Institut für Veterinärpharmakologie und -toxikologie

der Vetsuisse-Fakultät Universität Zürich

Direktor: Prof. Dr. med. vet. Hanspeter Nägeli

Arbeit unter wissenschaftlicher Betreuung von

Dr. med. vet. Dr. sc. nat. Enni Markkanen

Investigating stromal gene expression in metastatic and non-metastatic canine mammary tumours

Inaugural-Dissertation

zur Erlangung der Doktorwürde der
Vetsuisse-Fakultät Universität Zürich

vorgelegt von

Julia Ettlin

Tierärztin
von Basel BS, Allschwil BL

genehmigt auf Antrag von

Prof. Dr. med. vet. Hanspeter Nägeli, Referent

Prof. Dr. med. vet. Carla Rohrer Bley, Korreferentin

2018

Table of contents

1 Summary

Canine mammary tumours (CMTs) are suggested as good model for human breast cancer to better understand tumour biology and discover new biomarkers. Cancer-associated stroma (CAS) occupies a central role in cancer development and progression, and presents an interesting diagnostic and therapeutic target for both humans and dogs. However, in contrast to human cancer, CAS in CMTs remains largely uncharacterised. To analyse CAS from CMTs, we established isolation of CAS and matched normal stroma from formalin-fixed paraffin embedded (FFPE) tissue samples by laser-capture microdissection (LCM), and analysed gene expression by quantitative real-time PCR (RT-qPCR) and next-generation RNA sequencing (RNAseq). Using this setup, we investigated the expression of known human CAS markers in canine CAS. Furthermore, to identify possible drivers of tumour progression, we analysed CAS and normal stroma from 15 metastatic and 16 non-metastatic CMTs. Our findings show that i) CAS in CMTs undergoes strong reprogramming towards a tumour supportive function comparable with human CAS, and ii) CAS from metastatic tumours clearly differs from non-metastatic tumours, potentially enabling the identification of novel biomarkers and therapeutic targets for metastatic disease. Among other targets, we identified MMP11 as a possible new biomarker for metastatic CMTs. In summary, our data demonstrates the usability of FFPE tissue for RNAseq, and supports the use of the dog as a model of human breast cancer.

Keywords: canine mammary tumour, breast cancer, CAS, FFPE, LCM, metastases, MMP11

2 Zusammenfassung

Mammakarzinome des Hundes (CMKs) werden als gutes Modell für die Erforschung von Brustkrebs diskutiert. Die zentrale Rolle des Tumorstromas (TS) in der Tumorbiologie macht das TS für Diagnostik und Therapie bei Mensch und Hund höchst interessant. Im Gegensatz zum Menschen ist jedoch das TS in CMKs grösstenteils unerforscht. Um TS von CMKs detailliert zu untersuchen, haben wir die Isolation von TS und normalem Stroma aus Formalin-fixierten und in Paraffin-eingebetteten (FFPE) Proben mittels Laser-capture microdissection (LCM) etabliert, und die Genexpression mittels quantitativer PCR (RT-qPCR) oder RNA Sequenzierung (RNAseq) analysiert. Mittels dieser Technik haben wir die Expression von humanen TS-Markern im TS des Hundes ermittelt. Des Weiteren, um mögliche Treiber der Tumorprogression zu identifizieren, haben wir TS und normales Stroma von 15 metastatischen und 16 nicht-metastatischen CMKs erforscht. Unsere Ergebnisse zeigen, dass i) TS von CMKs, ähnlich dem humanen TS, umprogrammiert und eine tumorunterstützende Funktion übernimmt, und ii) TS von metastatischen Tumoren sich klar von nicht-metastatischen unterscheidet, was zur Identifikation neuer Biomarker und therapeutischer Ansatzpunkte für metastasierenden Krebs führen kann. Neben weiteren Kandidaten haben wir MMP11 als möglichen neuen Biomarker für CMKs identifiziert. Zusammenfassend beweisen unsere Daten die Verwendbarkeit von FFPE Gewebe für RNAseq und unterstützen die Verwendung des Hundes als Modell für Brustkrebs.

Schlüsselwörter: Mammakarzinom des Hundes, Brustkrebs, CAS, FFPE, LCM, Metastasen, MMP11

3 Abbreviations

ACTA2/αSMA	alpha smooth muscle actin
ASCs	adipose tissue-derived stem cells
AVCs	angiogenic vascular cells
CAFs	cancer-associated fibroblasts
CAS	cancer-associated stroma
CMTs	canine mammary tumours
CAV1	caveolin 1
COL1A1	collagen type I alpha 1 chain
COL14A1	collagen type XIV alpha 1 chain
CXCL12	C-X-C-motif chemokine ligand 12
DER-2	dog epidermal growth factor receptor-2
DIO3	deiodinase 3
E1	elution 1
ECM	extracellular matrix
EMT	epithelial-to-mesenchymal transition
ER	oestrogen receptor
FAP	fibroblast activation protein
FFPE	formalin-fixed paraffin embedded
FGF2	fibroblast growth factor 2
GnRH	gonadotropin-releasing hormone
HER-2	human epidermal growth factor receptor-2
HIF-1	hypoxia-inducible factor 1
IICs	infiltrating immune cells
IL6	interleukin 6
LCM	laser-capture microdissection
MMP2	matrix metalloproteinase 2
MMP11	matrix metalloproteinase 11
MSCs	mesenchymal stem cells
NK cells	natural killer cells
NST	invasive carcinoma of no special type
PCOLCE2	procollagen C-endopeptidase enhancer 2
PDGFRB	platelet derived growth factor receptor beta
PR	progesterone receptor
RIN	RNA integrity number
RNAseq	RNA sequencing
RT-qPCR	quantitative real-time PCR
SEMA3G	semaphorin 3G
SFRP1	secreted frizzled related protein 1
SLIT2	slit guidance ligand 2
TAMs	tumour-associated macrophages
TCGA	The Cancer Genome Atlas
TGFβ	transforming growth factor beta
TGFB2	transforming growth factor beta 2
TGFBR3	transforming growth factor receptor 3
Tregs	regulatory T-cells
VIT	vitrin

4 Introduction

4.1 Breast cancer as a challenge for the global healthcare system

The term “cancer” encompasses a large group of complex diseases that is responsible for an estimated 9.6 million deaths in 2018 all over the world. This makes cancer the second leading cause of death after cardiovascular diseases, both in Europe and worldwide [1-3]. The formation of cancer is a multistage process starting with the transformation of normal cells into tumour cells, which start to divide uncontrollably and give rise to a primary tumour. Moreover, some of these cells can overcome their physiological barriers, invade the surrounding tissues and even spread to distant organs. This final stage of cancer, known as metastasis, represents the main reason for cancer-related deaths [1].
In Switzerland over 40’000 people are diagnosed with cancer each year, with a rising tendency due to the increasing average age of the population. In contrast to this, the mortality for most cancer types is decreasing thanks to a good healthcare system, the continuous expansion of the knowledge on cancer, and the implementation of screening methods and more efficient treatments. Nevertheless, over 16’000 cancer patients die each year in Switzerland [4]. Breast cancer is the most frequent cancer type in women both worldwide and in Switzerland [4-6]. In the period from 2008 to 2012 in Switzerland, over 5700 patients were newly diagnosed with breast cancer, and 1400 patients died of breast cancer each year. Currently, the risk for Swiss women to develop breast cancer over a lifetime accounts for 12.7% (13 of 100 women) [4]. These high numbers clearly demonstrate that, despite significant advances in treating breast cancer over the last decades, there is still a large need for improved understanding of the disease to develop better therapeutic approaches, especially so for metastatic breast cancer.

4.2 The importance of the cancer-associated stroma (CAS) in cancer biology

Tumour cells have been in the focus of attention of cancer research for many decades, and the accumulation of genetic and epigenetic changes in these cells were classically considered as the main driving force for tumour development [7-10]. However, more recent results show that tumorigenesis is not a cell-autonomous process, but results from a reciprocal interaction between the tumour cells and their surrounding tissue. This surrounding tissue is also known as cancer-associated stroma (CAS) or tumour stroma [2, 7-9, 11-14]. The CAS consists of a mixture of various stromal cells and extracellular matrix (ECM) that have been shown to support growth and survival of the tumour cells [7, 8, 11, 12, 14]. The cells in CAS can be divided into three main cell types: i) angiogenic vascular cells (AVCs) including endothelial cells and pericytes, ii) cancer-associated fibroblastic cells (CAFs) comprising activated tissue resident fibroblasts and myofibroblasts, mesenchymal stem cells (MSCs), and activated adipocytes, and iii) infiltrating immune cells (IICs), such as lymphocytes, neutrophils and tumour-associated macrophages (TAMs) [11]. Under physiological conditions, epithelial and stromal interaction is essential for normal tissue formation and maintenance. The stroma maintains epithelial polarity and serves as an important barrier to prevent neoplastic transformation and uncontrollable cell proliferation. However, the presence of cancerous cells leads to reprogramming of the stromal compartment towards a tumour supportive function

[11, 13, 14]. This reprogramming of the stroma through tumour cells is achieved through a multitude of mechanisms, including exchange of signals through direct cell-cell contact, secretion of soluble factors like growth factors, cytokines, hormones as well as metabolites, secretion of exosomes containing miRNA, RNA and proteins, and others. All these mechanisms lead to gene expression changes in stromal cells that promote a tumour-cell supportive phenotype [7, 12, 14]. All of the CAS resident cells have been shown to significantly influence and contribute to the hallmarks of cancer [11]. Indeed, CAS has been shown to influence cancer initiation, growth and metastasis, and even to drive the development of resistance towards cancer therapy [7, 9, 11, 12, 14]. The different mechanisms by which CAS influences tumour growth and progression in general, and breast cancer in particular, is outlined in more detail in the following sections.

4.2.1 Influence of CAS on tumour growth

One of the major characteristics of cancer is the uncontrolled growth of tumour cells. This is partly a cell-intrinsic characteristic, but can also be strongly influenced through different cell types present in CAS.
CAFs represent a central component of the CAS in breast cancer, as they are responsible for building, maintaining and altering the structural framework of the tissue by secretion of ECM components [2, 7-9, 11, 12, 14]. CAFs derive from various sources such as normal fibroblasts, bone marrow-derived MSCs, adipose tissue-derived stem cells (ASCs), smooth muscle cells, and endothelial cells [2, 7-9, 11, 12]. These cells can be identified through a combination of different markers, including fibroblast activation protein (FAP), alpha smooth muscle actin (αSMA), tenascin C (TNC), and loss of markers like caveolin 1 (CAV1) and phosphatase and tensin homolog (PTEN) [7-9, 12]. CAFs have been shown to strongly impact on tumour growth and progression through the secretion of various growth factors including hepatocyte growth factor (HGF), epidermal growth factor (EGF), insulin like growth factor 1 and 2 (IGF1/2), platelet-derived growth factor (PDGF), transforming growth factor beta (TGFβ), basic fibroblast growth factor (bFGF) and vascular endothelial growth factor (VEGF), and many more. Furthermore, cytokines like interleukin 6 (IL6) and chemokines such as C-X-C-motif chemokine ligand 12 (CXCL12) are released by CAFs to promote epithelial cell growth [7-12, 14]. In breast cancer, these factors have also been shown to influence tumour growth indirectly by increasing tissue estradiol (E2) levels, which in turn results in enhanced proliferation of breast cancer cells [9]. Additionally, CAFs disrupt normal tissue structure by secretion of proteases like matrix metalloproteinases (MMPs) that dissolve epithelial cell-cell contacts, thus circumventing growth suppression pathways through contact inhibition [2, 8, 11].
Aside from CAFs, also IICs are known to contribute to tumour growth by secretion of growth factors (TGFβ, EGF, FGF), proteases and cytokines like C-C motif chemokine ligand 2 (CCL2) or interleukin (IL10) [11, 14]. Furthermore, IICs are involved in suppressing cell death pathways by binding to disconnected epithelial cancer cells, thus allowing them to survive in the new microenvironment [11].
To grow at an increased rate, tumour cells do not only depend on growth promoting signalling pathways, but also on an appropriate supply with adequate levels of oxygen and energy-rich metabolites. To this end, they trigger angiogenesis through a variety of proangiogenic factors including VEGF, CXCL12, interleukin 8/ C-X-C-motif chemokine ligand 8 (IL8/CXCL8), platelet derived growth factor receptor beta (PDGFRβ), TGFβ, MPPs, and FGF that are secreted by CAFs, IICs, pericytes as well as cancer cells themselves [8, 9, 11, 12]. Angiogenesis does not only play an

important role in primary tumour growth, but also supports invasion of the surrounding tissue and metastasis to distant organs [8, 11, 12]. To increase their supply with energy-rich metabolites, tumour cells have been shown to induce metabolic reprogramming in CAFs by releasing reactive oxygen species. This drives CAFs towards aerobic glycolysis, which results in the secretion of lactate and pyruvate that is taken up by the tumour cells to fuel their energetic demands [8, 10, 11].

Another key feature of malignant cancer cells is their ability to develop distant metastases, which are responsible for most cancer deaths [1, 8, 15]. For a tumour to form metastases, both tumour cells and the neighbouring CAS have to undergo multiple changes to enable this complex process. The first step in this process is for cancer cells to start invading the local tissue, and gain access to blood or lymph vessels (intravasation). Once in the circulation, cancer cells have to survive in the vasculature and exit from the vessels (extravasation) at the target organ, where they need to restart growing in order to form new colonies of tumour cells (colonisation) [8, 9, 14, 15]. The ability to degrade the ECM, an enhanced motility as well as undergoing epithelial-to-mesenchymal transition (EMT) have been shown to be important for tumour cells to invade their cellular surroundings and enter the vascular system [8, 9, 15]. Cancer cells do not achieve all these milestones on their own, but are strongly supported by the surrounding stroma in many of these aspects. Interestingly, the genes that are deregulated the most in CAS are related to ECM remodelling [16]. CAFs and IICs alter the ECM by secreting digestive enzymes like MMP2, MMP9, MMP11, serine proteases like urokinase-type plasminogen activator (uPA), and cysteine proteases influencing ECM components like collagen, fibronectin and tenascin C, thus leading to degradation and disorganisation of the ECM [2, 7, 8, 11, 14, 17]. The ECM alteration is reflected in the clinical presentation of breast cancer patients, where increased collagen deposition, collagen crosslinking and tissue density can be observed by palpation and diagnostic imaging [14, 16, 18]. For successful intravasation, tumour cells need to acquire an invasive phenotype, which can be triggered through expression of TGFβ by CAFs as well as IL6 or tumour necrosis factor alpha (TNFα) that are secreted by IICs [8, 11, 19]. Furthermore, looser tight junctions and rarer coverage through pericytes can be found around VEGF induced tumour vasculature, both of which facilitates cancer cell intra- and extravasation at the metastatic site [11]. To survive in circulation tumour cells do normally not spread as single cells, but instead travel together with fibroblasts from the primary mass. Finally, it has been shown that the pre-metastatic niche gets prepared by bone marrow-derived cells recruited by chemokines and cytokines released from the primary tumour, thus allowing the tumour cells to preferentially invade this niche and grow more easily [8, 14]. Taken together, the different components of CAS have been shown to influence all steps of cancer growth, development, invasion and metastasis directly as well as indirectly through a variety of mechanisms.

4.2.2 The role of CAS in cancer-associated inflammation and suppression of the immune system

Cancer-associated inflammation is another important component of the tumour stroma. It is mediated through different immune cells such as lymphocytes, neutrophils, eosinophils, mast cells, dendritic cells and macrophages. Presence of these IICs is usually associated with higher tumour grade, enhanced necrosis, loss of

hormone receptors and worse prognosis [9, 12, 14, 20]. Normally, IICs are able to destroy cancer cells, as these can be recognised as non-physiological cells within the tissue. The paradoxically worsened prognosis in the presence of immune cells is caused by a reprogramming of the IICs through the tumour cells towards a cancer cell tolerant phenotype. As a result, instead of fighting against tumour cells, the reprogrammed IICs actually promote tumour growth, angiogenesis, and metastasis [8, 9, 21]. Among the major players that exert pro-tumorigenic properties are tumour associated macrophages (TAMs). They originate from blood monocytes which are recruited to the tumour via cytokines including CCL2, IL6, TNFα and CXCL12 that are expressed by both tumour and stromal cells [8, 12, 14]. Most TAMs show a so-called proinflammatory or M2 phenotype, and secrete various cytokines such as IL4, IL10, CCL2, CCL17, CCL22, TGFβ as well as VEGF, PDGF, FGF, MMPs, and uPA which are involved in tissue remodelling, angiogenesis, tissue and blood vessel invasion and immunosuppression [9-12, 14, 17, 20].
Another group of IICs are lymphocytes, mostly regulatory T-cells (Treg), CD8+ T-cells, CD4+ helper cells and natural killer (NK) cells. Tregs normally protect the body against autoimmune responses. However, in the tumour tissue they enable the cancer cells to evade the immune system by supressing various immune cells, including the main effector cells CD8+ T-cells and NK cells that mediate elimination of tumour cells [11, 14, 21]. IICs express a molecule called programmed cell death 1 (PD-1), which inhibits inappropriate T-cell function in normal tissues. In cancer however, PD-1 binds its ligand PD-L1 that is expressed by tumour cells, which leads to inactivation of T-cells and thus the establishment of an immunosuppressive microenvironment [14, 22]. Dendritic cells in CAS have also been shown to exhibit an altered function, as most of them remain in an immature state unable to inhibit tumour growth, but instead promote angiogenesis through secretion of proangiogenic factors [14, 21]. Finally, not only IICs themselves, but also CAFs and ACV influence cancer-associated inflammation by inhibiting the T-cell function via TGF-β and impeding T-cell extravasation [8, 11].
In summary, tumour cells are not self-sufficient and heavily depend on the surrounding stroma. CAS influences growth and metastasis of tumour cells through complex interactions of a multitude of direct and indirect mechanisms deriving from various cellular sources. Thus, the interplay between tumour cells and CAS is emerging as centrally relevant for the growth and development of cancer cells. However, even though the details of this interplay between tumour cells and components of the CAS are slowly being unveiled, we are still far from a complete understanding of the mechanisms involved in this dialogue. A better understanding of the factors involved and their effects has the potential to uncover novel therapeutic strategies to inhibit both cancer cell growth and metastasis.

4.3 Spontaneous tumours in dogs as a model for human cancer

A plethora of *in vitro* and *in vivo* models have been used over the last century to gather knowledge about cancer biology. While these models have been highly informative in many aspects, there are inherent limits in using such models, as they cannot fully replicate the conditions of real, spontaneously developing patient tumours [23-27]. A rather novel field of research, referred to as comparative oncology, aims at opening up new possibilities by shifting the focus from classical rodent models to other animals including dogs. This additional perspective is seen as a chance to better understand complex diseases like cancer, as the comparison of

tumour development and risk factors across species provides the opportunity to discover basic mechanisms of tumorigenesis [23, 24, 28].
The domestic dog is considered one of the best examples for comparative oncology as it shares many similarities with humans. First of all, dogs have about the same number of genes as humans and share evolutionarily conserved alterations in the genome [23, 24, 26, 28-30]. Cancer in both species develops spontaneously, and manifests in a similar clinical presentation, pathophysiology, and histology. As such, development of spontaneous tumours in dogs has strong parallels with the natural progression of cancer development in humans, and is considered a better proxy of tumour biology than animal models with induced tumorigenesis. The higher life expectancy compared to rodent models and the similar environmental factors that dogs and humans are exposed to, combined with the fact that dogs often receive a high level of healthcare further strengthens the value of comparatively analysing canine and human cancers [1, 23, 24, 25, 31]. Furthermore, canine tumours have been shown to harbour genetic aberrations in the same genes as the corresponding human tumour types, including for instance BRCA1 and BRCA2 mutations which lead to an enhanced risk of hereditary breast and ovarian cancer in humans [23, 25, 30, 32, 33]. Additionally, certain breeds of dogs carry genetic predispositions for certain cancer types as a result of inbreeding and high degrees of consanguinity, thus facilitating the discovery of risk alleles responsible for the disease [23-25, 28, 30, 34]. Altogether, these insights emphasise the potential of the dog as models for human cancer and offers the possibility to overcome limits of xenograft and genetically engineered rodent models leading to improved understanding of tumour biology and facilitating biomarker discovery [23-25, 27, 28].

4.4 Comparing canine mammary tumours and human breast cancer

Among many different cancer types, canine mammary tumours (CMTs) are regarded as good models for human mammary carcinomas [35, 38]. The age of onset is comparable in both women and bitches when converting dog years into human years. The incidence of CMTs starts to increase after the age of 6 (humans 40 years) and peaks between 8 to 14 years (humans 50 to 70 years) [4, 26, 36, 38]. Furthermore, it is the most frequent cancer diagnosed both among female dogs as well as women suffering from cancer [25, 32, 35]. A retrospective study on tumours in dogs in Switzerland between 1955 and 2008 found that 20.53% of all canine tumours were located in the mammary gland [37]. On a global level, CMTs occur in more than 40% of female dogs and show and annual incidence rate varying between 192 to 205/100’000 dogs, which is even higher than incidence rates of 125/100’000 women in the United Stated and 144/100’000 women in Switzerland [4, 25, 34, 36, 38]. Interestingly, the United States have lower numbers for CMTs than other countries like Sweden, presumably because dogs get neutered at an early age and receive less gestagen preparations for heat prevention. Particularly neutering before the first oestrus minimizes the risk of CMTs to 0.5% compared to intact bitches, rising to 8% when neutered after the first oestrus, and rising to 26% when neutered after the second oestrus. However, no protective effects of neutering after the second oestrus has been found in dogs older than 2.5 years [34, 36]. The protective effect of neutering is indicative of a significant contribution of sex hormones to the development of CMTs. Under physiological conditions and in early stages of human and canine breast cancer development, sex hormones, such as oestrogen and progesterone, stimulate mammary tissue growth through specific binding of

hormones to their cognate receptors oestrogen receptor (ER) and progesterone receptor (PR). This effect can also be induced by synthetic gestagen used for oestrus preventions. Especially progesterone derivates have been shown to promote increased growth hormone production in the mammary gland, thus leading to IGF1 secretion, which stimulates cell proliferation. However, during disease progression, expression of hormone receptors can be lost, resulting in hormone-independent proliferation [34-36, 38, 39].

The anatomy of the normal mammary gland is similar in dogs and women. The alveoli and ducts of the mammary gland consist of luminal epithelial cells lined by myoepithelial cells and are separated from the surrounding connective tissue by the basement membrane [10, 36]. In both species tumorigenesis is seen as a dynamic process starting with benign hyperplastic lesions potentially turning into carcinoma *in situ* and finally becoming invasive, a stage which is marked by the disruption of the basement membrane [35, 40-42].
Histological classification of human breast cancer consists of more than 20 subtypes from which the invasive carcinoma of no special type (NST) is diagnosed most frequently, accounting for 40% to 75% of diagnoses [4, 32]. The wide range of NST cases is usually explained by improperly applied inclusion criteria leading to the inclusion of many specific subtypes in this type. This is not surprising, as NST morphology is very variable and includes tumour cells arranged in clusters, trabeculae and cords or some that even show a solid or syncytial tissue structure [32, 43]. Thus, relevance of histological classification is limited, not least because many studies show differences between different NST in clinics and treatment response [44].
In canines, most malignant mammary tumours arise from epithelial cells and are either defined as simple carcinomas or, in cases where myoepithelial cell proliferation can be simultaneously observed, complex carcinomas [34, 36, 45]. Canine simple carcinomas strongly resemble human breast cancer both histologically and at the molecular level, whereas complex carcinomas are rarely diagnosed in women [25, 46, 47]. Histological classification of CMTs slightly differs from the human classification and has been modified stepwise over the past 40 years. The WHO histologic classification from 1999 defined simple carcinoma subtypes for the first time including the tubulopapillary carcinoma, solid carcinoma and anaplastic carcinoma. In 2010 a new classification was proposed by Goldschmidt et al dividing simple carcinomas into a tubular, tubulopapillary, cystic-papillary and cribriform subtype. Moreover, solid and anaplastic carcinomas were specified as independent types, and new tumour types like the comedocarcinoma were added [45]. Nevertheless, the clinical relevance of the exact histologic classification into subtypes remains questionable [48].
Tumour grading is an additional feature that is assed in histological examination of invasive human breast carcinomas, and which has been adapted to invasive canine carcinomas. On the basis of tubule formation, nuclear pleomorphism and mitotic counts, carcinomas can be divided into three grades. Grade I tumours are well differentiated, grade II tumours are moderately differentiated and grade III tumours are poorly differentiated. Grade III is associated with worse survival in both species, and accordingly lymphatic invasion as well as lymph node metastasis is spotted more frequently in these cases [32, 45, 49-51]. In dogs, reports have associated different grades with different histological subtypes, showing most tubular and tubulopapillary carcinomas being well differentiated, whereas solid, comedocarcinoma and anaplastic carcinoma exhibited higher grades [49, 51, 52].

Besides clinical factors like tumour size, lymph node involvement, clinical stage, histological tumour type and grade, molecular subtypes (named luminal A, luminal B, HER2-enriched and basal-like) have been found to be prognostic in both canine and human breast cancer [30, 32, 34, 38, 49, 51-54]. The luminal A subtype is characterised by ER and/or PR expression, well differentiated cells and low proliferation rates [38, 44, 55]. Luminal B tumours also express ER and/or PR but have a higher proliferation rate and grade, with worse prognosis than luminal A [44]. Human epidermal growth factor receptor-2 (HER-2) enriched cancers are associated with high tumour grades and result from amplification of the erb-b2 receptor tyrosine kinase 2 (ERBB2) gene [44]. In dogs, contradictory results of HER-2 expression in CMTs have been reported. However, a homologue of HER-2 has been found in CMTs, termed dog epidermal growth factor receptor-2 (DER-2), showing similar biological effects [30, 34, 47, 53, 56-58]. The basal-like subtypes express basal cell markers and show no ER, PR or HER-2 expression. Therefore, this phenotype is also known as triple negative breast cancer associated with high malignancy, poor differentiation, enhanced proliferation and lymphatic invasion resulting in shorter overall survival [30, 38, 44, 52, 55]. To conclude, expression of hormone receptors and HER-2 in CMTs has been associated with similar clinics in human breast cancer. This suggests that they can serve as biomarkers in dogs, and also points out an additional commonality between the two species [38, 55]. However, assessment of molecular subtypes is still limited to research purposes and not routinely applied in CMT diagnosis [34, 54].
Taken together, the similarities between CMTs and human breast cancer indicate comparable tumour biology, and studying CMTs offers the opportunity to find novel biomarkers not only for dogs but also humans. Comparing the same disease in two different species additionally helps differentiating the molecular ‘driver’ of the disease from mere ‘passengers’, as the central drivers should be conserved between species. Finally, clinical trials in dogs can be conducted in a shorter period than human studies, due to a reduced lifespan and associated earlier manifestation of cancer [24].

4.5 Largely uncharted territory: cancer-associated stroma in canine mammary tumours

Studies investigating human cancer cells and their TME have started to reveal the importance of CAS in cancer initiation and progression, and emphasise the potential of targeting CAS in cancer therapy. One of the currently most promising strategies is immunotherapy, used as additional treatment modality to complement chemotherapy, radiotherapy and/or surgery [59, 60]. As CAS plays such a pivotal role in the biology of human cancer, it very likely also strongly influences tumour growth and development in dogs. However, to date, data regarding CAS in canine cancers is very rare. Most studies investigating CMTs have analysed the whole tumour tissue by sequencing or microarray analysis. In cases where CAS was looked at specifically, only single markers were analysed using immunohistochemistry [25, 27, 38, 61, 62].

A well-known CAF marker αSMA and the ECM molecule TNC were found to be expressed in myofibroblasts within CAS of canine simple mammary carcinomas. The presence of stromal myofibroblasts and the expression of TNC were associated with higher histological grade, vessel invasion, metastasis, and worse prognosis, correlating with findings in human breast cancer [63].

Similarly, the role of inflammatory cells and their gene expression signature in the canine CAS is still understudied. Very few studies have been conducted in CMTs considering the number of TAMs, T and B-cells in the tumour bed and their influence on clinical outcome. Most studies demonstrated that the amount of IICs is higher in malignant and metastasizing tumours and also Treg were shown to be associated with high histological grade and metastasis [10]. There is not much published data regarding the gene expression profile of IICs in CMTs. One immunohistochemistry study shows an increased expression of IL1 and TNFα in the stroma as well as in epithelial cells, associated with tumour malignancy and metastasis [64]. A second study investigating TAMs found upregulated genes like CXCL10 and Wnt ligands, both of which are suggested to be involved in angiogenesis [65].
The most thoroughly investigated enzymes regarding invasion in CMTs are MMP2, MMP9, and uPA [10]. These factors were shown to be expressed by both CAFs and tumour cells [10, 66, 67]. MMP2 up-regulation was shown to be associated with tumour malignancy including higher tumour stage [66, 67]. MMP9 expression was higher in malignant tumours compared to benign neoplasms and related with high histologic grade, invasion, metastasis and shorter survival times [66, 68]. Expression of uPA was also associated with malignant behaviour including increase in tumour size, higher histological grade, proliferation, invasive growth, metastasis in lymph nodes and distant organs as well as reduced overall survival and disease-free survival [10, 69]. In a multivariable survival study MMP9 and uPA presented better prognostic factors than classic histological parameters like tumour size and grade. Therefore, they are discussed as potential prognostic and therapeutic targets in CMTs [10, 70].
Other main biomarkers analysed in CMT by immunohistochemistry are VEGF and vascular endothelial growth factor receptor (VEGFR2). In CMTs VEGF was shown to be expressed in endothelial cells, TAMs and tumour cells with higher expression levels in malignant, high grade, and necrotic tumours leading to endothelial cell proliferation [71-73]. Expression of VEGFR2, shown to be expressed in endothelial cells, was also associated with malignancy and metastasis to the lungs. Highest VEGFR2 levels were detected in comedocarcinomas suggesting it may play an important role in this subtype [71, 74].

While adding important information to the field of CAS in canine tumours, all these reports have only investigated a very limited number of targets, and no unbiased analyses have been performed to investigate gene expression patterns in CAS from CMTs. Thus, it remains largely unknown whether CAS in canine and human breast cancer are comparable, and what the molecular similarities and differences are. A better understanding of the biology of CAS in CMTs is imperative to understand whether canine breast cancer really is comparable to the human disease in all of its aspects, and to understand how CAS influences growth and progression of CMTs.

4.6 Aim of this thesis

Given the central role of CAS for the biology of human breast cancer, it is also very likely to be a very important component in the growth and development of CMTs. To date however, CAS in CMTs remains practically uncharacterised, and it is unclear to what extent CAS from canine and human tumours can be compared. An improved understanding of the canine CAS will serve to validate CMTs as model for the human disease, and comparative studies with human breast cancer have the potential to identify key drivers of tumour growth and metastasis.
To better understand the mechanisms involved in CAS formation of CMTs and be able to identify commonalities and differences between canine and human CAS, we set out to analyse the gene expression of CAS from canine simple mammary carcinomas. Specifically, the aims of my thesis were the following:

1) Establish a protocol to analyse the expression of selected CAS markers for human breast cancer in CAS from canine mammary carcinomas.
2) Develop a protocol to analyse CAS and normal stroma from FFPE tissues by next-generation RNA sequencing (RNAseq).
3) Analyse CAS and normal stroma from non-metastatic versus metastatic canine mammary carcinomas to investigate the changes in canine CAS and identify differentially regulated genes that could potentially be used as prognostic or therapeutic targets.

5 Materials and methods

A large part of the materials and methods that were used have already been described in detail in my master thesis [75] as well as the two studies that are included in this thesis of which I am first and shared first author, namely “Analysis of gene expression signatures in cancer-associated stroma from canine mammary tumours’’[76] and “An optimised protocol for isolation of RNA from small sections of laser-capture microdissected FFPE tissue amenable for next-generation sequencing” [77]. In the following section the entire procedure is outlined in brief to give a complete overview of all materials and methods used.

5.1 Selection criteria for tissue specimens

Twenty-one canine simple mammary carcinomas were provided by the Institute of Veterinary Pathology of the Vetsuisse Faculty Zurich. These are cases that were either from the Small Animal Hospital of Zurich or external cases sent in by Swiss veterinarians. Additional ten cases were provided by Prof. R. Klopfleisch from the Institute of Veterinary Pathology of the Freie Universität Berlin and have already been part of a previously published study [61]. These cases had slight differences in fixation and histological classification criteria, the details of which can be found in [61] and further below. All samples were formalin-fixed, paraffin embedded (FFPE) and selected by a pathologist. The criteria for inclusion in this study were as follows: female dogs, simple mammary carcinomas, histological tumour grade I-III, sufficient tumour and normal stroma for isolation, and available information on lymph nodes regarding metastases.
The decision to include simple mammary carcinoma was based on its similarity to human breast cancer regarding histology and molecular pattern [25, 46, 75, 78]. Selection criteria of the modified WHO classification and the histologic grading system from Clemente et al were applied [45, 51, 79]. Following simple carcinoma subtypes were included: tubular, tubulopapillary, cribriform, cystic-papillary, solid and comedocarcinoma [45]. The anaplastic subtype was excluded as the highly invasive growth pattern with scattered epithelial cells impeded the selective extraction of stromal cells. Furthermore, instead of a primary mass, the tumour cells of anaplastic carcinomas were often found in lymphatic vessels, which made it difficult to define the appropriate distance for isolating normal stroma. The selection criterion for metastatic tumours was presence of metastases in histological sections of regional lymph nodes found by microscopic examination, whereas non-metastatic tumours were defined by regional lymph nodes free of metastases.
The cases were reviewed by a board-certified veterinary pathologist using routinely stained H & E slides cut at 2 µm. If no clear identification was achieved, the cases were discussed with colleagues of the institute. When difficulties in the distinction between simple and complex carcinomas appeared, immunohistochemistry using the myoepithelial cell marker p63 (1:50, ab735, Abcam) was conducted to detect myoepithelial cell proliferation. The slides were stained according to a standard protocol established at the Institute of Veterinary Pathology, University of Zürich (available upon request).

5.2 Tissue preparation for laser-capture microdissection (LCM)

Tissue specimens were fixed in 10% neutral buffered formalin (Zürich), or 4% neutral buffered formalin (Berlin), and subsequently embedded in paraffin. The microtome HM 360 (ThermoFisher Scientific) was used to cut 10 µm tissue sections. The water

was treated with DEPC and the blade was cleaned with RNase away™ (Ambion) to avoid mRNA degradation during cutting. After cutting the sections were mounted on PEN Membrane Glass Slides (Applied Biosystems™) and dried at room temperature overnight. To enable identification of stroma, tissue sections were stained with Cresyl violet according to [80] with slight modifications (Figure 1). Following reagents were used: xylene (Thommen-Furler AG), ethanol (Sigma-Aldrich), cresyl violet (acetate) for microscopy Certistain® (Merck), and DEPC treated water (Carl Roth).

Cresyl violet staining for FFPE tissue sections
Xylene, 20 s
Xylene, 20 s
Xylene, 20 s
100% ethanol, 30 s
100% ethanol, 30 s
95% ethanol, 30 s
95% ethanol, 30 s
70% ethanol, 30 s
70% ethanol, 30 s
75% ethanol, 2 min
Cresyl violet (0.2 g cresyl violet in 40 ml 100% ethanol), 1 min
75% ethanol, 5 s
90% ethanol, 5 s
100% ethanol, 5 s
100% ethanol, 1 min
Air-dry, 2 min

Figure 1: *Cresyl violet staining protocol for FFPE tissue sections.*

5.3 Stroma isolation by LCM

The stained slides were reviewed by a veterinary pathologist before microdissection to identify the stromal areas. Cell types included for isolation were fibroblasts, endothelial cells, pericytes, and inflammatory cells. Normal stroma was isolated from the same slides as the tumour-associated stroma and at least 2 mm away from the tumour cells [81]. Further, the normal stroma had to be located between the normal mammary glands and not within the dermis. If the sample did not meet the criteria for normal stroma, normal stroma was isolated from another mammary tissue specimen of the same dog, extracted and fixed on the same day. Isolation was conducted according to manufacturer's protocol using the ArcturusXT™ Laser Capture Microdissection System (Thermo Scientific) and the Arcturus® CapSure® Macro LCM Caps (Life Technologies). To validate the proper excision of stromal cells, the LCM cap and the region of excision were both checked through microscopy after microdissection (Figure 2). The UV-laser or an RNase-away treated scalpel blade was used to clean the cap from contaminating epithelial cells in cases where small residual amounts of unwanted tissue were co-isolated. The caps containing the isolated tissue were placed on 0.5 ml microcentrifuge tubes (Eppendorf® Safe-Lock Tubes) and stored at 4°C until microdissection of this sample was concluded, and the samples were stored maximum one week at -20°C until mRNA isolation.

5.4 Isolation of mRNA

Extraction of mRNA was performed using the Covaris® truXTRAC FFPE RNA kit according to manufacturer's protocol with small adjustments. To transfer the sample into the microTUBE Screw-Cap (Covaris®) a sterile scalpel blade was used to remove the membrane from the LCM cap containing the tissue specimen. For sonication, the E220 focused ultrasonicator (Covaris®) was used according to manufacturer's protocol. The centrifugation step after crosslink reversal at 80°C was skipped (as paraffin had already been removed during staining). In step 13 the RNA Elution Buffer was preheated to 70°C to achieve higher mRNA yields. Subsequently, mRNA was eluted in two elutions using 30 µl of RNA Elution Buffer in the first round and 20 µl in the second round, each of which was collected in a separate tube. After finishing mRNA extraction the samples were kept on ice. The mRNA quality and mRNA yield was measured according to manufacturer's protocol using the High Sensitivity RNA ScreenTape kit (Agilent Technologies). The eluate was stored at -80°C before proceeding further analysis.

5.5 Next-generation RNA sequencing

10 ng of RNA from Elution 1 (E1) diluted to a concentration of 0.33 ng/µl in a total volume of 30 µl was submitted for next-generation RNA sequencing. The SMARTer Stranded Total RNA-seq Kit—Pico Input Mammalian (Clontech/ Takara Bio USA) was used according to manufacturer's protocol for RNA library preparation and ribosomal RNA depletion. Single-read sequencing (125bp) was run using the Illumina HiSeq 4000 according to standard protocols of the Functional Genomics Centre Zurich (FGCZ). Quality control for the resulting NGS reads was performed with FastQC (http://www.bioinformatics.babraham.ac.uk/projects/fastqc). Trimmomatic [82] (v.0.36, 4 bases hard-trimming from the start, and adapter trimming at the end) was used to trim the reads and STAR [83] (version 2.6.0c) was applied to align the trimmed reads with the reference genome and transcriptome (FASTA and GTF files, respectively, Ensembl, release89, CanFam3.1). Kallisto [84] (version 0.43.1) was used for gene expression quantification. For identification of differently expressed genes the R/Bioconductor package edgeR [85] (R version: 3.5.0, EdgeR version: 3.22.1) with the implemented count based negative binominal model was applied using the normalisation factor calculated by the trimmed mean of M values (TMM) method [86].

5.6 Analysis of RNA sequencing data

Unsupervised hierarchical clustering ($p \leq 0.01$, log2 ratio threshold of 0.5) was conducted for both, comparison of tumour and normal stroma as well as comparison of CAS of metastatic and non-metastatic tumours.
Gene ontology (GO) enrichment analysis was performed using goseq R Bioconductor package [87]. The analysis was run for each cluster as well as for all significantly deregulated, up-regulated, and down-regulated genes separately and dividing them into the three GO categories termed biological process (BP), molecular function (MF), and cellular composition (CC). For the comparison of CAS of metastatic and non-metastatic tumours no results were displayed for most categories, due to low numbers of significantly deregulated genes. Therefore, an additional GO enrichment analysis was performed, using the Enrichr software [88, 89].
Pathway analysis was performed using the MetaCore™ software (Thomson Reuters) analysing the gene set of the 500 most deregulated genes for both comparison

conditions mentioned above. As the MetaCore ™ database allows only analysis of human, mouse and rat genes, the gene symbol was used for uploading the experiment and 'human' was selected as the target species. Pathway analysis using 'Pathway Maps' was conducted for the up-regulated, down-regulated, and also for all deregulated genes separately ($p \leq 0.03$, fold change ≥ 0.5).
For identification of stromal gene candidates involved in metastasis, all significantly deregulated genes of the comparison metastatic versus non-metastatic CAS ($p \leq 0.03$, fold change ≥ 0.5) were analysed by the Explore DEG app of the FGCZ using 'Feature view'.

5.7 Validation of selected genes by quantitative real-time PCR

To validate the next-generation RNA sequencing results 16 cases were randomly selected (8 metastatic, 8 non-metastatic). The iScript™ cDNA Synthesis Kit (BioRad) was used for cDNA preparation according to manufacturer's protocol. A maximum of 15 µl of mRNA per reaction were used with a total mRNA input of 15 ng per sample. To increase the yield of cDNA for quantitative real-time PCR (RT-qPCR) analysis, the TaqMan® PreAmp Master Mix (2x) (Applied Biosystems™) was used to perform cDNA preamplification according to manufacturer's protocol applying 14 PCR cycles. After preamplification the samples were diluted by adding 20 µl of nuclease free water. To perform RT-qPCR the KAPA PROBE FAST qPCR Kit Master Mix (2X) Universal reagents (Kapa Biosystems) was used. The samples were run in duplicates on the CFX384 Touch™ Real-Time PCR detection system (BioRad) using 2 µl preamlified cDNA per reaction, in a total volume of 10 µl. Relative gene expression was quantified as = 2^-(CtTarget-CtHousekeeping), where CtTarget is obtained by normalising the resulting CT values against the mean of the three housekeeping genes GAPDH, PPIA and B2M. Details regarding primers can be found in (Table 1). The TaqMan® primers were obtained from ThermoFisher Scientific and the primers for GAPDH from Microsynth (Balgach, Switzerland). All primers were used at final concentrations of 900 nM primers and 250 nM probes, except GAPDH used at final concentrations of 300 nM primers and 200 nM probe [90]. Validation of the primers was either conducted by the manufacturer, or for GAPDH by [90], showing approximately 100% amplification efficiency.

Table 1: *List of primers used in this study for RT-qPCR.*

Gene target	Sequence	Amplicon length (nt)	Taqman® order number or Reference
DIO3	Manufacturer's proprietary information	96	Cf02688456_g1
MMP11	Manufacturer's proprietary information	75	ARFVK2U
VIT	Manufacturer's proprietary information	68	Cf02657286_m1
TGFBR3	Manufacturer's proprietary information	70	Cf02637773_m1
TGFB2	Manufacturer's proprietary information	112	Cf02676763_m1
SFRP1	Manufacturer's proprietary information	69	Cf02654440_m1
GAPDH	Fw: 5'-GCTGCCAAATATGACGACATCA-3' Rev: 5'-GTAGCCCAGGATGCCTTTGAG-3' Probe: 5'-TCCCTCCGATGCCTGCTTCACTACCTT-3'	75	[90]
B2M	Manufacturer's proprietary information	87	Cf02659077_m1
PPIA	Manufacturer's proprietary information	92	Cf03986523_gH

5.8 Graphical representation and statistical analysis of qPCR results

For all statistical analysis and graphical displays of RT-qPCR results, the program GraphPad Prism (www.graphpad. com) was used. Relative mRNA levels/expression values of the four different sample categories were analysed through 1-way ANOVA (p-value with $\alpha = 0.05$), followed by Bonferroni's Multiple Comparison Test to assess significance between each of the categories. Data is displayed as scatter plots, with mean ±SEM.

5.9 Survival analysis of stromal candidate genes

To analyse the association of the deregulated genes with survival, the Tumor Immune Estimation Resource (TIMER; cistrome.shinyapps.io/timer) web application was used [91]. The software checks human data from The Cancer Genome Atlas (TCGA). Covariates included in the analysis were age, tumour stage, Breast Invasive Carcinoma (BRCA) and its subtype HER-2. For the display of survival differences, a Kaplan-Meier Curve was drawn. The parameters were set at 50% for the split percentage and 100 months for the survival time.

6 Results

6.1 Paper: “Analysis of Gene Expression Signatures in Cancer-Associated Stroma from Canine Mammary Tumours Reveals Molecular Homology to Human Breast Carcinomas.”

Int. J. Mol. Sci. (2017), 18, 1101; doi:10.3390/ijms18051101

In this first paper, we analysed the expression of nine known human CAS markers by RT-qPCR and/or immunohistochemistry in CAS isolated from canine simple carcinoma. This was the first report to provide comprehensive expression analysis of all these markers in CAS from canine mammary carcinomas.
My contribution to this paper, of which I am the first author, was to set up the entire workflow for LCM of CAS and normal stroma in FFPE tissue samples, and to select and analyse the expression of known CAS markers. I also significantly contributed to writing of the manuscript.

International Journal of
Molecular Sciences

MDPI

Article

Analysis of Gene Expression Signatures in Cancer-Associated Stroma from Canine Mammary Tumours Reveals Molecular Homology to Human Breast Carcinomas

Julia Ettlin [1], Elena Clementi [1], Parisa Amini [1], Alexandra Malbon [2] and Enni Markkanen [1,*]

[1] Institute of Veterinary Pharmacology and Toxicology, Vetsuisse Faculty, University of Zürich, Winterthurerstr. 260, 8057 Zürich, Switzerland; julia.ettlin@uzh.ch (J.E.); elena.clementi@vetpharm.uzh.ch (E.C.); parisa.amini@vetpharm.uzh.ch (P.A.)

[2] Institute of Veterinary Pathology, Vetsuisse Faculty, University of Zürich, Winterthurerstr. 268, 8057 Zürich, Switzerland; alexandra.malbon@uzh.ch

* Correspondence: enni.markkanen@vetpharm.uzh.ch; Tel.: +41-44-635-8770

Academic Editor: Sanjay K. Srivastava
Received: 14 February 2017; Accepted: 17 May 2017; Published: 20 May 2017

Abstract: Cancer-associated stroma (CAS) plays a key role in cancer initiation and progression. Spontaneously occurring canine mammary carcinomas are viewed as excellent models of human breast carcinomas. Considering the importance of CAS for human cancer, it likely plays a central role in canine tumours as well. So far, however, canine CAS lacks characterisation, and it remains unclear whether the biology between CAS from canine and human tumours is comparable. In this proof-of-principle study, using laser-capture microdissection, we isolated CAS and normal stroma from 13 formalin-fixed paraffin embedded canine simple mammary carcinomas and analysed the expression of seven known human CAS markers by RT-qPCR (Reverse Transcription quantitative PCR) and validated some targets by immunohistochemistry. We found that Col1a1 (Collagen1α1), αSMA (alpha Smooth Muscle Actin), FAP (Fibroblast activation protein), PDGFRβ (Platelet-derived growth factor receptor beta), and Caveolin-1 were significantly upregulated in canine CAS, and the expression of CXCL12 (Stromal cell derived factor 1) significantly decreased, whereas MMP2 (Matrix Metalloproteinase 1) and IL6 (Interleukin 6) did not change. Our results suggest strong similarities in CAS biology in canine and human mammary carcinomas but also reveal some differences. To the best of our knowledge, this is the first report to provide a comprehensive expression analysis of the most important CAS markers in canine simple mammary carcinomas and further supports the validity of the dog as model for human cancer.

Keywords: cancer; dog; tumour; mammary carcinoma; tumour stroma; gene expression; cancer-associated stroma; tumour microenvironment

1. Introduction

The majority of all cancers are of epithelial origin and derive from a corrupted epithelial cell population that gives rise to aggressively growing tumour cells. However, these epithelial tumour cells are not living in an isolated environment, and, far from being self-sufficient, heavily depend on their microenvironment for growth and survival (reviewed in [1]). While the vast majority of research in the past has focused on the neoplastic cells themselves, recent progress has started to unveil the central importance of the tumour microenvironment in cancer formation and progression. The so-called cancer stroma consists of an extracellular matrix as well as a variety of cells, including endothelial cells, immune cells, and fibroblasts (reviewed in [2]). Under physiological conditions, stroma serves

as an important barrier to prevent epithelial transformation (reviewed in [3]). However, in response to emerging epithelial cancerous lesions, the stromal compartment undergoes a reprogramming towards a tumour-supportive function, termed cancer-associated stroma (CAS), and plays a key role in cancer initiation and progression [1]. The pivotal role of CAS in many human carcinomas (such as breast, lung, prostate, and colorectal carcinomas) has been widely documented [4]. It has even been suggested that components of CAS serve as actual drivers, initiating the development of a tumour from precancerous cells (e.g., [2]). Abundant literature shows that CAS directly supports the growth of tumour cells through secretion and/or activation of cytokines, growth factors, nutrients, and proteases (e.g., reviewed in [1,4]). Studies performed in human clinical tumour samples have begun to shed light on mechanisms driving the formation of CAS as well as the molecular dialogue between CAS and tumour cells (e.g., [5–8]).

Due to the closely related pathophysiology, naturally occurring cancers in the domestic dog are progressively leveraged as a valuable source of information to better understand the biology behind tumour development and possibly find novel anti-cancer treatments [9–11]. Indeed, the study of canine cancer overcomes several of the limitations of genetically modified or xenograft rodent models for tumours [12,13]. Canine mammary tumours in particular are viewed as excellent models for human breast cancer due to strong clinical and molecular similarities and also availability of specimens [13,14]. In dogs, the majority of mammary cancer cases are classified either as simple carcinomas or as complex carcinomas [15]. Histologically, canine simple carcinomas very closely replicate the biology of human simple carcinomas (e.g., reviewed in [14]). Even at the molecular level, canine simple carcinomas replicate the genomic aberrations found in the human counterpart and have thus been demonstrated to faithfully represent human breast carcinoma [13]. Finally, canine mammary tumours are highly relevant in the veterinary clinical setting due to their incidence, as the most frequent cancer in intact female dogs, as well as the difficulties of therapeutic intervention (such as e.g., control of metastases and development of resistance to therapy) that are associated with all current cancer treatments [16].

Given the importance of CAS for the biology of human cancer, it likely plays a central role in the development and growth of canine tumours as well. So far, however, canine CAS greatly lacks characterisation, and it remains completely unclear whether similar markers are expressed in canine and human CAS. Therefore it remains unclear whether CAS has a role in the growth of canine tumours, what mechanisms are involved in its formation, and if canine CAS is comparable to human CAS. For these reasons, we set out to analyse the expression of several genes known to be expressed in the CAS of human breast tumours in formalin-fixed paraffin embedded (FFPE) specimens from canine simple mammary carcinoma cases. Our results provide a comprehensive overview, the first of its kind to our knowledge, of the expression of the most important CAS markers in dogs and suggest that CAS-related biology is very comparable between canine and human breast carcinoma.

2. Results

2.1. Selection of Cases Included in the Study

The main aims of our study were, firstly, to characterise the expression of known CAS-associated targets from human cancer in canine mammary tumour associated stroma and, secondly, to understand if large aspects of the underlying biology of CAS could be compared between dog and human breast cancer. To this end, we chose to include only canine simple carcinoma cases, as this type of tumour is recognised as a very close clinical, histological, and molecular correlate of human simple breast carcinoma [13,14]. Cases with obvious inflammation were excluded to avoid introducing unnecessary variability (for details, see Materials and Methods). With these criteria in mind (also see the Materials and Methods section), we selected a total of 13 canine simple mammary carcinomas, as defined by a board-certified veterinary pathologist (A.M.), from the archives to be included in the analysis. The mean age of the dogs at sample collection was 9.8 years, and further characteristics of patients and tumour samples can be found in Table 1.

Table 1. Overview of cases included in this study. Clinical data from dogs with simple mammary carcinoma; Case # = case number as referred to within this study; f/n = female, neutered; n.d. = not disclosed; age = age at excision of tumour; age of sample = time between initial tumour excision and sampling of stroma/RNA extraction.

Case #	Gender	Breed	Age (Years)	Subtype of Simple Carcinoma	Age of Sample (Months)
1	f	Basset	12	tubular	3
2	f	Vizsla	10	cystic-papillary	18
3	f	Samoyed	5	tubulo-papillary	7
4	f	Maltese	14	tubular	3
5	f	Tibetan Terrier	12	tubular	15
6	f/n	West Highland White Terrier	12	tubular-solid	13
7	f	Havanese	13	tubular	11
8	f	Chihuahua	8	tubulo-papillary	7
9	f/n	Bracke	9	cribriform	14
10	f/n	n.d.	13	tubular	7
11	f/n	Appenzell Mountain Dog	6	tubular	18
12	f	Boxer	9	tubulo-papillary	8
13	f	n.d.	4	cystic-papillary	23

2.2. Selection of Cancer Associated Stroma Markers to be Analysed in This Study

One of the inherent challenges in identifying CAS is that, because of its cellular and molecular heterogeneity, there is no single molecule that could specifically and reliably differentiate CAS from normal stroma. However, several studies performed with human breast cancer material have reported a variety of factors that are produced by CAS, the expression of some of which is correlated with a clinically unfavourable outcome. Using the available literature for gene expression changes in human breast cancer stroma, we selected targets that have been reported by several studies as typical CAS markers and represent a variety of different classes of molecules (Table 2).

Table 2. List of the cancer-associated stromal targets selected for analysis in this study. List of gene names and their respective protein names that were assessed by RT-qPCR (Reverse Transcription quantitative PCR), immunohisto–chemistry, or both. "Expression in CAS" summarises the expression trend as observed in human studies (see References). The column "qPCR" denotes which of the targets were analysed by RT-qPCR, whereas the column "HC" specifies which targets were assessed by immunohistochemistry. The "Ref." column indicates selected references to either original publications or reviews. * For Cav1, expression studies are somewhat discordant, although generally a decreased Cav1 expression in CAS is associated with poor prognosis.

Gene Name	Protein Name	Function	Expression in CAS	qPCR	IHC	Ref.
PDGFRB	PDGFRβ (Platelet-derived growth factor beta)	Cell-surface tyrosine kinase receptor	upregulated	×	×	[17–19]
MMP2	MMP2 (Matrix metalloproteinase 2)	Metalloproteinase	upregulated	×	×	[20–23]
COL1A1	Col1a1 (Collagen 1 α 1)	Extracellular matrix	upregulated	×		[22–26]
FAP	FAP, Fibroblast activation protein	Serine protease	upregulated	×		[27,28]
ACTA2	αSMA (α smooth muscle actin, aorta)	Cytoskeleton	upregulated	×	×	[29–34]
CXCL12	SDF1 (Stromal cell-derived factor 1)	Chemokine	upregulated	×	×	[20,35,36]
IL6	IL-6 (Interleukin-6)	Cytokine	upregulated	×		[37,38]
FGF2	bFGF (Basic fibroblast growth factor)	Growth factor	upregulated		×	[2,39]
CAV1	Cav1 (Caveolin-1)	Possibly stabilisation of caveolar membranes	Downregulated *		×	[2,40]

2.3. Isolation of mRNA from Tumour Stroma and Matched Normal Stroma from Patient Material

To specifically isolate RNA from CAS and normal stroma from FFPE tissue sections of clinical mammary carcinoma cases, we established a protocol for laser-capture microdissection (LCM), a technique that allows the precise excision of areas of interest from microscopic tissue sections, for canine FFPE tissue sections, followed by RNA isolation (Figure 1). Using the ArcturusXT™ Laser Capture Microdissection System (ThermoFisher Scientific, Waltham, MA, USA), we isolated matched normal stroma and CAS from 13 clinical cases of simple mammary carcinoma (Table 1). Importantly, normal stroma and CAS were both isolated from the exact same tissue section to minimise differences in tissue quality and processing, thus allowing for optimal comparability of the two correlates. The areas of interest were defined by a board-certified veterinary pathologist (Alexandra Malbon, A.M.), and microscopic validation of the tissue before and after excision ensured the selective isolation of CAS and normal stroma (Figure 2). RNA isolation, analysis, and preamplification were performed as specified in the Materials and Methods section. As expected for FFPE tissue samples [41], the analysis of mRNA quality and quantity revealed highly fragmented RNA and low yields (Table S1). Nevertheless, the mRNA was amenable to analysis by RT-qPCR.

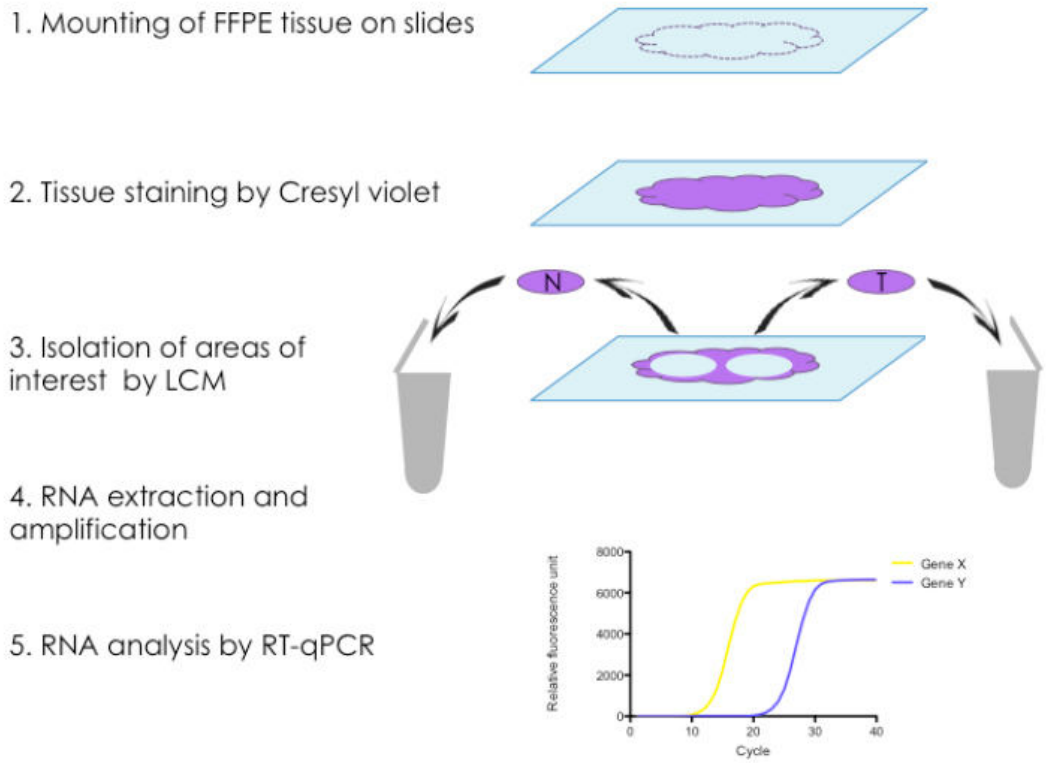

Figure 1. Protocol for isolation and analysis of matched normal and cancer-associated stroma from FFPE tissue sections. (1) Formalin-fixed paraffin-embedded (FFPE) tissue sections are cut and mounted onto PEN (Polyethylene naphthalate) Membrane Glass Slides (Applied Biosystems™); (2) Tissue is stained with Cresyl violet to facilitate visualisation of areas of interest under the microscope; (3) Areas of normal stroma (N) and tumour stroma (T) are isolated from the same slide under the microscope using Laser-Capture Microdissection, and harvested into separate tubes; (4) RNA extraction, quality control, quantitation, and preamplification; (5) Relative mRNA levels of selected genes are analysed by RT-qPCR.

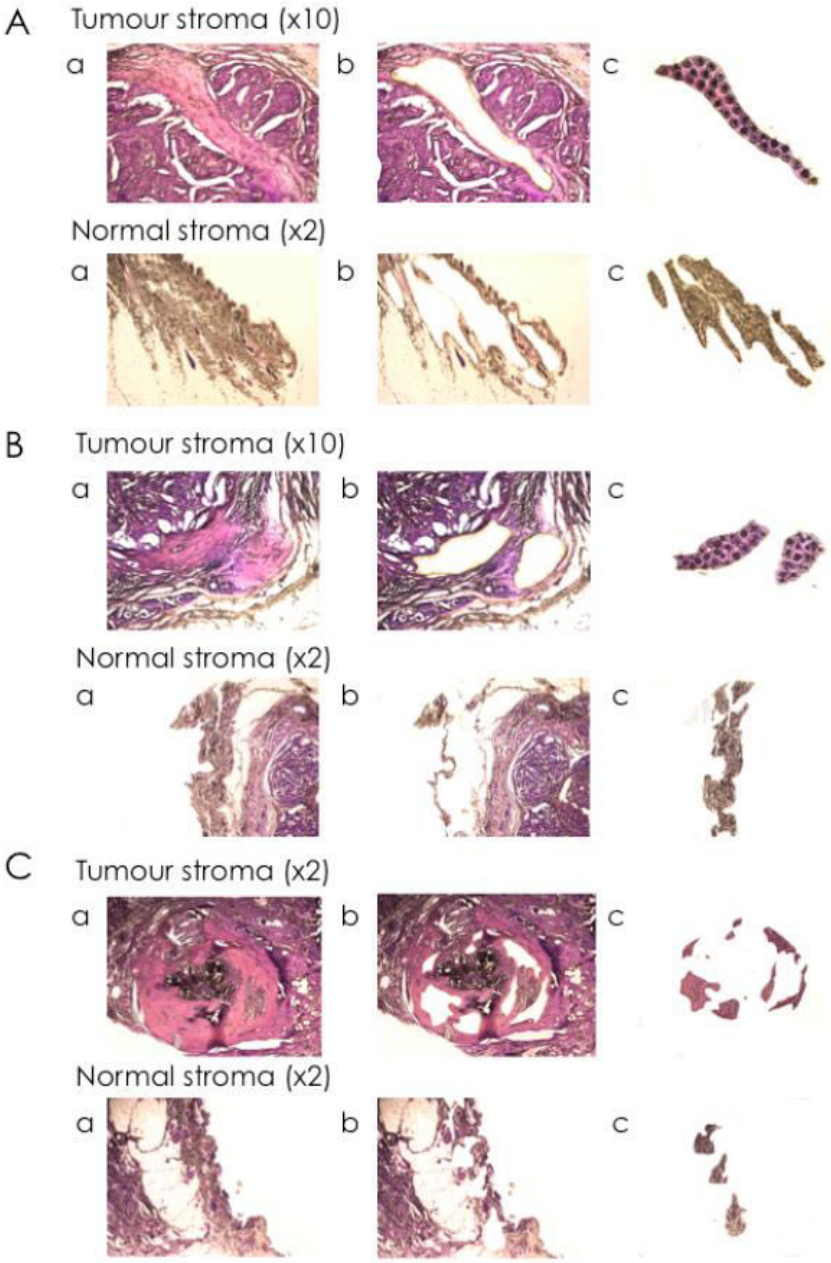

Figure 2. Selective isolation of cancer-associated stroma and normal stroma from canine simple mammary carcinomas by laser-capture microdissection. Representative images of tissue mounted on the slide were taken at ×2 and ×10 magnification, as indicated, (a) before dissection; (b) after dissection; and (c) of the CapSure® Cap containing the excised tissue sections to validate the isolation of the selected cells. The dark spots visible in the CapSure® Cap samples denote the area of the melted thermoplastic film of the cap by the infrared laser and thus of adhering tissue. Three representative cases were chosen. Cases: (**A**): Case #3; (**B**): Case #4; (**C**): Case #6.

2.4. Expression Analysis of Cancer Associated Stroma Markers by RT-qPCR

To analyse expression of the targets of interest (Table 2) in the RNA isolated from the FFPE tissue sections, RT-qPCR was performed, comparing CAS with the respective matching normal stroma. Three cases had to be excluded from the analysis due to insufficient housekeeping gene performance,

probably due to low RNA abundance. PDGFRB, ACTA2, and CXCL12, as well as IL6, could not be reliably amplified in all cases, leading to different numbers of cases that were analysed for each gene, as indicated in the respective panels (Figure 3). For details on which cases yielded data for which primers, see Table S1.

We found that the mRNA levels of ACTA2, COL1A1, and FAP were all significantly increased in CAS compared to the normal stroma (Figure 3A–C). These findings are consistent with data obtained from studies on human material (Table 2 and references therein) and validate our approach to specifically isolate RNA from CAS and normal stroma from canine FFPE mammary carcinoma samples. No significant difference in mRNA expression levels could be detected for PDGFRB or MMP2 (Figure 3D,E), possibly due to a combination of a small sample size and relatively modest changes in expression of the gene, or perhaps simply because they might not change. Interestingly, the levels of CXCL12 were significantly lower in CAS compared to normal stroma (Figure 3), which is in contrast to the literature analysing human samples (Table 2 and references therein). The reasons for this discrepancy are currently unclear but might suggest a difference in the role of CXCL12 in stroma of canine compared to human mammary carcinomas. Taken together, our results showed that at least COL1A1, ACTA2, and FAP were significantly upregulated on mRNA levels in CAS from canine mammary carcinoma similar to human mammary carcinoma samples, whereas CXCL12 is downregulated. These data suggest that the underlying biology of CAS is highly comparable, at least in some aspects, between dogs and humans and that COL1A1, ACTA2, and FAP can be used as markers of CAS in canine mammary carcinomas.

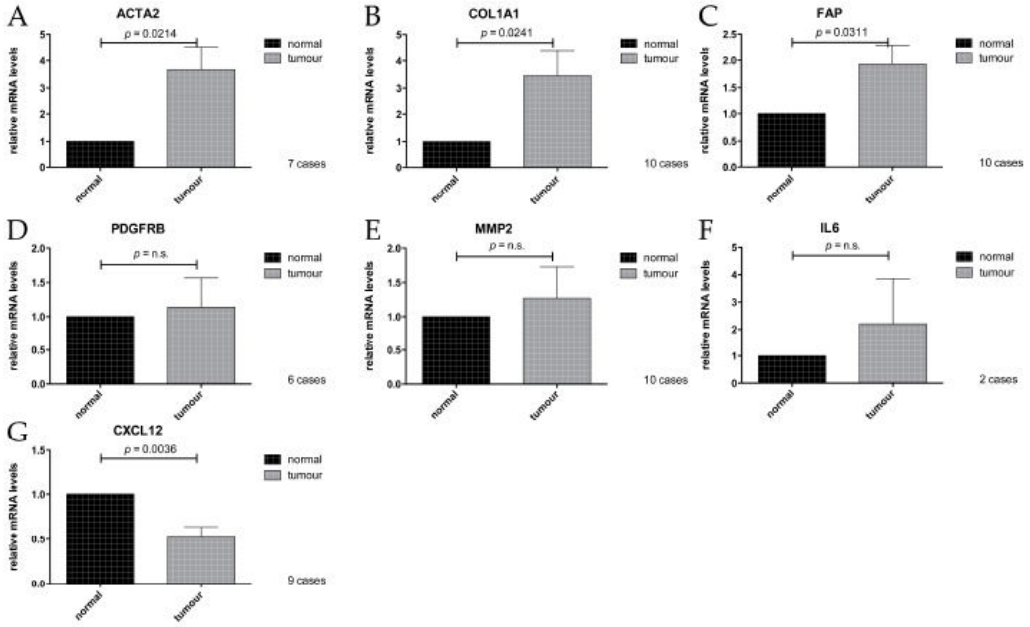

Figure 3. Relative mRNA levels of CAS-associated genes in normal stroma and tumour stroma isolated by laser-capture microdissection (LCM), measured by RT-qPCR. (**A**): ACTA2; (**B**): COL1A1; (**C**): FAP; (**D**): PDGFRB; (**E**): MMP2; (**F**): IL6; (**G**): CXCL12. Values are mean values ±SEM, normalised to expression levels in normal stroma. *p*-values were calculated using student's *t*-test, and significance was set at $p \leq 0.05$. n.s. = not significant.

2.5. Expression Analysis of Cancer Associated Stroma Markers by Immunohistochemistry

In order to validate our mRNA expression findings (Figure 3), to confirm that the measured changes were derived specifically from cells deriving from the stromal compartment and not influenced by contamination by regions containing epithelial cancer cells, and to possibly still extract data from

the cases that had not yielded mRNA data, immunohistochemical (IHC) analysis of all thirteen cases was performed for αSMA (alpha Smooth Muscle Actin, the product of *ACTA2* gene), FAP (Fibroblast Activation Protein), PDGFRβ (Platelet-derived Growth Factor Receptor beta), MMP2 (Matrix Metalloproteinase 1), and SDF1 (Stromal Derived Factor 1, the product of *CXCL12* gene) (Figure 3). Additionally, we analysed the expression of Caveolin-1 (Cav1), a protein that is sometimes shown to be increased in CAS but, if decreased in CAS, has been shown to predict early recurrence and poor clinical outcome in human breast cancer (e.g., reviewed in [42]), and FGF2, another marker upregulated in CAS [2,39].

Immunohistochemically stained tumour sections were scored by a board-certified veterinary pathologist (A.M.), according to the following score-system: 0 = negative, 0.5 = negligible, 1 = mild, 2 = moderate, 3 = strong (see also Materials and Methods). We found αSMA, FAP, PDGFRβ, and Caveolin-1 to be significantly upregulated in CAS compared to normal stroma (Figures 4A–D and 5A–D).

Staining for αSMA was only detectable in CAS as well as all vessel walls, whereas normal stroma or epithelial cancer cells remained negative (Figure 4A), and the IHC staining score was significantly higher in CAS compared to normal stroma (Figure 5A). These findings are in accordance with the literature from human breast cancer studies showing an upregulation of αSMA in CAS (Table 2) and validate our RT-qPCR results (Figure 3A). Importantly, these results further underline the specificity of our isolation protocol for CAS and normal stroma.

Mild to moderate FAP staining could be clearly detected in the tumour stroma and was significantly stronger than in the normal stroma, where only negligible staining could be detected, except for vessel walls (Figures 4B, 5B and S1). Staining for FAP in epithelial cancer cells was mostly negligible. These findings are in accordance with our RT-qPCR data (Figure 3C) and with literature from human breast cancer studies that have demonstrated FAP upregulation in CAS (Table 2).

Staining for PDGFRβ was significantly more intense in CAS compared to normal stroma, and no staining could be detected in epithelial cancer cells (Figures 4C and 5C). This suggested that even though no significant increase in PDGFRB mRNA levels using RT-qPCR could be detected (Figure 3D), possibly due to a combination of low sample size with small expression changes, protein levels of PDGFRβ increased in CAS, which is similar to findings from human breast cancer stroma (Table 2 and references therein).

Tissue analysed with Cav1 antibody showed mild to moderate staining for the tumour stroma and only mild staining for the normal stroma (Figure 4D). Additionally to CAS, other cell types such as neoplastic epithelial cells, myoepithelial cells lining tubules, smooth muscle cells, and cells of blood vessels showed positive staining with the Caveolin-1 antibody. The IHC staining score for Cav1 was significantly higher for CAS compared to normal stroma (Figure 5D).

While the RT-qPCR of CXCL12 mRNA levels showed a significant decrease in CAS (Figure 3G), analysis of SDF1 protein expression by IHC revealed no significant changes between CAS and normal stroma, while neoplastic epithelial cells stained strongly (Figures 4E and 5E). The reason for the discrepancy between the RT-qPCR and the IHC results remains to be further investigated. One possible explanation for this could be that stabilisation of the protein via posttranslation modifications interferes with protein turnover, even though the transcription of the corresponding mRNA has been downregulated. Furthermore, MMP2 and FGF2 failed to show any significant differences in IHC staining scores between CAS and normal stroma (Figures 4F,G and 5F,G). The fact that MMP2 staining intensity did not change significantly is in accordance with the result of RT-qPCR (Figure 3E). Thus, the results from our IHC studies show clearly that αSMA, FAP, PDGFRβ, and Cav1 are all significantly upregulated in canine CAS, largely mimicking the events known from human CAS.

In summary, this study provides, to the best of our knowledge, the first thorough analysis of the gene expression signatures of known CAS-related genes from human tumour samples by RT-qPCR and IHC in FFPE tissues from dog mammary carcinomas.

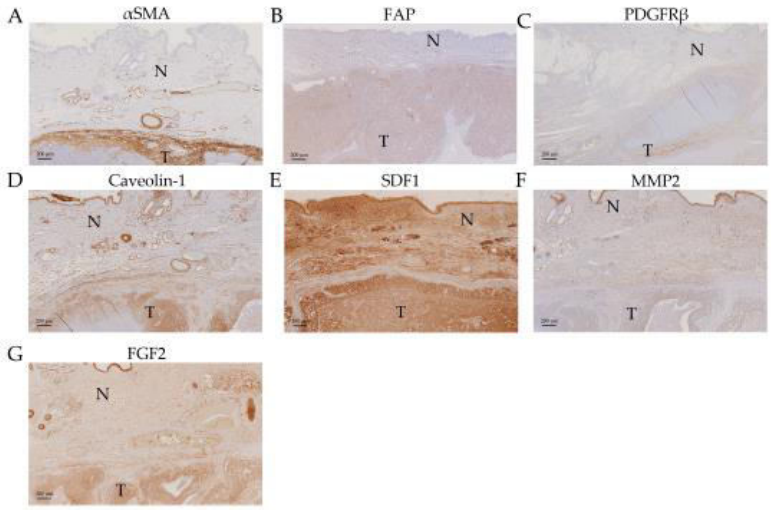

Figure 4. Immunohistochemical staining of a canine simple mammary carcinoma sample. Images are from Case #6), except for FAP, for which the image was taken from case #5. Pictures were taken at ×2 (for PDGFRβ) and ×5 (for the other gene products) magnification. T = tumour stroma, N = normal stroma. (**A**): αSMA; (**B**): FAP; (**C**): PDGFRβ; (**D**): Caveolin-1; (**E**): SDF1; (**F**): MMP2; and (**G**): FGF2.

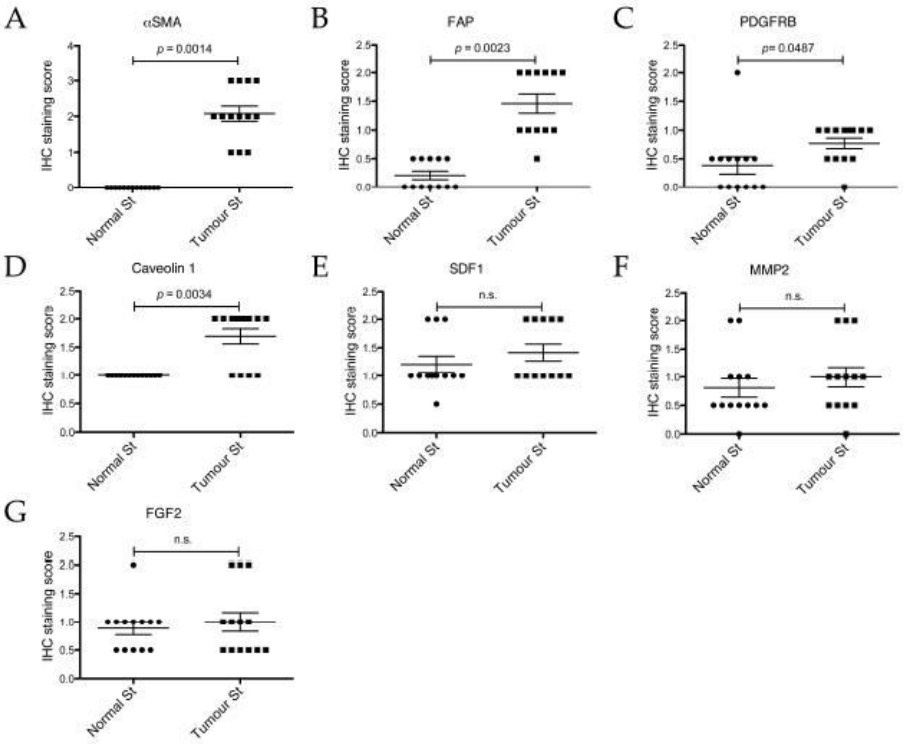

Figure 5. Immunohistochemical staining scores of the normal and tumour stroma (normal st and tumour st, respectively) from the 13 different cases for different proteins. Slides were stained with the indicated antibodies and scored. (**A**): αSMA; (**B**): FAP; (**C**): PDGFRβ; (**D**): Caveolin 1; (**E**): SDF1; (**F**): MMP2; (**G**): FGF2. IHC for FAP could only be performed on 12 cases due to the unavailability of case #7 at the time of processing. Plotted are all individual values and the mean ± SEM of the IHC staining scores. *p*-values are two-tailed and were calculated using the Wilcoxon signed rank test, with significance set at $p \leq 0.05$. n.s. = not significant.

3. Discussion

Recent cancer research has expanded its focus from mutated cancer cells to their microenvironment since the importance of the tumour stroma in cancer initiation, progression, and metastasis and the development of adaptive resistance to therapies has been unveiled [1,43,44]. To reveal the biology of cancer, the dog represents an ideal model organism as canine cancer occurs spontaneously, shows similar clinical presentation, and overcomes some limitations of rodent models. So far however, there are only very limited data regarding the reprogramming of normal stroma into CAS in canine cancers compared to studies performed in human samples [12,13]. To expand the knowledge regarding the biology of CAS in canine cancers, we set out to investigate the expression of known human CAS markers in the tumour stroma of canine simple mammary carcinoma specimens. To do this, we established the isolation of CAS and matched normal stroma by laser-capture microdissection (LCM) using FFPE canine simple mammary carcinoma samples (Figure 1). So far, few studies have been performed using LCM for analysing FFPE tissue samples [45,46], whereas most studies were performed using fresh frozen tissue samples [21,47] since fresh-frozen specimens promise a higher yield and much increased quality of mRNA. Despite low quantity and quality of the extracted RNA, as expected from the literature (Table S1), we were able to analyse the expression of all selected target genes (Table 2) by RT-qPCR (Reverse Transcription quantitative PCR) (Figure 3). These analyses were complemented by immunohistochemical staining to validate the procedure as well as the obtained data and further extend our observations (Figure 4). In the following, the findings for each target are discussed in detail.

3.1. ACTA2/αSMA

The upregulation of ACTA2 in CAS of our canine mammary carcinoma samples is consistent with the results from human studies in which the increase of its gene product, αSMA, is associated with poor prognosis [29–34]. αSMA plays a role in cell motility as it is a major constituent of the cytoskeleton and is expressed by myofibroblasts during wound healing as well as cancer-associated fibroblasts (CAFs) [2]. Importantly, we could further validate our observations by an IHC analysis of αSMA protein levels, which were significantly upregulated in stromal cells of the tumour but not in normal stroma (Figures 3A, 4A and 5A). This finding is consistent with another report demonstrating an increase in aSMA immunoreactivity in stroma of canine simple mammary carcinomas [48]. The specific localisation of staining with αSMA to CAS but not normal stroma or neoplastic epithelial cells further underlined the specificity of our approach in isolating CAS and normal stroma by LCM.

3.2. COL1A1/Collagen 1

We found COL1A1 to be upregulated in the canine tumour stroma by RT-qPCR (Figure 3B). This gene encodes the Collagen1 alpha chain 1, which forms part of the extracellular matrix. This upregulation of COL1A1 in CAS is consistent with findings in human studies [22–25] and matches the finding that collagen is progressively deposited during breast cancer development resulting in increased tissue stiffness as a classical fibrosis-type response of neoplasms [49].

3.3. Fibroblast Activation Protein, FAP

FAP, a serine protease expressed in the reactive stromal fibroblasts of epithelial cancers and the granulation tissue of healing wounds, was also found significantly overexpressed in the CAS of our canine tumour specimens by RT-qPCR (Figure 3C). Importantly, IHC for FAP confirmed this upregulation on protein levels (Figures 4B and 5B, Figure S1). An increase in FAP expression in canine mast cell tumour stroma by IHC has been recently demonstrated [50]. FAP is known to be overexpressed in CAS from human breast cancer as well [27,28], and has the capacity to degrade gelatin and type 1 collagen and therefore influences the remodelling of the ECM, supporting the formation of a tumour-permissive milieu [28,51].

3.4. PDGFRB/PDGFRβ

PDGFRB encodes a tyrosine kinase receptor of the platelet-derived growth factor (PDGF) family. This protein, PDGFRβ, is secreted by CAFs and triggers cancer growth and increased pericyte coverage of vessels, resulting in increased vessel function [18]. High stromal PDGFRβ is associated with metastasis, larger tumour size, high histopathological grade, and shorter survival in human breast cancer [17–19,51]. In our dataset, no significant change in relative mRNA levels comparing tumour and normal stroma was observed (Figure 3D). However, it is possible that the inability of our analysis to determine any significant change is caused by a combination of a small sample size and a moderate effect size, which would necessitate a larger dataset for reliable detection. Therefore, the six cases included in this analysis are not enough to give a proper assessment of the situation in canine mammary cancers. Therefore, more samples would need to be analysed in order to draw a valid conclusion for the mRNA levels of PDGFRβ in canine mammary cancer stroma. Indeed, by IHC staining, we detected a statistically significant increase in staining of the tumour stroma compared to the normal stroma for PDGFRβ, indicating an increase in PDGFRβ protein in CAS (Figures 4C and 5C). This finding is well in accordance with published data for human CAS [18].

3.5. CXCL12/SDF1

CXCL12 is a chemokine secreted by cancer associated myofibroblasts and binds to the CXCR4 receptor on epithelial cells, enhancing their proliferation, migration, and invasion and thus playing a role in tumorigenesis [20,33,35,43]. Moreover, CXCL12 is involved in angiogenesis by playing a part in the recruitment of endothelial progenitor cells into cancerous tissue [35,43]. Instead of being upregulated, as observed in many human studies [20,35,36], we found a downregulation of CXCL12 in the CAS of our specimens (Figure 3G). A lack of an adequate amount of myofibroblasts collected of the tumour stromal compartment compared to the normal stromal compartment seems not to be the main cause since ACTA2 and FAP are also expressed in myofibroblasts and show an opposing result (Figure 3A,C). Poor mRNA quality and an overall low amount of tissue samples may have had an influence on the validity and proper detection of CXCL12, or, quite simply, the canine isoform of CXCL12 may not play the same role in tumorigenesis in dogs as in humans. IHC staining for SDF1, the gene product of CXCL12, did not reveal differences between CAS and normal stroma in our analysis (Figures 4E and 5E). This could be a consequence of the stabilisation of the protein via posttranslation modifications, which interferes with protein turnover, even though the transcription of the corresponding mRNA has been downregulated. Another explanation would be unspecific antibody crossreactivity with other targets that covers the real effect. Further analysis of a larger dataset as well as validation and extension of these findings are required to draw further conclusions.

3.6. MMP2

An analysis of MMP2 revealed no significant change in gene expression (Figure 3E) or protein levels by IHC (Figure 4F, Figure 5F), even though several breast cancer studies [20–23] have found an upregulation of MMP2 in the tumour stroma of human patients. MMP2 is a metalloproteinase secreted by CAFs and also tumour associated macrophages and functions by remodelling the ECM, resulting in tumour progression, invasion, and metastasis and the support of angiogenesis [21,43]. It is possible that a lack of increase of MMP2 expression in canine tumour stroma is due to lack of isolation of tumour associated macrophages in our case, as we sought to avoid areas of obvious inflammation when isolating stroma (see Materials and Methods). Moreover, CAFs may have not expressed high amounts of MMP2 since most CAS areas collected in this study were from areas inside the tumour mass and not at its border, where most of the remodelling processes are thought to take place. Malignant canine mammary tumours have been found to express higher levels of MMP2 than benign tumours or normal mammary tissue [52]. Importantly, the expression of MMP2 in these cases was detected in the myoepithelial cells lining the basement membrane of tubuloalveolar structures in benign tumours,

while malignant tumours showed MMP2 expression in the neoplastic cells themselves. This study did not specify any expression of MMP2 in the stroma. Similarly, another report showed elevated levels of MMP2 expression by IHC and protein activity in neoplastic cells, with the highest levels in malignant tumours, whereas no differences in mRNA levels using the whole tumour could be found [53]. This study also found a higher level of MMP2 expression in the stroma of tumours, with the highest immunoreactivity found in the fibroblasts closest to the epithelial cells. Taking into account these results, it is possible that the cell layer closest to the tumours was not always excised during the isolation of CAS in order not to not risk a contamination of CAS material with neoplastic cells. If the protein was indeed produced in this cell layer, this would explain why we did not detect an increase in mRNA levels. Again, this needs to be further investigated in a larger cohort. Finally, it remains unclear why we were not able to detect an increase in MMP2 staining by IHC as demonstrated by [53], which could also be related to differences in the antibody used.

3.7. Interleukin 6, IL6

Examination of IL6 levels by RT-qPCR was successful for both tumour and normal stroma in only two cases and therefore clearly showed no significant difference in gene expression, which precludes any further interpretation of these data (Figure 3F). The cytokine is primarily secreted during acute or chronic inflammation by inflammatory cells or CAFs promoting tumorigenesis, angiogenesis. and metastasis [51]. Low amounts of tissue and bad mRNA quality may have had an influence on the proper detection of IL6 as well as the avoidance of inflammatory areas during tissue collection (see Materials and Methods section), which contain most of the IL6 secreting cells. Indeed, the study of Chavey et al. [37] showed a correlation between the number of tumour associated macrophages and IL6 levels in breast cancer, supporting this hypothesis.

3.8. Caveolin-1

Caveolin-1 is known to be expressed in cancer-associated fibroblasts, myoepithelial cells underlying the luminal epithelial cells, endothelial cells, and adipocytes, which clearly correlates with our detection (Figure 4D, Figure 5D) [54,55]. While, in humans, a decrease in expression of Cav1 in tumour stroma is generally considered to be a marker of poor prognosis [42], increases in Cav1 in CAS have also been documented to be associated with higher tumour aggressiveness [56]. Data on Cav1 expression in CAS from canine mammary tumours is less clear, mainly because studies have mostly focused on staining intensities in the tumour epithelia themselves and not in CAS particularly (e.g., [55]). Further studies are warranted for a more thorough analysis and an evaluation of the significance of these results.

Concluding, our data show that canine CAS shows similar changes in key CAS-molecules to those found in human cancer samples, suggesting that the underlying biology is very comparable. This further validates the use of canine simple mammary carcinomas as a model for human breast cancer [9,10,12,13,57]. Furthermore, it is possible that some of these changes in canine CAS render the cancer similarly more aggressive in its malignant behaviour and that such changes are associated with poor prognosis, as is the case with human cancers [51]. Unfortunately however, as our dataset is yet too small and there are no survival data available, these questions can not be addressed at this point in time.

Since difficulties with primer performance in a subset of samples reduced cases that could be included in the statistical analysis, analysis of more samples is needed to further validate our findings and unveil more reliable and more subtle changes. It is likely that next-generation RNA sequencing technologies would yield much more and precise data from these samples. Though technically challenging with such small amounts of highly degraded RNA, the establishment of this approach is expected to yield much more valuable information regarding the biology of CAS in dogs, to further our understanding of tumour biology, and perhaps lead to biomarker discovery and the development of new therapies for human and canine mammary carcinomas.

4. Materials and Methods

4.1. Selection of Cases for LCM

Thirteen dog mammary carcinoma samples were provided by the Institute of Veterinary Pathology of the Vetsuisse Faculty, Zürich. All of the samples were formalin-fixed, paraffin-embedded tissue samples from either the Small Animal Hospital of Zurich or external cases sent in by veterinarians practising in Switzerland. Cases were selected with the help of a board-certified veterinary pathologist (A.M.) using the following criteria; female dogs, simple mammary carcinomas, appropriate tumour stroma content, FFPE samples not older than two years [58], areas with no obvious or only negligible inflammation, and samples were paraffin-embedded on their arrival day at the Pathology, (i.e., no prolonged storage in formalin). During our initial screening for suitable cases, those which contained only highly inflamed stroma were excluded. In selecting areas for LCM from our chosen cases, no regions with aggregates of inflammatory cells were included. The cells were not specifically counted per field as this would be highly variable according to the proportion of the field taken up by stroma. Rather, if only individualised leukocytes (i.e., single figures of most commonly lymphocytes and plasma cells) were present within a stromal region, it was considered appropriate to select and any areas with aggregated inflammatory cells were removed.

4.2. Tissue Processing and Staining

Biopsy samples had been fixed immediately in 10% neutral buffered formalin and subsequently routinely embedded in paraffin. For total mRNA analysis, formalin-fixed, paraffin-embedded tissue sections cut at 10 µm were used. Diethylpyrocarbonate (DEPC) treated water was used for the microtome HM 360 (ThermoFisher Scientific, Waltham, MA, USA), and the blade was cleaned with RNase away™ (ThermoFisher Scientific, Waltham, MA, USA). The tissue was mounted on PEN Membrane Glass Slides (Applied Biosystems™, Waltham, MA, USA). The mounted tissue sections were left to dry overnight at room temperature (http://support.moleculardevices.com). To visualise the areas of interest, the tissue sections were stained for initial scrape tests with H&E, and for all other interventions with Cresyl Fast Violet according to [59] with slight modifications (Table 3). The slides were completely air dried before microdissection to allow for proper excision performance. For every tissue sample that underwent LCM, a second tissue slide was stained with conventional Hematoxylin-Eosin staining to allow for validation of tissue morphology in case of uncertainty using the Cresy violet stain. The reagents used were xylene (Thommen-Furler AG, Rüti bei Büren, Switzerland), ethanol (Sigma-Aldrich, St. Louis, MO, USA), Hematoxylin Solution modified acc. to Gill II (Merck KGaA, Darmstadt, Germany), Ammonium Hydroxide Solution (Sigma-Aldrich), Cresyl Fast Violet (Fluka AG, Buchs, Switzerland), and DEPC treated water (Carl Roth, Karlsruhe, Germany).

Table 3. Staining protocol for Cresyl violet staining of formalin-fixed paraffin embedded (FFPE) tissue sections.

Cresyl Violet Staining for FFPE Tissue Sections	
100% Xylene, bath 1	5 min
100% Xylene, bath 2	5 min
100% Ethanol	30 s
95% Ethanol	30 s
70% Ethanol	30 s
dH_2O	10 s
Cresyl violet (75% Ethanol with Diethylpyrocarbonate (DEPC) treated dH_2O, pH 8.0)	15 s
dH_2O	10 s
70% Ethanol	10 s
95% Ethanol, bath 1	10 s
95% Ethanol, bath 2	10 s
100% Ethanol, bath 1	30–60 s
100% Ethanol, bath 2	30–60 s

4.3. Laser-Capture Microdissection (LCM)

Tumour grading (Table S2) was performed by a veterinary pathologist (A.M.), according to the grading system adapted for canine simple mammary carcinoma by Clemente et al. ([60] from an existing human grading system [61]. Before microdissection, the identification of tumour stroma in samples was performed by a veterinary pathologist (A.M.). The criteria for stroma were fibroblastic cells, endothelial cells and pericytes of small vessels, only single inflammatory cells to avoid areas with heavy inflammation, and no adipocytes. We also excluded medium or large vessels to maximize the fibrous portion of the sampled stroma. The chosen stroma was morphologically different to normal stroma, being more compact and frequently sclerotic. Using the criteria of previous papers (e.g., [21,47]), we ensured that "normal" was at least 2 mm away from the neoplasm, but in practice the overlying epidermis was almost always included in the biopsy so that the normal dermis immediately beneath was sampled whenever possible (excluding adnexal structures).

For microdissection, the ArcturusXT™ Laser Capture Microdissection System (Thermo Scientific) and Arcturus® CapSure® Macro LCM Caps (Life Technologies) were used. Highly enriched populations of normal or tumour-associated stroma from the specimen were identified and isolated according to the manufacturer's protocol. Normal stroma samples were isolated from the same slides as tumour-associated stroma, from regions specified by a veterinary pathologist (A.M.) that presented no obvious alterations or were at least 2 mm away from the tumour [47]. The isolation of cells of interest was verified by microscopic examination of the LCM cap as well as the excised region after microdissection (Figure 2). After excision, the caps were put on 0.5 mL microcentrifuge tubes (Eppendorf® Safe-Lock Tubes, Hamburg, Germany) and placed on ice until proceeding with mRNA isolation.

4.4. Isolation of mRNA from FFPE Tissue Sections Isolated by LCM

Extraction of mRNA was performed immediately after microdissection within three hours after staining, due to potential RNase contamination during storage [59]. A Recover All™ Total Nucleic Acid Isolation Kit for FFPE (Ambion™) was used to extract the mRNA according to the manufacturer's protocol with the following small adjustments. As long exposure to xylene has been shown to be detrimental to mRNA integrity [62] and deparaffinisation by xylene had already been performed to stain the sections, the first deparaffinisation step using xylene and 100% ethanol was skipped, and the excised tissue was directly immersed in a 0.5 mL microcentrifuge tube containing 100 µL Digestion Buffer and 4 µL Protease. To get the tissue into the solution, a sterile blade and forceps were used to peel off the thermoplastic film on the cap containing the captured cells. The heating time and temperature in step C-2a were adjusted to 3 h at 50 °C, followed by 20 min at 70 °C, according to manufactures protocol "Optimized Extraction and Quantification of RNA from FFPE Samples for Gene Expression Analyses" (https://tools.thermofisher.com). To elute the mRNA from the column, RNase-free water was used to avoid the effects of the elution buffer on downstream applications. The eluate was aliquoted before analysis and stored at −80 °C. mRNA abundance and quality was analysed using the 4200 or 2200 Tape Station Software using the High Sensitivity RNA ScreenTape kit (Agilent Technologies, Santa Clara, CA, USA), according to the manufacturer's protocol.

4.5. cDNA Synthesis and Preamplification

To retrotranscribe mRNA into cDNA, the iScript™ cDNA Synthesis Kit by Bio-Rad was used according to the manufacturer's protocol, using a maximum of 15 µL of mRNA per reaction. This kit allows generation of cDNA with combination of oligo (dT) and random hexamer primers using low mRNA inputs and is optimized for fragments below 1 kb of length. cDNA preamplification was done using the TaqMan® PreAmp Master Mix (2×) (Applied Biosystems™) to produce sufficient cDNA for qPCR analysis. The preamplification was performed according to the manufacturer's protocol using 14 PCR cycles.

4.6. Reverse Transcription quantitative PCR

Quantitative real-time PCR (RT-qPCR) was performed using KAPA PROBE FAST qPCR Kit Master Mix (2×) Universal reagents (Kapa Biosystems, Wilmington, MA, USA), with 2.5 µL preamplified cDNA per reaction in a total volume of 10 µL. RT-qPCR reactions were run in duplicates on the CFX384 Touch™ Real-Time PCR detection system (BioRad, Hercules, CA, USA). The primers used in this study are detailed in Table 4. The comparative CT (Cycle threshold) method was applied for the quantification of gene expression, and the values were normalised against GAPDH, PPIA, and B2M as endogenous controls. The results were expressed as fold changes in mRNA levels of cancer-associated stroma over normal stroma. The primers were either customised Taqman® gene expression assays specifically designed to detect the canine isoforms of the targeted genes (ThermoFisher Scientific), used at final concentrations of 900 nM primers and 250 nM probes, or, for canine GAPDH, purchased from Microsynth (Balgach, Switzerland) and used at a final concentration of 300 nM primers and 200 nM probe [63]. All primer pairs have been validated by the manufacturer, or in the case of GAPDH by [63], and displayed at approximately 100% amplification efficiency.

Table 4. List of primers used for RT-qPCR. The "c" before each gene indicates that primers were designed to detect the canine isoforms of the intended targets.

Gene Target	Sequence	Amplicon Length (nt)	Taqman® Order Number or Reference
cGAPDH	Fw: 5′-GCTGCCAAATATGACGACATCA-3′ Rev: 5′-GTAGCCCAGGATGCCTTTGAG-3′ Probe: 5′-TCCCTCCGATGCCTGCTTCACTACCTT-3′	75	[63]
cPPIA	Manufacturer's proprietary information	92	Cf03986523_gH
cB2M	Manufacturer's proprietary information	87	Cf02659077_m1
cPDGFRB	Manufacturer's proprietary information	60	Cf02626568_g1
cMMP2	Manufacturer's proprietary information	58	Cf02623423_m1
cCOL1A1	Manufacturer's proprietary information	87	Cf02623126_m1
cFAP	Manufacturer's proprietary information	69	Cf02657429_m1
cACTA2	Manufacturer's proprietary information	86	Cf02668774_mH
cCXCL12	Manufacturer's proprietary information	86	Cf02625258_m1
cIL6	Manufacturer's proprietary information	68	Cf02624151_m1

4.7. Graphical Display of Results and Statistical Analysis

For all statistical analysis and graphical displays, the program GraphPad Prism (www.graphpad.com) was used. The data was first tested for normality using the D'Agostino and Pearson omnibus normality test and the Shapiro-Wilk normality test. If the data followed a Gaussian distribution (normally distributed data), student's *t*-test was performed to assess significance for a two-tailed *p*-value with $\alpha = 0.05$. If data did not pass the normality test (non-normally distributed data), a Wilcoxon Signed Tank Test was performed to assess the significance for a two-tailed *p*-value with $\alpha = 0.05$.

4.8. Immunohistochemistry

Formalin-fixed paraffin-embedded (FFPE) tissue sections (2 µm thickness) were mounted on positively charged slides and dried overnight at 37 °C. Drying was followed by the deparaffinisation of the slides with four xylene baths for 5 min each using the Tissue-Tek® Prisma® and Film® (Sysmex, Horgen, Switzerland). For rehydration, a degressive alcohol series using 100% ethanol, 95% ethanol, 70% ethanol, and distilled water was performed. Slides used for SDF1 immunohistochemical staining underwent an antigen-retrieval pretreatment after rehydration by putting the slides into EDTA-buffer (basic buffer pH 9.0) and then into a pressure cooker for 20 min at 98 °C, followed by rinsing with distilled water. Thereafter all the sections were put in TBS wash-buffer 3006 (Dako, Carpinteria, CA, USA). Immunohistochemical staining for FAP was performed as specified in [50]. Staining for PDGFR-β, MMP-2, SDF1, FGF-2, and Caveolin-1 was performed with the Dako Autostainer

(Agilent Technologies) using polyclonal rabbit antibodies (Table 5) overnight at 4 °C and for αSMA using monoclonal mouse antibody (Table 5) for 1h at room temperature. The antibodies were diluted in the dilution-buffer S2022 (Dako, Carpinteria, CA, USA). After incubation with the primary antibody, the slides were rinsed with TBS wash-buffer and blocked with peroxidase (peroxidase blocking buffer, Dako S2023) for 10 min at room temperature. The αSMA slides were treated with a link biotinylated secondary antibody for 15 min at room temperature and rinsed with TBS before peroxidase blocking. Next, the slides were rinsed with TBS and incubated with the EnVision™ + System HRP Rabbit Kit (Dako K4003) for 30 min at room temperature or, for αSMA, incubated with the Dako Real™ Detection Kit (Dako K5001, K5003) for 15 min at room temperature. Before removing the slides from the Autostainer, they were rinsed with TBS and incubated with DAB (diaminobenzidine) Dako K3468 (Dako, Carpinteria, CA, USA) for 10 min at room temperature. Removing the slides from the Autostainer, they were rinsed with distilled water and counterstained for 2 s in Hematoxylin (modified acc. to Gill II, Merck KGaA, Darmstadt, Germany). Finally the sections were rinsed with tap water, dehydrated in the Prisma® machine (70% ethanol, 95% ethanol, 100% ethanol and xylene), and covered with the Tissue-Tek®-Film®.

The immunohistochemical staining was scored semi-quantitatively by a board-certified veterinary pathologist (A.M.) without prior knowledge of the PCR results. Scores were based on the section as a whole, e.g. if one region composing <25% stained strongly whilst the majority remained unstained, the score was given as mild. As the aim was to identify differences between groups, comparisons were performed between groups for a given antibody rather than between antibodies. The scoring system was therefore adapted slightly to suit the staining behaviour of the antibody and allow maximum discrimination between cases. When a stain showed scant variation in staining intensity (e.g., αSMA), the slides were assessed purely numerically. Where intensity was highly variable, the two were factored together. Therefore a sample with strong staining in <25% would score moderate, and if in two cases 90% of cells stained but one weakly and the other strongly, the latter would score strong and the former moderate. Furthermore, neoplastic epithelial cells were examined for positive staining to check if the selected genes were specifically expressed in stromal cells. The staining intensity was scored in a scale from 0 to 3 (0: negative, 0.5: negligible (rare individual cells/barely perceptible staining), 1: mild (up to 25% positively staining cells), 2: moderate (25–75% positively staining cells), 3: strong (>75% positively staining cells).

Table 5. Details of the primary antibodies used for Immunohistochemistry.

Antibody	Source, Order Information	Type	Dilution	Reference
PDGFR-β	Santa Cruz Biotechnology, sc-432	Rabbit polyclonal	1:50	[64]
FAP	Abcam, ab53066	Rabbit polyclonal	1:100	[50]
MMP-2	Thermo Scientific, Ab-7, #RB-1537-P1	Rabbit polyclonal	1:100	[53]
αSMA	Dako, Clone 1A4, Code M0851	Mouse monoclonal	1:400	-
SDF1	Abcam, ab9797	Rabbit polyclonal	1:100	-
FGF-2	Santa Cruz Biotechnology, (147) sc-79	Rabbit polyclonal	1:100	[65]
Caveolin-1	Santa Cruz Biotechnology, (N-20) sc-894	Rabbit polyclonal	1:100	[55]

Supplementary Materials: Supplementary materials can be found at www.mdpi.com/1422-0067/18/5/1101/s1.

Acknowledgments: This study was financially supported by the Heuberger Stiftung, awarded to to Enni Markkanen, and the Forschungskredit of the University of Zurich, awarded to Enni Markkanen and Parisa Amini.

Author Contributions: Enni Markkanen was responsible for the study design. Julia Ettlin performed most of the experiments and was helped by Elena Clementi and Parisa Amini. Alexandra Malbon is a board-certified veterinary pathologist and supervised the choice of clinical cases, helped to implement the LCM process, supervised the use of the LCM, and provided histopathological expertise to evaluate the LCM and IHC samples. Data analysis was done by Julia Ettlin and Enni Markkanen. Enni Markkanen wrote the initial draft of the manuscript with help from Julia Ettlin, and all authors contributed to the final manuscript.

Conflicts of Interest: The authors declare no conflict of interest.

References

1. Hanahan, D.; Coussens, L.M. Accessories to the Crime: Functionsof Cells Recruited to the Tumor Microenvironment. *Cancer Cell* **2012**, *21*, 309–322. [CrossRef] [PubMed]
2. Luo, H.; Tu, G.; Liu, Z.; Liu, M. Cancer-associated fibroblasts: A multifaceted driver of breast cancer progression. *Cancer Lett.* **2015**, *361*, 155–163. [CrossRef] [PubMed]
3. Bissell, M.J.; Radisky, D. Putting tumours in context. *Nat. Rev. Cancer* **2001**, *1*, 46–54. [CrossRef] [PubMed]
4. Bissell, M.J.; Hines, W.C. Why don't we get more cancer? A proposed role of the microenvironment in restraining cancer progression. *Nat. Med.* **2011**, *17*, 320–329. [CrossRef] [PubMed]
5. Calon, A.; Espinet, E.; Palomo-Ponce, S.; Tauriello, D.V.F.; Iglesias, M.; Céspedes, M.V.; Sevillano, M.; Nadal, C.; Jung, P.; Zhang, X.; et al. Dependency of colorectal cancer on a TGF-β-driven program in stromal cells for metastasis initiation. *Cancer Cell* **2012**, *22*, 571–584. [CrossRef] [PubMed]
6. Calon, A.; Lonardo, E.; Berenguer-Llergo, A.; Espinet, E.; Hernando-Momblona, X.; Iglesias, M.; Sevillano, M.; Palomo-Ponce, S.; Tauriello, D.V.F.; Byrom, D. Stromal gene expression defines poor-prognosis subtypes in colorectal cancer. *Nat. Genet.* **2015**, *47*, 320–329. [CrossRef] [PubMed]
7. Finak, G.; Bertos, N.; Pepin, F.; Sadekova, S.; Souleimanova, M.; Zhao, H.; Chen, H.; Omeroglu, G.; Meterissian, S.; Omeroglu, A. Stromal gene expression predicts clinical outcome in breast cancer. *Nat. Med.* **2008**, *14*, 518–527. [CrossRef] [PubMed]
8. Pepin, F.; Bertos, N.; Laferriere, J.; Sadekova, S.; Souleimanova, M.; Zhao, H.; Finak, G.; Meterissian, S.; Hallett, M.T.; Park, M. Gene expression profiling of microdissected breast cancer microvasculature identifies distinct tumor vascular subtypes. *Breast Cancer Res.* **2012**, *14*, R120. [CrossRef] [PubMed]
9. Rogers, N. Canine clues: Dog genomes explored in effort to bring human cancer to heel. *Nat. Med.* **2015**, *21*, 1374–1375. [CrossRef] [PubMed]
10. Karlsson, E.K.; Lindblad-Toh, K. Leader of the pack: Gene mapping in dogs and other model organisms. *Nat. Rev. Genet.* **2008**, *9*, 713–725. [CrossRef] [PubMed]
11. Gardner, H.L.; Fenger, J.M.; London, C.A. Dogs as a Model for Cancer. *Annu. Rev. Anim. Biosci.* **2015**, *4*, 199–222. [CrossRef] [PubMed]
12. Schiffman, J.D.; Breen, M. Comparative oncology: What dogs and other species can teach us about humans with cancer. *Philos. Trans. R. Soc. Lond. B Biol. Sci.* **2015**, *370*. [CrossRef] [PubMed]
13. Liu, D.; Xiong, H.; Ellis, A.E.; Northrup, N.C.; Rodriguez, C.O.; O'Regan, R.M.; Dalton, S.; Zhao, S. Molecular homology and difference between spontaneous canine mammary cancer and human breast cancer. *Cancer Res.* **2014**, *74*, 5045–5056. [CrossRef] [PubMed]
14. Queiroga, F.L.; Raposo, T.; Carvalho, M.I.; Prada, J.; Pires, I. Canine mammary tumours as a model to study human breast cancer: Most recent findings. *In Vivo* **2011**, *25*, 455–465. [PubMed]
15. Kessler, M. *Kleintieronkologie. Diagnose und Therapie von Tumorerkrankungen bei. Hund und Katze*, 3rd ed.; Enke Verlag: Stuttgart, Germany, 2012.
16. Salas, Y.; Márquez, A.; Diaz, D.; Romero, L. Epidemiological Study of Mammary Tumors in Female Dogs Diagnosed during the Period 2002–2012: A Growing Animal Health Problem. *PLoS ONE* **2015**, *10*, e0127381. [CrossRef] [PubMed]
17. Paulsson, J.; Ehnman, M.; Ostman, A. PDGF receptors in tumor biology: Prognostic and predictive potential. *Future Oncol.* **2014**, *10*, 1695–1708. [CrossRef] [PubMed]
18. Paulsson, J.; Sjöblom, T.; Micke, P.; Pontén, F.; Landberg, G.; Heldin, C.-H.; Bergh, J.; Brennan, D.J.; Jirström, K.; Ostman, A. Prognostic significance of stromal platelet-derived growth factor beta-receptor expression in human breast cancer. *Am. J. Pathol.* **2009**, *175*, 334–341. [CrossRef] [PubMed]
19. Frings, O.; Augsten, M.; Tobin, N.P.; Carlson, J.; Paulsson, J.; Pena, C.; Olsson, E.; Veerla, S.; Bergh, J.; Ostman, A.; et al. Prognostic significance in breast cancer of a gene signature capturing stromal PDGF signaling. *Am. J. Pathol.* **2013**, *182*, 2037–2047. [CrossRef] [PubMed]
20. Allinen, M.; Beroukhim, R.; Cai, L.; Brennan, C.; Lahti-Domenici, J.; Huang, H.; Porter, D.; Hu, M.; Chin, L.; Richardson, A.; et al. Molecular characterization of the tumor microenvironment in breast cancer. *Cancer Cell* **2004**, *6*, 17–32. [CrossRef] [PubMed]
21. Ma, X.-J.; Dahiya, S.; Richardson, E.; Erlander, M.; Sgroi, D.C. Gene expression profiling of the tumor microenvironment during breast cancer progression. *Breast Cancer Res.* **2009**, *11*, R7. [CrossRef] [PubMed]

22. Bergamaschi, A.; Tagliabue, E.; Sørlie, T.; Naume, B.; Triulzi, T.; Orlandi, R.; Russnes, H.G.; Nesland, J.M.; Tammi, R.; Auvinen, P.; et al. Extracellular matrix signature identifies breast cancer subgroups with different clinical outcome. *J. Pathol.* **2008**, *214*, 357–367. [CrossRef] [PubMed]
23. Triulzi, T.; Casalini, P.; Sandri, M.; Ratti, M.; Carcangiu, M.L.; Colombo, M.P.; Balsari, A.; Ménard, S.; Orlandi, R.; Tagliabue, E. Neoplastic and stromal cells contribute to an extracellular matrix gene expression profile defining a breast cancer subtype likely to progress. *PLoS ONE* **2013**, *8*, e56761. [CrossRef] [PubMed]
24. Beck, A.H.; Espinosa, I.; Gilks, C.B.; van de Rijn, M.; West, R.B. The fibromatosis signature defines a robust stromal response in breast carcinoma. *Lab. Investig.* **2008**, *88*, 591–601. [CrossRef] [PubMed]
25. West, R.B.; Nuyten, D.S.A.; Subramanian, S.; Nielsen, T.O.; Corless, C.L.; Rubin, B.P.; Montgomery, K.; Zhu, S.; Patel, R.; Hernandez-Boussard, T.; et al. Determination of stromal signatures in breast carcinoma. *PLoS Biol.* **2005**, *3*, e187. [CrossRef] [PubMed]
26. Helleman, J.; Jansen, M.P.H.M.; Ruigrok-Ritstier, K.; van Staveren, I.L.; Look, M.P.; Meijer-van Gelder, M.E.; Sieuwerts, A.M.; Klijn, J.G.M.; Sleijfer, S.; et al. Association of an Extracellular Matrix Gene Cluster with Breast Cancer Prognosis and Endocrine Therapy Response. *Clin. Cancer Res.* **2008**, *14*, 5555–5564. [CrossRef] [PubMed]
27. Lee, J. Tumor Immunotherapy Targeting Fibroblast Activation Protein, a Product Expressed in Tumor-Associated Fibroblasts. *Cancer Res.* **2005**, *65*, 11156–11163. [CrossRef] [PubMed]
28. Park, J.E.; Lenter, M.C.; Zimmermann, R.N.; Garin-Chesa, P.; Old, L.J.; Rettig, W.J. Fibroblast activation protein, a dual specificity serine protease expressed in reactive human tumor stromal fibroblasts. *J. Biol. Chem.* **1999**, *274*, 36505–36512. [CrossRef] [PubMed]
29. Surowiak, P.; Murawa, D.; Materna, V.; Maciejczyk, A.; Pudelko, M.; Ciesla, S.; Breborowicz, J.; Murawa, P.; Zabel, M.; Dietel, M.; et al. Occurence of stromal myofibroblasts in the invasive ductal breast cancer tissue is an unfavourable prognostic factor. *Anticancer Res.* **2007**, *27*, 2917–2924. [PubMed]
30. Sappino, A.P.; Skalli, O.; Jackson, B.; Schürch, W.; Gabbiani, G. Smooth-muscle differentiation in stromal cells of malignant and non-malignant breast tissues. *Int. J. Cancer* **1988**, *41*, 707–712. [CrossRef] [PubMed]
31. Elenbaas, B.; Weinberg, R.A. Heterotypic signaling between epithelial tumor cells and fibroblasts in carcinoma formation. *Exp. Cell Res.* **2001**, *264*, 169–184. [CrossRef] [PubMed]
32. Yamashita, M.; Ogawa, T.; Zhang, X.; Hanamura, N.; Kashikura, Y.; Takamura, M.; Yoneda, M.; Shiraishi, T. Role of stromal myofibroblasts in invasive breast cancer: Stromal expression of α-smooth muscle actin correlates with worse clinical outcome. *Breast Cancer* **2012**, *19*, 170–176. [CrossRef] [PubMed]
33. Surowiak, P.; Suchocki, S.; Győrffy, B.; Gansukh, T.; Wojnar, A.; Maciejczyk, A.; Pudełko, M.; Zabel, M. Stromal myofibroblasts in breast cancer: Relations between their occurrence, tumor grade and expression of some tumour markers. *Folia Histochem. Cytobiol.* **2006**, *44*, 111–116. [PubMed]
34. Yazhou, C.; Wenlv, S.; Weidong, Z.; Licun, W. Clinicopathological significance of stromal myofibroblasts in invasive ductal carcinoma of the breast. *Tumour Biol.* **2004**, *25*, 290–295. [CrossRef] [PubMed]
35. Orimo, A.; Gupta, P.B.; Sgroi, D.C.; Arenzana-Seisdedos, F.; Delaunay, T.; Naeem, R.; Carey, V.J.; Richardson, A.L.; Weinberg, R.A. Stromal fibroblasts present in invasive human breast carcinomas promote tumor growth and angiogenesis through elevated SDF-1/CXCL12 secretion. *Cell* **2005**, *121*, 335–348. [CrossRef] [PubMed]
36. Kojima, Y.; Acar, A.; Eaton, E.N.; Mellody, K.T.; Scheel, C.; Ben-Porath, I.; Onder, T.T.; Wang, Z.C.; Richardson, A.L.; Weinberg, R.A.; et al. Autocrine TGF-β and stromal cell-derived factor-1 (SDF-1) signaling drives the evolution of tumor-promoting mammary stromal myofibroblasts. *Proc. Natl. Acad. Sci. USA* **2010**, *107*, 20009–20014. [CrossRef] [PubMed]
37. Chavey, C.; Bibeau, F.; Gourgou-Bourgade, S.; Burlinchon, S.; Boissière, F.; Laune, D.; Roques, S.; Lazennec, G. Oestrogen receptor negative breast cancers exhibit high cytokine content. *Breast Cancer Res.* **2007**, *9*, R15. [CrossRef] [PubMed]
38. Schafer, Z.T.; Brugge, J.S. IL-6 involvement in epithelial cancers. *J. Clin. Investig.* **2007**, *117*, 3660–3663. [CrossRef] [PubMed]
39. Kalluri, R.; Zeisberg, M. Fibroblasts in cancer. *Nat. Rev. Cancer* **2006**, *6*, 392–401. [CrossRef] [PubMed]
40. Witkiewicz, A.K.; Dasgupta, A.; Sotgia, F.; Mercier, I.; Pestell, R.G.; Sabel, M.; Kleer, C.G.; Brody, J.R.; Lisanti, M.P. An absence of stromal caveolin-1 expression predicts early tumor recurrence and poor clinical outcome in human breast cancers. *Am. J. Pathol.* **2009**, *174*, 2023–2034. [CrossRef] [PubMed]

41. Burgemeister, R. Nucleic acids extraction from laser microdissected FFPE tissue sections. *Methods Mol. Biol.* **2011**, *724*, 117–129. [PubMed]
42. Martinez-Outschoorn, U.E.; Sotgia, F.; Lisanti, M.P. Caveolae and signalling in cancer. *Nat. Rev. Cancer* **2015**, *15*, 225–237. [CrossRef] [PubMed]
43. Zischek, C. Das Tumorstroma als Angriffspunkt Einer Stammzellbasierten CCL5-Promoter/HSV-TK Suizidgentherapie in einem Murinen Pankreastumormodell. Ph.D. Thesis, Ludwig-Maximilians-Universität München, Munich, Germany, 2011.
44. Gandellini, P.; Andriani, F.; Merlino, G.; D'Aiuto, F.; Roz, L.; Callari, M. Complexity in the tumour microenvironment: Cancer associated fibroblast gene expression patterns identify both common and unique features of tumour-stroma crosstalk across cancer types. *Semin. Cancer Biol.* **2015**, *35*. [CrossRef] [PubMed]
45. Mihala, A.; Alexa, A.A.; Samoilă, C.; Dema, A.; Vizitiu, A.C.; Anghel, A.; Tămaş, L.; Marian, C.V.; Sîrbu, I. A pilot study on the expression of microRNAs resident on chromosome 21 in laser microdissected FFPE prostate adenocarcinoma samples. *Rom. J. Morphol. Embryol.* **2015**, *56*, 1063–1068. [PubMed]
46. Morton, M.L.; Bai, X.; Merry, C.R.; Linden, P.A.; Khalil, A.M.; Leidner, R.S.; Thompson, C.L. Identification of mRNAs and lincRNAs associated with lung cancer progression using next-generation RNA sequencing from laser micro-dissected archival FFPE tissue specimens. *Lung Cancer* **2014**, *85*, 31–39. [CrossRef] [PubMed]
47. Finak, G.; Sadekova, S.; Pepin, F.; Hallett, M.; Meterissian, S.; Halwani, F.; Khetani, K.; Souleimanova, M.; Zabolotny, B.; Omeroglu, A.; et al. Gene expression signatures of morphologically normal breast tissue identify basal-like tumors. *Breast Cancer Res.* **2006**, *8*, R58. [CrossRef] [PubMed]
48. Yoshimura, H.; Michishita, M.; Ohkusu-Tsukada, K.; Takahashi, K. Increased presence of stromal myofibroblasts and tenascin-C with malignant progression in canine mammary tumors. *Vet. Pathol.* **2011**, *48*, 313–321. [CrossRef] [PubMed]
49. Giussani, M.; Merlino, G.; Cappelletti, V.; Tagliabue, E.; Daidone, M.G. Tumor-extracellular matrix interactions: Identification of tools associated with breast cancer progression. *Semin. Cancer Biol.* **2015**, *35*, 3–10. [CrossRef] [PubMed]
50. Giuliano, A.; Santos Horta Dos, R.; Constantino-Casas, F.; Hoather, T.; Dobson, J. Expression of Fibroblast Activating Protein and Correlation with Histological Grade, Mitotic Index and Ki67 Expression in Canine Mast Cell Tumours. *J. Comp. Pathol.* **2017**, *156*, 14–20. [CrossRef] [PubMed]
51. Zhang, J.; Liu, J. Tumor stroma as targets for cancer therapy. *Pharmacol. Ther.* **2013**, *137*, 200–215. [CrossRef] [PubMed]
52. Santos, A.; Lopes, C.; Frias, C.; Amorim, I.; Vicente, C.; Gärtner, F.; Matos, A. Immunohistochemical evaluation of MMP-2 and TIMP-2 in canine mammary tumours: A survival study. *Vet. J.* **2011**, *190*, 396–402. [CrossRef] [PubMed]
53. Aresu, L.; Giantin, M.; Morello, E.; Vascellari, M.; Castagnaro, M.; Lopparelli, R.; Zancanella, V.; Granato, A.; Garbisa, S.; Aricò, A.; et al. Matrix metalloproteinases and their inhibitors in canine mammary tumors. *BMC Vet. Res.* **2011**, *7*, 33. [CrossRef] [PubMed]
54. Wang, S.-W.; Xu, K.-L.; Ruan, S.-Q.; Zhao, L.-L.; Chen, R.-L. Overexpression of caveolin-1 in cancer-associated fibroblasts predicts good outcome in breast cancer. *Breast Care* **2012**, *7*, 477–483. [PubMed]
55. Shinoda, H.; Legare, M.E.; Mason, G.L.; Berkbigler, J.L.; Afzali, M.F.; Flint, A.F.; Hanneman, W.H. Significance of ERα, HER2, and CAV1 expression and molecular subtype classification to canine mammary gland tumor. *J. Vet. Diagn. Investig.* **2014**, *26*, 390–403. [CrossRef] [PubMed]
56. Goetz, J.G.; Minguet, S.; Navarro-Lérida, I.; Lazcano, J.J.; Samaniego, R.; Calvo, E.; Tello, M.; Osteso-Ibáñez, T.; Pellinen, T.; Echarri, A.; et al. Biomechanical remodeling of the microenvironment by stromal caveolin-1 favors tumor invasion and metastasis. *Cell* **2011**, *146*, 148–163. [CrossRef] [PubMed]
57. Rowell, J.L.; McCarthy, D.O.; Alvarez, C.E. Dog models of naturally occurring cancer. *Trends Mol. Med.* **2011**, *17*, 380–388. [CrossRef] [PubMed]
58. Hester, S.D.; Bhat, V.; Chorley, B.N.; Carswell, G.; Jones, W.; Wehmas, L.C.; Wood, C.E. Editor's Highlight: Dose-Response Analysis of RNA-Seq Profiles in Archival Formalin-Fixed Paraffin-Embedded Samples. *Toxicol. Sci.* **2016**, *154*, 202–213. [CrossRef] [PubMed]
59. Espina, V.; Wulfkuhle, J.D.; Calvert, V.S.; VanMeter, A.; Zhou, W.; Coukos, G.; Geho, D.H.; Petricoin, E.F.; Liotta, L.A. Laser-capture microdissection. *Nat. Protoc.* **2006**, *1*, 586–603. [CrossRef] [PubMed]

60. Clemente, M.; Pérez-Alenza, M.D.; Illera, J.C.; Peña, L. Histological, immunohistological, and ultrastructural description of vasculogenic mimicry in canine mammary cancer. *Vet. Pathol.* **2010**, *47*, 265–274. [CrossRef] [PubMed]
61. Elston, C.W.; Ellis, I.O. Pathological prognostic factors in breast cancer. I. The value of histological grade in breast cancer: Experience from a large study with long-term follow-up. *Histopathology* **1991**, *19*, 403–410. [CrossRef] [PubMed]
62. Vincek, V.; Nassiri, M.; Knowles, J.; Nadji, M.; Morales, A.R. Preservation of Tissue RNA in Normal Saline. *Lab. Investig.* **2003**, *83*, 137–138. [CrossRef] [PubMed]
63. Kowalewski, M.P.; Kautz, E.; Högger, E.; Nadji, M.; Morales, A.R. Interplacental uterine expression of genes involved in prostaglandin synthesis during canine pregnancy and at induced prepartum luteolysis/abortion. *Reprod. Biol. Endocrinol.* **2014**, *12*, 46. [CrossRef] [PubMed]
64. Iussich, S.; Maniscalco, L.; Di Sciuva, A.; Iotti, B.; Morello, E.; Martano, M.; Gattino, F.; Buracco, P.; De Maria, R. PDGFRs expression in dogs affected by malignant oral melanomas: Correlation with prognosis. *Vet. Comp. Oncol.* 2016. [CrossRef] [PubMed]
65. Kodama, A.; Sakai, H.; Matsuura, S.; Murakami, M.; Murai, A.; Mori, T.; Maruo, K.; Kimura, T.; Masegi, T.; Yanai, T. Establishment of canine hemangiosarcoma xenograft models expressing endothelial growth factors, their receptors, and angiogenesis-associated homeobox genes. *BMC Cancer* **2009**, *9*, 363. [CrossRef] [PubMed]

6.2 Paper: “An optimised protocol for isolation of RNA from small sections of laser-capture microdissected FFPE tissue amenable for next-generation sequencing.”

BMC Molecular Biol. (2017) 18:22 doi: 10.1186/s12867-017-0099-7

In this second paper we presented a novel protocol for isolation and analysis of RNA from small sections of FFPE tissue that results in much higher RNA yields than the conventional extraction protocols and makes it possible to perform next-generation RNA sequencing. This was the first report to demonstrate that it is possible to perform RNAseq with such small samples isolated from FFPE tissue.
I contributed to this paper, of which I am shared first author, through teaching of the method to the other authors, isolation of several of the cases that were included in the study, and by demonstrating that it is feasible to do RNAseq with these samples through coordinating a collaboration with the Functional Genomics Center Zurich (FGCZ).

Amini et al. BMC Molecular Biol (2017) 18:22
DOI 10.1186/s12867-017-0099-7

BMC Molecular Biology

METHODOLOGY ARTICLE Open Access

An optimised protocol for isolation of RNA from small sections of laser-capture microdissected FFPE tissue amenable for next-generation sequencing

Parisa Amini[1†], Julia Ettlin[1†], Lennart Opitz[2], Elena Clementi[1], Alexandra Malbon[3] and Enni Markkanen[1*]

Abstract

Background: Formalin-fixed paraffin embedded (FFPE) tissue constitutes a vast treasury of samples for biomedical research. Thus far however, extraction of RNA from FFPE tissue has proved challenging due to chemical RNA–protein crosslinking and RNA fragmentation, both of which heavily impact on RNA quantity and quality for downstream analysis. With very small sample sizes, e.g. when performing Laser-capture microdissection (LCM) to isolate specific subpopulations of cells, recovery of sufficient RNA for analysis with reverse-transcription quantitative PCR (RT-qPCR) or next-generation sequencing (NGS) becomes very cumbersome and difficult.

Methods: We excised matched cancer-associated stroma (CAS) and normal stroma from clinical specimen of FFPE canine mammary tumours using LCM, and compared the commonly used protease-based RNA isolation procedure with an adapted novel technique that additionally incorporates a focused ultrasonication step.

Results: We successfully adapted a protocol that uses focused ultrasonication to isolate RNA from small amounts of deparaffinised, stained, clinical LCM samples. Using this approach, we found that total RNA yields could be increased by 8- to 12-fold compared to a commonly used protease-based extraction technique. Surprisingly, RNA extracted using this new approach was qualitatively at least equal if not superior compared to the old approach, as Cq values in RT-qPCR were on average 2.3-fold lower using the new method. Finally, we demonstrate that RNA extracted using the new method performs comparably in NGS as well.

Conclusions: We present a successful isolation protocol for extraction of RNA from difficult and limiting FFPE tissue samples that enables successful analysis of small sections of clinically relevant specimen. The possibility to study gene expression signatures in specific small sections of archival FFPE tissue, which often entail large amounts of highly relevant clinical follow-up data, unlocks a new dimension of hitherto difficult-to-analyse samples which now become amenable for investigation.

Keywords: FFPE, RNA isolation, RNAsequencing, LCM, RT-qPCR, Dog, Cancer, Mammary carcinoma, Mammary tumour

*Correspondence: enni.markkanen@vetpharm.uzh.ch
†Parisa Amini and Julia Ettlin are joint first authors
[1] Institute of Veterinary Pharmacology and Toxicology, Vetsuisse Faculty, University of Zürich, Winterthurerstr. 260, 8057 Zurich, Switzerland
Full list of author information is available at the end of the article

Introduction

Formalin-fixed paraffin-embedded (FFPE) tissue samples constitute a vast and valuable resource of patient material that can potentially be used for biomedical research. In most cases such specimen also entail large amounts of clinically relevant data, such as clinical history, further laboratory findings, follow-up data, and much more. To date however, the extraction of macromolecules in general, and RNA in particular, from FFPE tissues has proved challenging due to chemical crosslinking of RNA with proteins and RNA fragmentation, both of which heavily decrease RNA quantity that can be extracted from such tissues, and also severely impact on RNA quality for downstream analysis (e.g. [1–4]).

Laser-capture microdissection (LCM) is a technique that allows the specific isolation of defined areas, such as particular subpopulations of cells, from within a tissue section by direct microscopic visualization [5]. This approach enables researchers to precisely dissect areas of interest and thus address the role(s) of specific subsets of cells within samples of a given pathology directly derived from patients. Such an approach is particularly valuable and important as the focus of research is switching towards deciphering the cellular and molecular interactions of different contributing cell types that underlie pathologies. For instance, as data from the tumour research field convincingly demonstrates, cancerous lesions are not only made up of neoplastic tumour cells, but can be rather thought of as an 'organism' in which vast contributions to support survival and proliferation derive from the surrounding microenvironment that consists of stromal cells, immune cells, tumour vasculature, extracellular matrix and other components [6, 7]. The problem that arises when addressing small subsections of tissue sections that are excised by LCM is often one of low abundance—the sections that can be isolated are more often than not very small, thus also yielding very low amounts of material to study. If, in addition to this complication, the isolated material has a rather low cellularity, such as stroma that consists in large parts of extracellular matrix, isolation of sufficient RNA can become a really taunting challenge.

Due to all these facts, to date most LCM analyses geared towards RNA expression analysis have used fresh-frozen rather than FFPE tissue sections [1]. However, the use of fresh-frozen tissues necessitates a high grade of coordination between surgical tissue resection and the analysis pipeline, which often proves difficult, and importantly also precludes the analysis of any archival samples that might be available. Furthermore, tissue morphology of FFPE tissue is vastly superior to fresh-frozen tissue, and staining procedures for specific subpopulations of cells are often more optimal for FFPE tissue. Therefore, a method that would allow better use of FFPE tissue for RNA expression analysis has the potential to benefit a vast array of research projects that are analysing patient-derived specimen.

We have recently established a procedure to extract cancer-associated stroma (CAS) from archival canine FFPE breast cancer tissue by LCM using reverse-transcription quantitative PCR (RT-qPCR) [8]. During the establishment of this procedure, a major problem we encountered was the low overall yield of RNA that could be extracted from the tiny amounts of tissue that were isolated, which rendered the tissue sampling and analysis slow and cumbersome, if not almost impossible. To be able to tap the valuable reserve of FFPE tissue specimen for analysis by LCM efficiently, we felt that a better protocol for RNA isolation could help improving the yields of RNA that is isolated from these tissues. To this end, we set out to improve the extraction of RNA from these very small and challenging deparaffinised and stained FFPE samples with the ultimate aim of performing next-generation sequencing (NGS) RNA analysis.

Materials and methods

Case selection and tissue processing for LCM

Thirteen dog mammary carcinoma samples were obtained from the Institute of Veterinary Pathology of the Vetsuisse Faculty Zürich (Table 1). All samples were formalin-fixed, paraffin-embedded tissue samples either from the Small Animal Hospital of Zurich or external cases sent in by veterinarians practising in Switzerland. Details regarding selection criteria are described in [8]. Paraffin blocks were routinely kept at room temperature. For LCM, tissue sections were cut at 10 µm. DEPC treated water was used for the microtome HM 360 (ThermoFisher Scientific), the blade was cleaned with RNase away™ (Ambion). The tissue was mounted on PEN Membrane Glass Slides (Applied Biosystems™) and mounted tissue sections were left to dry overnight at room temperature (http://support.moleculardevices.com). To visualise the areas of interest, tissue sections were stained with Cresyl Fast Violet according to [5] with slight modifications (Table 2). To allow for proper excision performance, slides were completely air dried before microdissection. For every tissue sample that underwent LCM, a second tissue slide was stained with conventional Hematoxylin–Eosin staining to allow for validation of tissue morphology in case of uncertainty using the Cresy violet stain.

Laser-capture microdissection (LCM)

Before microdissection, identification of tumour stroma in samples was performed by a pathologist (Alexandra Malbon AM). Criteria for stroma: fibroblastic cells, endothelial cells and pericytes of small vessels, only single

Table 1 Overview of cases included in this study

Case #	Gender	Breed	Age (years)	Subtype of simple carcinoma
1	f	Basset	12	Tubular
2	f	Vizsla	10	Cystic-papillary
3	f	Samoyed	5	Tubulo-papillary
4	f	Maltese	14	Tubular
5	f	Tibetan terrier	12	Tubular
6	f/n	West highland white terrier	12	Tubular-solid
7	f	Havanese	13	Tubular
8	f	Chihuahua	8	Tubulo-papillary
9	f/n	Bracke	9	Cribriform
10	f/n	N.d.	13	Tubular
11	f/n	Appenzell mountain dog	6	Tubular
12	f	Boxer	9	Tubulo-papillary
13	f	N.d.	4	Cystic-papillary

Clinical data from dogs with simple mammary carcinoma; Case# case number as referred to within this study, f/n female, neutered, n.d not disclosed. Age age at excision of tumour

Table 2 Protocol for Cresyl violet staining of FFPE tissue sections

Cresyl violet staining procedure for FFPE tissue sections	
100% Xylene, bath 1	5 min
100% Xylene, bath 2	5 min
100% Ethanol	30 s
95% Ethanol	30 s
70% Ethanol	30 s
dH_2O	10 s
Cresyl violet (75% Ethanol with DEPC treated dH_2O, pH 8.0)	15 s
dH_2O	10 s
70% Ethanol	10 s
95% Ethanol, bath 1	10 s
95% Ethanol, bath 2	10 s
100% Ethanol, bath 1	30–60 s
100% Ethanol, bath 2	30–60 s

inflammatory cells to avoid areas with heavy inflammation, no adipocytes. For Microdissection the ArcturusXT™ Laser Capture Microdissection System (Thermo Scientific) and Arcturus® CapSure® Macro LCM Caps (Life Technologies) were used. Highly enriched populations of normal or tumour-associated stroma from the specimen were identified and isolated according to the manufacturer's protocol. Normal stroma samples were isolated from the same slides, from regions specified by a pathologist (AM) that presented no obvious alterations or at least 2 mm away from the tumour [9]. Isolation of cells of interest was verified by microscopic examination of the LCM cap as well as the excised region after microdissection (Fig. 1). After excision, the caps were put on 0.5 ml microcentrifuge tubes (Eppendorf® Safe-Lock Tubes) and placed on ice until proceeding with mRNA isolation. 1–2 caps were used per sample.

'Old' (protease-based) isolation protocol for RNA from FFPE tissue sections

Extraction of mRNA was performed immediately after microdissection using the Recover All™ Total Nucleic Acid Isolation Kit for FFPE (Ambion™) according to the manufacturer's protocol with the following small adjustments. As long exposure to xylene has been shown to be detrimental to mRNA integrity [10], and deparaffinisation by xylene had already been performed to stain the sections, the first deparaffinisation step using xylene and 100% ethanol was skipped and the excised tissue was directly immersed into a 0.5 ml microcentrifuge tube containing 100 µl Digestion Buffer and 4 µl Protease. To get the tissue into the solution a sterile blade and forceps were used to peel off the thermoplastic film from the cap containing the captured cells. The heating time and temperature in step C-2a was adjusted to 3 h at 50 °C followed by 20 min at 70 °C, according to manufactures protocol "Optimized Extraction and Quantification of RNA from FFPE Samples for Gene Expression Analyses" (https://tools.thermofisher.com). To elute the RNA from the column, RNase-free water was used to avoid the effects of elution buffer on downstream applications. The eluate was aliquoted before analysis and stored at −80 °C. RNA abundance and quality was analysed using the 4200 or 2200 Tape Station Software using the High Sensitivity RNA ScreenTape kit (Agilent Technologies), according to the manufacturer's protocol.

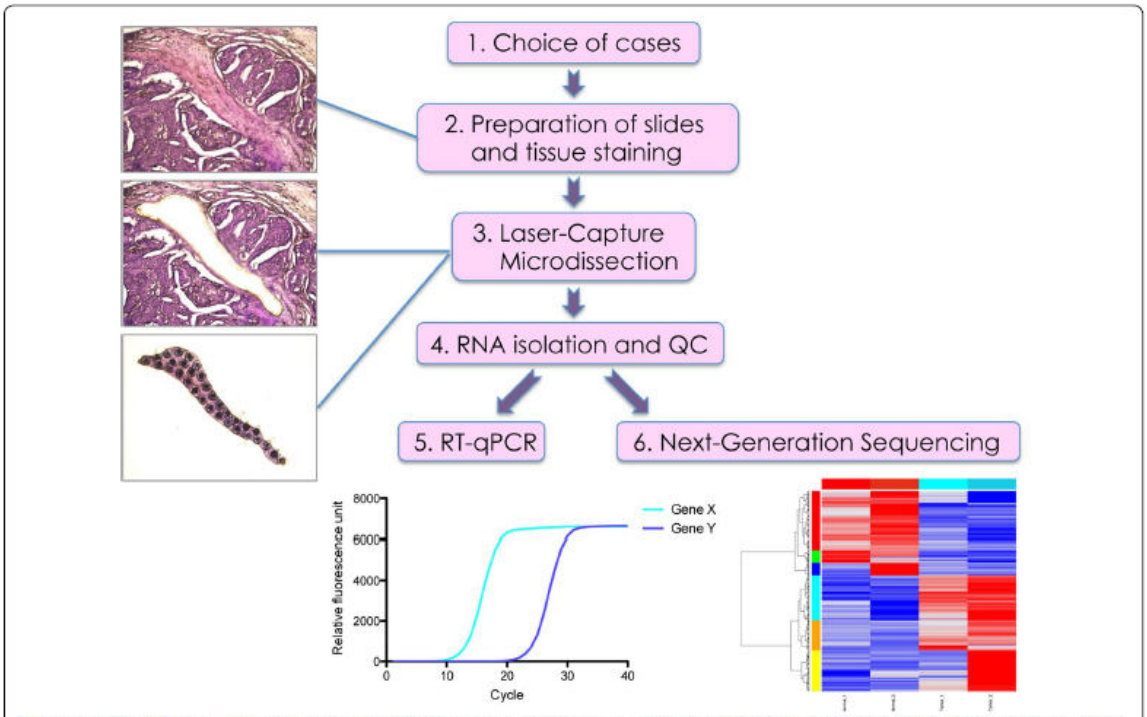

Fig. 1 Workflow for the isolation and analysis of RNA from normal and cancer-associated stroma from FFPE tissue by Laser-capture microdissection. (*1*) Canine simple mammary carcinoma cases to be analysed are chosen from the archives. (*2*) Sectioning and mounting of FFPE sections is followed by tissue deparaffinisation and staining to visualise structures under the microscope (*top panel on the left*). (*3*) Laser-capture microdissection allows excision of areas of interest, and visual validation of the excised area (*middle panel on the left*) as well as the excised tissue piece (*bottom panel on the left*). The black spots that appear on the excised tissue piece are a result of the thermoplastic film that is welded to the tissue, and not tissue damage. (*4*) RNA is isolated from the excised tissue of interest, and quality control is performed to measure RNA quality and quantity. (*5*) RT-qPCR or (*6*) NGS can be used to analyse the extracted RNA

'New' (sonication-based) isolation protocol for RNA from FFPE tissue sections

Extraction of RNA was performed immediately after microdissection using the Covaris® truXTRAC FFPE RNA kit according to the manufacturer's protocol with following adjustments. A sterile blade was used to peel off the thermoplastic film from the LCM cap and transfer the tissue isolated by LCM into glass vials for sonication. Sonication of samples was performed with the E220 focused ultrasonicator (Covaris®). After reverse crosslinking at 80 °C, the soluble fraction was transferred into clean eppendorf tubes and DNAse treated without prior centrifugation, as due to the absence of paraffin, the samples did not contain any solids that could be precipitated. RNA was eluted from the spin columns using 30 µl of elution buffer prewarmed to 70 °C to increase RNA yield. A second elution into fresh collection tubes was performed using 20–30 µl prewarmed elution buffer using the identical elution protocol. The eluate was aliquoted before analysis and stored at −80 °C. RNA abundance and quality was analysed using the 4200 or 2200 Tape Station Software using the High Sensitivity RNA ScreenTape kit (Agilent Technologies), according to the manufacturer's protocol.

cDNA Synthesis, preamplification and quantitative real-time PCR

Reverse transcription was performed using the iScript™ cDNA Synthesis Kit (BioRad) according to the manufacturer's protocol, using a maximum of 10 µl of RNA per reaction. Due to the limiting concentration extractions using the old method, RNA inputs per reaction ranged between 0.5 and 2.3 ng of total RNA per sample. This kit allows generation of cDNA with combination of oligo(dT) and random hexamer primers using low RNA inputs and is optimized for fragments below 1 kb of length. To increase the number of RT-qPCR analyses that could be performed, cDNA was preamplified using the TaqMan® PreAmp Master Mix (2×) (Applied Biosystems™). This step was necessary due to the very low concentrations of

RNA extracted using the old protocol, but can be omitted using the new protocol that yields much higher RNA amounts and concentration. For comparability reasons it was performed identically in parallel for all samples. The preamplification was performed according to the manufacturer's protocol using 14 PCR cycles. RT-qPCR was performed using KAPA PROBE FAST qPCR Kit Master Mix (2×) Universal reagents (Kapa Biosystems), with 2.5 µl cDNA per reaction, in a total volume of 10 µl. RT-qPCR were run in duplicates on the CFX384 Touch™ Real-Time PCR detection system (BioRad). Details regarding primers can be found in [8], and other details regarding the setup of the RT-qPCR can be found in [11].

Next-generation sequencing

RNA library preparation and depletion of ribosomal RNA was performed using the SMARTer Stranded Total RNA-seq Kit—Pico Input Mammalian from Clontech/Takara Bio USA according to the manufacturer's protocol with 2 ng input RNA for the 'old' extraction protocol, and 10 ng input RNA for the 'new' extraction protocol. Single-read sequencing (125 bp) was run on the Illumina HiSeq 2500 using the HiSeq SBS Kit v4 and HiSeq cluster kits v4 according to standard protocols used at the Functional Genomics Centre Zurich (FGCZ). Resulting NGS reads were quality-checked with FastQC (http://www.bioinformatics.babraham.ac.uk/projects/fastqc). Reads were trimmed with Trimmomatic [12] (v0.33, 4 bases hard-trimming from the start, and adapter trimming at the end). We aligned the trimmed reads to the reference genome and transcriptome (FASTA and GTF files, respectively, Ensembl, release88, CanFam3.1) with STAR [13] version 2.5.1b. Gene expression was quantified using the R/Bioconductor package Rsubread (version 1.24.1) [14]. To detect differentially expressed genes, we applied the count based negative binomial model implemented in the R/Bioconductor package edgeR (R version: 3.3.2, edgeR version: 3.16.5) [15], in which the normalization factor was calculated by trimmed mean of M values (TMM) method [16]. The sequence data of this study have been deposited in the European Nucleotide Archive with the primary accession code PRJEB20761.

Graphical display of results and statistical analysis

For all statistical analysis and graphical display the program GraphPad Prism (http://www.graphpad.com) was used.

Results

Workflow for the isolation of RNA from normal and cancer-associated stroma from FFPE tissue

To specifically isolate normal stroma and CAS from within a section of FFPE tissue, we had previously established a workflow for case selection, tissue preparation and staining, LCM, and isolation of RNA, which can be followed by RNA analysis by either RT-qPCR or NGS (Fig. 1) and [8]. We used the ArcturusXT™ Laser Capture Microdissection System (Thermo Scientific) to isolate matched normal and CAS from 13 clinical cases of canine simple mammary carcinoma (Table 1). Of note, to minimise differences in tissue quality and processing, normal stroma and CAS were both isolated from the identical tissue section. This allows optimal comparability of the two correlates. The areas to be isolated were defined by a board-certified veterinary pathologist (AM), and microscopic validation of tissue before and after excision, as well as the excised portion, ensured selective isolation of the tissue of interest (Fig. 1). RNA isolation, performed as specified later, was followed by control of RNA quality and quantity as described in "Materials and methods" section.

Optimization of the RNA isolation procedure

Most classically available protocols and kits for extraction of RNA from FFPE tissue depend entirely on a Proteinase K (or another equivalent protease) digestion step to lyse the tissue and liberate RNA (Fig. 2a), usually following deparaffinisation of the sample (e.g. [17–21]). Proteinase K digests proteins, which leads to unravelling of the tissue, and also removes at least a part of the proteins from protein–RNA crosslinks that are the result of formalin fixation [22]. This digestion step is usually followed by a heating step to inactivate the enzyme and further promote the reversal of protein-RNA crosslinks. The resulting mixture of macromolecules is then treated with DNAse I to remove unwanted DNA, and cleaned up using an affinity purification step, often consisting of a spin-column, or similar.

In our experiments, the major bottleneck of RNA extraction using the classical approach seemed to derive from the inefficiency of Proteinase K to completely digest the very fibrous tissue (CAS and normal stroma) that had been isolated by LCM. Despite trying marked increases in digestion time (as suggested by several available protocols, e.g. [17, 20]), we could still observe clearly macroscopically visual pieces of tissue that would not dissolve, and most likely still contained substantial amounts of RNA that remained inaccessible to our extraction efforts, contributing to low total RNA yields (Fig. 3a; Additional file 1: Table S1 and [8]).

To overcome this problem, we decided to test a novel approach for isolation of RNA from FFPE tissue, which relies on tissue disruption using focused ultrasonication prior to the proteinase K treatment step (Fig. 2b). The main problem was that this approach has been developed for use with paraffinised tissue sections exclusively, and was not supposed to work with deparaffinised and

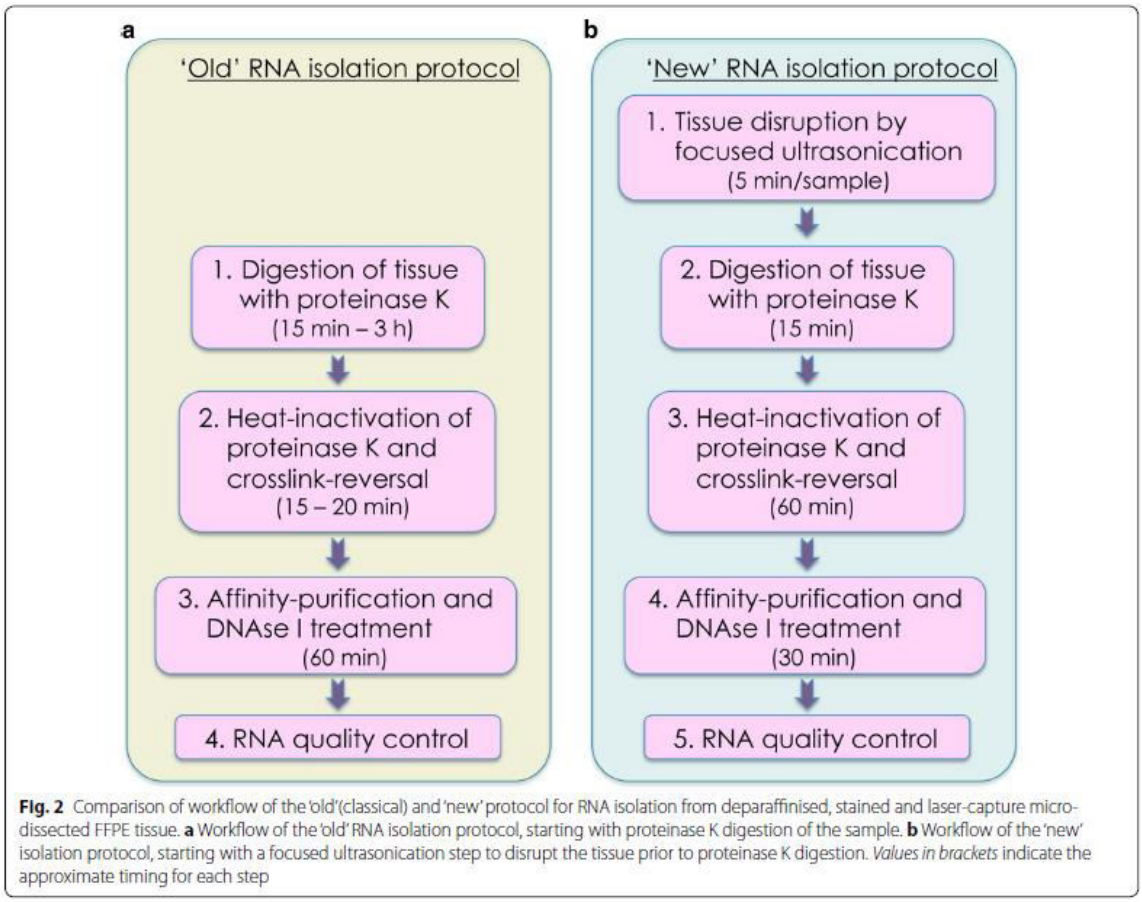

Fig. 2 Comparison of workflow of the 'old'(classical) and 'new' protocol for RNA isolation from deparaffinised, stained and laser-capture microdissected FFPE tissue. **a** Workflow of the 'old' RNA isolation protocol, starting with proteinase K digestion of the sample. **b** Workflow of the 'new' isolation protocol, starting with a focused ultrasonication step to disrupt the tissue prior to proteinase K digestion. *Values in brackets* indicate the approximate timing for each step

stained tissue. For paraffinised tissue, the ultrasonication step leads to an emulsification of the paraffin with the lysis solution, which helps removing paraffin from the sample, improves tissue rehydration, and enhances dissociation of biomolecules for improved isolation of RNA [23, 24]. However, deparaffinisation is a prerequisite for tissue staining in order to properly visualise tissue for LCM. Nevertheless, we reasoned that tissue disruption using focused sonication should still be efficient even in the absence of paraffin, and adapted the workflow of the kit slightly to suit our samples (for details see "Materials and methods"). Apart from the first tissue disruption step, this novel RNA isolation protocol is very comparable to the other available kits, also in terms of hands-on time (compare Fig. 2a, b).

Direct comparison of the old versus new FFPE RNA isolation protocol

To analyse the performance of the 'new' RNA isolation protocol, we isolated comparable amounts of normal stroma and CAS by LCM from the identical FFPE tissue blocks that had been used for our previous study, in which RNA had been isolated by the conventional 'old' method ([8] and Table 2). In order to keep the conditions as comparable as possible, we kept slide handling identical, and we sought to isolate similar surface areas visually and by using the same number of LCM caps (1–2 caps per sample) while also maintaining a similar timing for the entire process.

Comparing the results from both extraction methods, we observed a vast increase in RNA yield that could be isolated from the LCM specimen using the new isolation method (Fig. 3a; Additional file 1: Table S1). On average, the yield of RNA from normal stroma increased by fourfold from 10.18 ng (range 2.9–34 ng, Std. deviation 8.8 ng) using the old protocol to 40.42 ng (range 9.7–143.6 ng, Std. deviation 36.4 ng) using the new protocol, while the RNA yield from CAS increased by 7.4-fold from 9.57 ng (range 1.7–31 ng, Std. deviation 7.6 ng) with the old protocol to 70.95 ng (range 14.6–194 ng, Std.

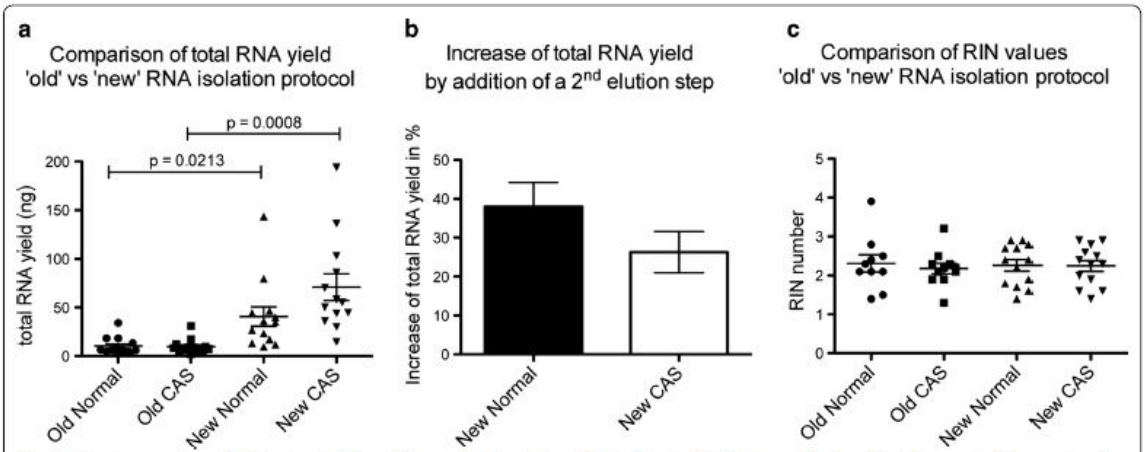

Fig. 3 Direct comparison of RNA extracted from LCM samples from deparaffinised, stained FFPE tissue with the old vs the new isolation protocol. **a** Scatter plot with mean ± SEM of total RNA yield from the 13 clinical cases analysed obtained using the old vs the new isolation protocol. Old normal shows data obtained from using the old protocol on LCM samples of normal stroma, while old CAS shows data for the old protocol on CAS. New normal and new CAS are the equivalent for the new extraction procedure, respectively. p-values were calculated using the Student's t test. **b** Bar graph displaying mean ± SEM of the increase of total RNA yield that could be achieved using a 2nd elution step with the new isolation protocol for normal and CAS samples, respectively, compared to a single elution step only. n = 8 for both types of tissue, respectively. **c** Scatter plot with mean ± SEM of the RIN values obtained from all 13 clinical cases isolated using the old or the new isolation procedure, respectively. RIN values could not be calculated for 3 samples of old normal and 2 samples of old CAS, and are thus omitted from this graph

deviation 49.1 ng) using the new protocol. These numbers are however still underestimating the total increase of RNA yield that can be achieved using the new method, as we discovered in the course of the experiments that the addition of a second elution step yielded an additional 32.2% of RNA on average using the new protocol (38.0% (range 15.8–63.3%, Std. deviation 17.6%) more RNA from the normal stroma, and 26.3% (range 10.2–53.5%, Std. deviation 14.9%) more RNA from CAS) (Fig. 3b). In the four specimen included in this study where a 2nd elution step was performed, the average yield increased by 8.2-fold in the normal stroma (from 8.0 ng (range 3.3–18.2 ng, Std. deviation 6.9 ng) with the old protocol to 65.4 ng (range 17–143.6 ng, Std. deviation 59.4 ng) using the new protocol), and by 12.8-fold in the tumour stroma (from 8.2 ng (range 3.1–12.4 ng, Std. deviation 3.9 ng) with the old protocol to 104.6 ng (range 43.9–194 ng, Std. deviation 73.7 ng) using the new protocol). RNA integrity (RIN) values did not differ significantly between the extraction procedures (Fig. 3c; Additional file 1: Table S1).

Comparison of the performance of the isolated RNA using RT-qPCR

To compare the performance of RNA extracted using the two methods by RT-qPCR, we randomly picked several of our samples, reverse transcribed identical amounts of RNA extracted using both methods into cDNA in parallel, and analysed expression of the two housekeeping genes GAPDH and B2M by RT-qPCR. RNA isolated using the new method performed in general better yielding lower mean Cq values in RT-qPCR than RNA deriving from the old isolation procedure (Table 3). On average, RNA from the new isolation procedure yielded lower mean Cq values by 2.06 cycles for GAPDH primers, and by 2.59 cycles for B2M primers compared to the mean Cq values using RNA from the old isolation protocol.

Comparison of the performance of the isolated RNA using Next-Generation RNA Sequencing

To compare the performance of the extracted RNA from both protocols using RNAseq, we checked the overall mapping rate for all generated reads. We observed that, regardless of the isolation protocol used, 49.45–79.51% of the reads were mappable to the dog genome (Fig. 4a). There was no systematic difference between both protocols ($p = 0.5936$). Furthermore, we investigated how many mapped reads were informative in respect to exonic regions of the genome. The fraction of reads mapping to exonic regions was between 14 and 17.07% (Fig. 4b). On average, 1.55% more reads using the new protocol were assigned to exonic regions ($p = 0.0323$). Finally, the gene body coverage was checked to determine biases at 3′- or 5′-end of expressed genes (FPKM > 10). The coverage profiles were very flat for all libraries, indicating even

Table 3 Comparison of Cq values obtained using RNA isolated with the old vs. the new protocol

Primer	Sample	Mean Cq old	Mean Cq new	Δ Mean Cq new – mean Cq old
GAPDH	#2 Normal	26.99	26.56	−0.43
	#2 Tumour	24.89	24.61	−0.29
	#3 Tumour	22.24	17.75	−4.49
	#4 Tumour	22.99	19.23	−3.75
	#5 Normal	26.74	24.40	−2.34
	#6 Tumour	20.97	20.98	0.00
	#7 Tumour	23.57	19.79	−3.78
	#8 Normal	23.72	23.28	−0.44
	#9 Normal	27.36	27.77	0.41
	#9 Tumour	24.82	19.33	−5.49
	#10 Normal	27.29	26.89	−0.40
	#10 Tumour	N.d.	25.68	n.a.
	Mean ΔCq New—Cq Old for GAPDH			−2.06
B2M	#2 Normal	25.83	24.62	−1.21
	#2 Tumour	21.88	21.27	−0.61
	#3 Tumour	22.76	17.48	−5.28
	#4 Tumour	22.70	18.83	−3.87
	#5 Normal	24.33	21.38	−2.95
	#6 Tumour	21.32	21.07	−0.25
	#7 Tumour	23.89	18.87	−5.02
	#8 Normal	24.13	24.46	0.33
	#9 Normal	27.63	26.14	−1.49
	#9 Tumour	25.94	21.36	−4.58
	#10 Normal	28.98	26.73	−2.25
	#10 Tumour	27.92	24.16	−3.76
	Mean ΔCq New—ΔCq Old for B2M			−2.59

Identical amounts of RNA were reverse transcribed and analysed by RT-qPCR using GAPDH or B2 M primers. First column: primers that were used for the analysis. Second column indicates the case and type of tissue from which the RNA that was analysed derived. "Mean Cq Old" denotes the mean Cq values obtained with RNA isolated using the old extraction protocol. "Mean Cq New" shows the Cq values obtained with RNA isolated using the new extraction protocol. "Δ Mean Cq New-mean Cq old" shows the difference in Cq values between the new extraction protocol and the old extraction protocol; a negative value here indicates better performance (lower Cq values) of the new extraction protocol. "Mean Δ Cq New-Cq old values" for GAPDH and B2 M list the mean difference of the Cq values between new and old extraction across all samples. N.d not detectable, n.a not applicable.

gene body coverage (Fig. 4c). Nevertheless we observed a small bias at the 3′-end in the libraries of the old protocol. In conclusion, RNA extracted using the new focused ultrasonication based method yields RNA that performs comparably to the old protease-based extraction techniques in NGS applications.

Concluding, the vastly increased yield combined by its compatibility with qPCR and NGS makes the new extraction method a preferential choice for extraction of RNA from limiting amounts of FFPE clinical specimen.

Discussion

FFPE tissue archives constitute a vast treasury of valuable samples for biomedical research. Thus far however, the extraction of RNA from FFPE tissues has proved challenging due to chemical crosslinking of RNA with proteins as well as RNA fragmentation, both of which heavily impact on RNA quantity and quality for downstream analysis. When, additionally to these difficulties, sample size become very small, e.g. due to the need to use LCM to isolate specific subpopulations of cells, it has been very difficult to recover enough RNA that is amenable for proper analysis using RT-qPCR or NGS.

Encountering this problem, we found that commonly used RNA isolation protocols were mostly inefficient due to insufficient initial steps of tissue disruption using proteinase K, which most of the time left behind still macroscopically visible pieces of tissue. To overcome this bottleneck, we successfully adapted an isolation protocol for paraffinised FFPE samples that uses focused ultrasonication for efficient tissue disruption to our deparaffinised, stained and laser-capture-microdissected samples.

Using this approach, we could show that total RNA yields could be increased 8–12-fold compared to the commonly used proteinase K-based tissue disruption techniques (Fig. 3). More importantly, RNA extracted

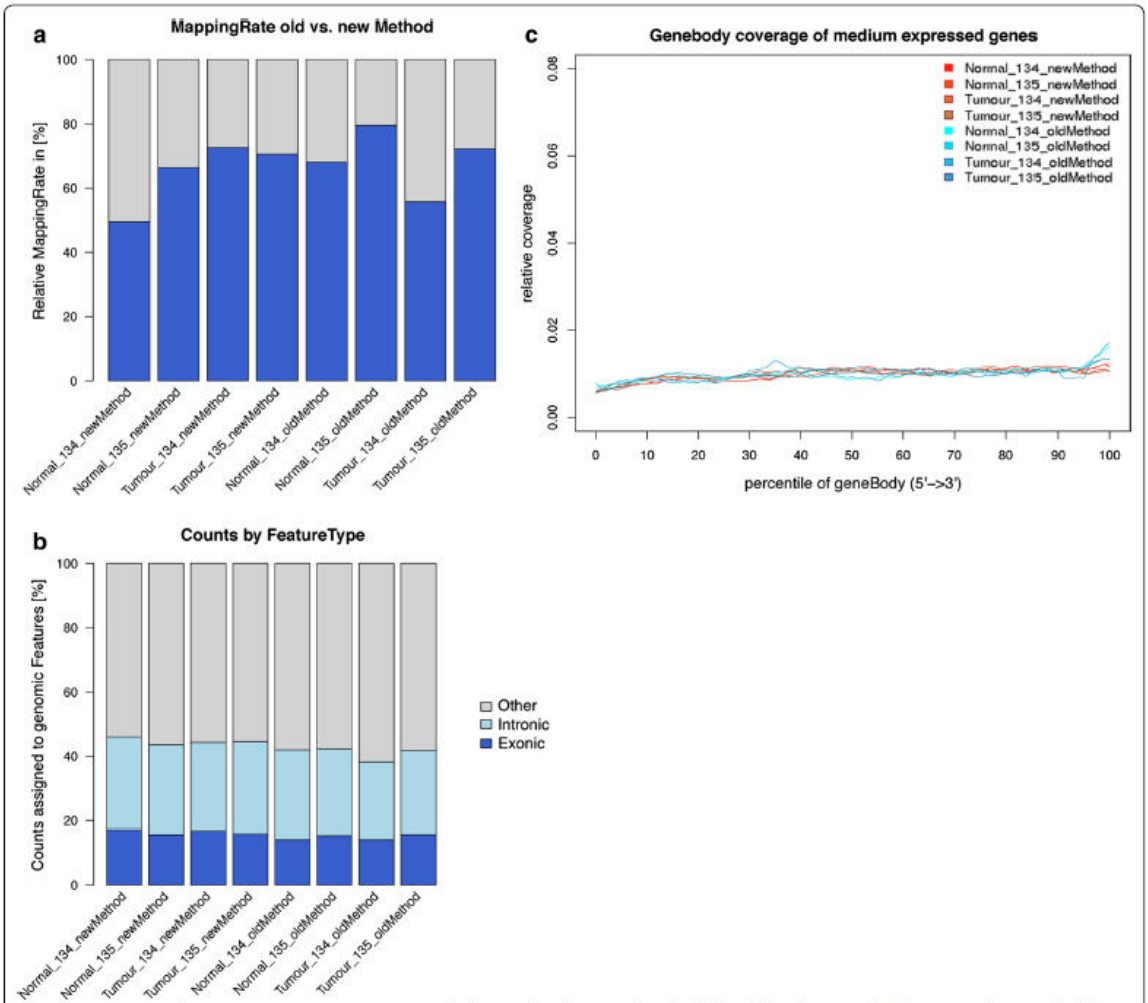

Fig. 4 Comparison of Next-Generation Sequencing results obtained with RNA isolated with the old and new method, respectively. **a** Barplot illustrating the relative amount of mapped (*blue*) vs. unmapped (*grey*) reads using the new protocol (*left*) or the old protocol (*right*). **b** Barplot showing fractions of mapped reads specific for exonic (*blue*), intronic (*light blue*) and other genomic (*grey*) regions. **c** Linegraph illustrating the calculated read-coverage over the genebody for expressed genes of medium length (400–1000 nt). Results for samples extracted by the new protocol are highlighted in *red* colors

with this new approach proved to be qualitatively at least equal if not superior to RNA extracted using the old approach, as RT-qPCR Ct values were on average 2.3-fold lower using the new method (Fig. 3b). This was surprising, as the RIN values did not differ significantly between the old and the new extraction method (Fig. 3c). As the most important determinants for RNA integrity in FFPE samples seem to be the fixation and storage steps, and can not be greatly influenced by the method of extraction [2], we hypothesize that the reason for this better performance is possibly lower amounts of protein-RNA crosslinks present when using the new method. This could be caused by better sample accessibility for proteinase K, which would explain a better 'usability' of RNA for cDNA generation. Finally, we demonstrate that the RNA extracted using the new method performs well in NGS and is thus amenable for analysis using this technique (Fig. 4).

Conclusions

Using this optimised RNA extraction protocol, analysis of limiting samples derived from LCM extracted deparaffinised and stained FFPE tissue samples becomes technically feasible. We thus envisage that the application of this

protocol can have a tremendous positive impact on the feasibility of RNA expression studies on archival patient-derived samples. The possibility to study gene expression signatures in specific sections of archival FFPE tissue, which often entail large amounts of highly relevant clinical follow-up data, unlocks a new dimension of hitherto difficult-to-analyse samples which now become amenable for investigation. Importantly, this approach is perfectly translatable to human tissue specimen and different pathologies, and we hope to enable a variety of studies to come to a successful completion using our RNA extraction and NGS-protocols.

Accession numbers

The sequence data of this study have deposited in the European Nucleotide Archive with the primary Accession Code PRJEB20761.

Additional file

Additional file 1: Table S1. Total extracted RNA amounts and RIN values for all samples. Table listing the total extracted RNA amounts and RIN values for all samples included in the study. N.d. = not detectable.

Abbreviations

FFPE: formalin-fixed paraffin embedded; LCM: Laser-capture microdissection; RT-qPCR: reverse-transcription quantitative PCR; CAS: cancer-associated stroma; NGS: next-generation RNA sequencing; DEPC: diethyl pyrocarbonate; PEN: polyethylene naphtalate.

Authors' contributions

EM was responsible for the study design. JE performed setup and isolation of all samples using the 'old' isolation protocol. PA and EM isolated all samples using the 'new' isolation protocol. JE and EM analysed samples by RT-qPCR and prepared samples for NGS. AM is a board-certified veterinary pathologist and supervised the choice of clinical cases, helped to implement the LCM process, supervised the use of and sampling by the LCM. Data quality assessment and analysis was done by EM. LO performed data analysis of the RNA sequencing. EM wrote the initial draft of the manuscript. All authors read and approved the final manuscript.

Author details

[1] Institute of Veterinary Pharmacology and Toxicology, Vetsuisse Faculty, University of Zürich, Winterthurerstr. 260, 8057 Zurich, Switzerland. [2] Functional Genomics Center Zurich, University of Zürich/ETH Zürich, Winterthurerstr. 190, 8057 Zurich, Switzerland. [3] Institute of Veterinary Pathology, Vetsuisse Faculty, University of Zürich, Winterthurerstr. 268, 8057 Zurich, Switzerland.

Acknowledgements

The authors thank Dr. Jelena Kühn-Georgijevic (Functional Genomics Center Zurich, University of Zurich, Winterthurerstr. 190, 8057 Zürich, Switzerland) for expertise regarding Next-Generation sequencing.

Competing interests

The authors declare that they have no competing interests.

Availability of data and materials

The sequence data of this study have been deposited in the European Nucleotide Archive with the primary accession code PRJEB20761. All other data supporting our findings is contained in the manuscript and in Additional file 1: Table S1.

Consent for publication

Not applicable.

Ethics approval and consent to participate

No animals were killed for the purpose of this research project, as the tissue analysed was surgically removed in a curative setting with the verbal consent of the patient owners. According to the Swiss Animal Welfare Law Art. 3 c, Abs. 4 the preparation of tissues in the context of agricultural production, diagnostic or curative operations on the animal or for determining the health status of animal populations is not considered an animal experiment and, thus, does not require an animal experimentation license. The use of FFPE material from canine patients which was obtained for diagnostic reasons therefore does not require a formal ethics approval and complies with national guidelines. These same samples have already been used before in [8].

Funding

This study was financially supported by the Heuberger Stiftung to EM and the Forschungskredit of the University of Zurich to EM/PA.

Publisher's Note

Received: 13 July 2017 Accepted: 17 August 2017
Published online: 23 August 2017

References

1. Liu H, McDowell TL, Hanson NE, Tang X, Fujimoto J, Rodriguez-Canales J. Laser capture microdissection for the investigative pathologist. Vet Pathol. 2014;51:257–69.
2. von Ahlfen S, Missel A, Bendrat K, Schlumpberger M. Determinants of RNA quality from FFPE samples. PLoS ONE. 2007;2:e1261.
3. Legres LG, Janin A, Masselon C, Bertheau P. Beyond laser microdissection technology: follow the yellow brick road for cancer research. Am J Cancer Res. 2014;4:1–28.
4. Erickson HS, Albert PS, Gillespie JW, Rodriguez-Canales J, Marston Linehan W, Pinto PA, Chuaqui RF, Emmert-Buck MR. Quantitative RT-PCR gene expression analysis of laser microdissected tissue samples. Nat Protoc. 2009;4:902–22.
5. Espina V, Wulfkuhle JD, Calvert VS, VanMeter A, Zhou W, Coukos G, Geho DH, Petricoin EF, Liotta LA. Laser-capture microdissection. Nat Protoc. 2006;1:586–603.
6. Hanahan D, Coussens LM. Accessories to the crime: functions of cells recruited to the tumor microenvironment. cancer cell. 2012;21:309–22.
7. Bissell MJ, Hines WC. Why don't we get more cancer? A proposed role of the microenvironment in restraining cancer progression. Nat Med. 2011;17:320–9.
8. Ettlin J, Clementi E, Amini P, Malbon A, Markkanen E. Analysis of gene expression signatures in cancer-associated stroma from canine mammary tumours reveals molecular homology to human breast carcinomas. Int J Mol Sci. 2017;18(5):1–19.
9. Finak G, Sadekova S, Pepin F, Hallett M, Meterissian S, Halwani F, Khetani K, Souleimanova M, Zabolotny B, Omeroglu A, Park M. Gene expression signatures of morphologically normal breast tissue identify basal-like tumors. Breast Cancer Res. 2006;8:R58.
10. Vincek V, Nassiri M, Knowles J, Nadji M, Morales AR. Preservation of tissue RNA in normal saline. Lab Invest. 2003;83:137–8.
11. Ettlin J. Analysis of gene expression signatures in cancer-associated stroma from canine mammary tumours. Thesis, Vetsuisse Faculty, University of Zurich; 2017
12. Bolger AM, Lohse M, Usadel B. Trimmomatic: a flexible trimmer for Illumina sequence data. Bioinformatics. 2014;30:2114–20.
13. Dobin A, Davis CA, Schlesinger F, Drenkow J, Zaleski C, Jha S, Batut P, Chaisson M, Gingeras TR. STAR: ultrafast universal RNA-seq aligner. Bioinformatics. 2013;29:15–21.
14. Liao Y, Smyth GK, Shi W. The subread aligner: fast, accurate and scalable read mapping by seed-and-vote. Nucleic Acids Res. 2013;41:e108.

15. Robinson MD, McCarthy DJ, Smyth GK. edgeR: a bioconductor package for differential expression analysis of digital gene expression data. Bioinformatics. 2010;26:139–40.
16. Robinson MD, Oshlack A. A scaling normalization method for differential expression analysis of RNA-seq data. Genome Biol. 2010;11:R25.
17. Bonin S, Hlubek F, Benhattar J, Denkert C, Dietel M, Fernandez PL, Höfler G, Kothmaier H, Kruslin B, Mazzanti CM, Perren A, Popper H, Scarpa A, Soares P, Stanta G, Groenen PJTA. Multicentre validation study of nucleic acids extraction from FFPE tissues. Virchows Arch. 2010;457:309–17.
18. Sengüven B, Baris E, Oygur T, Berktas M. Comparison of methods for the extraction of DNA from formalin-fixed, paraffin-embedded archival tissues. Int J Med Sci. 2014;11:494–9.
19. Neasy R. FFPE Handbook—QIAGEN . https://www.qiagen.com/us/resources/resourcedetail?id=7b8ed707-c2d6-4b9e-a1ba-8893935622f9&lang=en. Accessed 23 May 2017.
20. Recover all total nucleic acid isolation kit. https://tools.thermofisher.com/content/sfs/manuals/cms_056616.pdf. Accessed 23 May 2017.
21. High pure FFPET RNA isolation kit. https://shop.roche.com/shop/products/high-pure-ffpet-rna-isolation-kit. Accessed 23 May 2017.
22. König J, Zarnack K, Luscombe NM, Ule J. Protein-RNA interactions: new genomic technologies and perspectives. Nat Rev Genet. 2012;13:77–83.
23. truXTRAC FFPE DNA and RNA kits. http://covarisinc.com/products/ffpe-extraction/truxtrac-ffpe-dna-and-rna-kits/. Accessed 23 May 2017.
24. Deparaffinization-Procedure for FFPE nucleic acid extraction with the Bioruptor. https://www.diagenode.com/protocols/bioruptor-deparaffinization-protocol. Accessed 23 May 2017.

6.3 Unpublished results: Comparing CAS from metastatic and non-metastatic canine mammary carcinomas

The main aim of this third project was to investigate, whether CAS from metastatic canine mammary carcinomas differs from that of non-metastatic ones, and if so, identify what these differences are.

6.3.1 Selection of clinical cases and description of tissue sample characteristics

Applying the criteria for case selection described in the Materials and Methods chapter, a total of 31 cases could be included in our analysis. 15 dogs (case no. 1-15) showed metastases in the lymph node at the time of tumour excision, whereas in 16 dogs (case no. 16-31) no metastases could be found by microscopic examination. All 31 samples derived from female dogs, of which 22 were purebreds, 8 were crossbreeds and for one dog the breed was not disclosed (Table 2). The age at sample collection ranged from 5 to 17 years with a mean age of 11 years. The age of tissue blocks included in this study ranged from 7 months to over 120 months, as experience in the lab has shown that the age of the block does not significantly impair its use for analysis. Cases No. 8, 9, 10, 11, 17, 18, 21, 24, 25 and 27 were kindly provided by Prof. R. Klopfleisch (Freie Universität Berlin). For these cases, we used the information provided by Prof. Klopfleisch, and no further specification of the simple carcinoma subtype was performed. Additionally, no information regarding the neutering status or the exact age of samples (at least 120 months) was available for these cases. A detailed tabulation of sample characteristics can be found in Table 2 and further information on the samples from Berlin can be found in [61].

6.3.2 mRNA isolation from normal and tumour stroma for next-generation RNA sequencing

To specifically analyse the stromal compartment of canine simple mammary carcinomas, LCM was used to specifically isolate CAS and matched normal stroma from each case listed in Table 2. The stroma enriched areas were defined by a veterinary pathologist before starting LCM to ensure the correct isolation of stromal cells. Further, validation was conducted by taking pictures of the area of interest before and after microdissection, which included the inspection of the excised tissue on the cap (for examples, see Figure 2).
To analyse the extracted tissue by next-generation RNA sequencing, mRNA was isolated according to our previously published protocol [77]. The total mRNA yield of the first elution (E1) ranged from 23.7 ng to 654 ng and the mRNA quality of E1, determined by the RNA integrity number (RIN), varied between 1 and 4 with a mean value of 2 (Table 3), as expected [77]. As these values were well within the range amenable to RNAseq [77], CAS and normal stroma from all 31 cases were submitted for RNAseq analysis.

Table 2: *Overview of cases included in this study. Clinical data from dogs with simple mammary carcinoma; Case # = case number as referred to within this study; Case-ID = case identification number; f/n = female, neutered; n.d. = not disclosed; age = age at excision of tumour; age of sample = time between initial tumour excision and sampling of stroma/RNA extraction. > 120 denotes samples from Berlin which are at least 120 months old, but for which no exact age could be defined.*

Case #	**Case-ID**	**Gender**	**Breed**	**Age (years)**	**Subtype of simple carcinoma** *not specified for samples from Berlin	**Metastases in lymph node**	**Histologic Grade**	**Age of sample (months)**
1	H11-0640-3 (M2)	f	Volpino Italiano	11	solid	+	Grade III	85
2	H12-0226-3/4 (M3)	f	Labrador Retriever	13	comedocarcinoma	+	Grade III	75
3	H12-2699-4 (M4)	f	Cocker Spaniel	11	solid	+	Grade III	67
4	H13-1198-1/3 (M5)	f	n.d.	11	solid	+	Grade III	60
5	H10-0986-2 (M6)	f	Irish Setter	10	tubulopapillary	+	Grade II	97
6	H16-0106-1/2 (M7)	f/n	Crossbreed	14	solid	+	Grade III	28
7	H14-1216-1/4 (M8)	f	Papillon	17	solid	+	Grade III	48
8	V822/07AF (M10)	f/n.d.	American Pitbull	9	*simple carcinoma	+	Grade III	> 120
9	V833/07BRK (M11)	f/n.d.	Rottweiler	10	*simple carcinoma	+	Grade III	> 120
10	2243/07CRK (M12)	f/n.d.	Bavarian Mountain Hound	13	*simple carcinoma	+	Grade III	> 120
11	1232/08RKC (M13)	f/n.d.	West Highland White Terrier	16	*simple carcinoma	+	Grade II	> 120
12	H13-1669-2 (M14)	f	American Staffordshire Terrier	12	tubular	+	Grade II	59
13	H11-2840-1 (M15)	f	Border Collie-Mix	14	tubulopapillary	+	Grade II	80
14	H16-1705-2/4 (M31)	f	Vizsla	11	micropapillary	+	Grade II	25
15	H15-0838-1 (M32)	f	Poodle-Mix	14	comedocarcinoma	+	Grade II	40
16	H17-0434-1 (M9)	f	Golden Retriever	9	tubular-solid	-	Grade I	15
17	V830/07BRK (M16)	f/n.d.	Cocker Spaniel-Mix	12	*simple carcinoma	-	Grade III	> 120
18	2047/07ARK (M17)	f/n.d.	Labrador Retriever	11	*simple carcinoma	-	Grade III	> 120
19	H11-0316-4 (M18)	f	Old English Sheepdog	11	tubular	-	Grade I	88
20	H17-1914-2 (M19)	f	Miniature Pinscher	13	tubular	-	Grade I	9
21	1937/07ARK (M20)	f/n.d.	Dalmatian	10	*simple carcinoma	-	Grade II	> 120
22	H17-2696-1 (M21)	f/n	Brittany	9	solid	-	Grade II	7
23	H17-2039-1 (M22)	f/n	Border Collie-Mix	10	tubular	-	Grade II	9
24	279/08RKA (M23)	f/n.d.	German Shepherd-Mix	13	*simple carcinoma	-	Grade III	> 120
25	264/08RKA (M24)	f/n.d.	German Shepherd-Mix	9	*simple carcinoma	-	Grade III	> 120
26	H11-0455-1 (M25)	f	Havanese	9	solid	-	Grade II	89
27	2194/07CRK (M26)	f/n.d.	Crossbreed	11	*simple carcinoma	-	Grade III	> 120
28	H16-2622-3 (M27)	f	French Bulldog	5	tubular	-	Grade I	21
29	H14-2512-2 (M28)	f	Staffordshire Bull Terrier	n.d	tubular	-	Grade I	45
30	H14-2537-1/2 (M29)	f	Jack Russell Terrier	9	cystic-papillary	-	Grade I	45
31	H16-2188-2 (M30)	f	Podenco	9	comedocarcinoma	-	Grade I	23

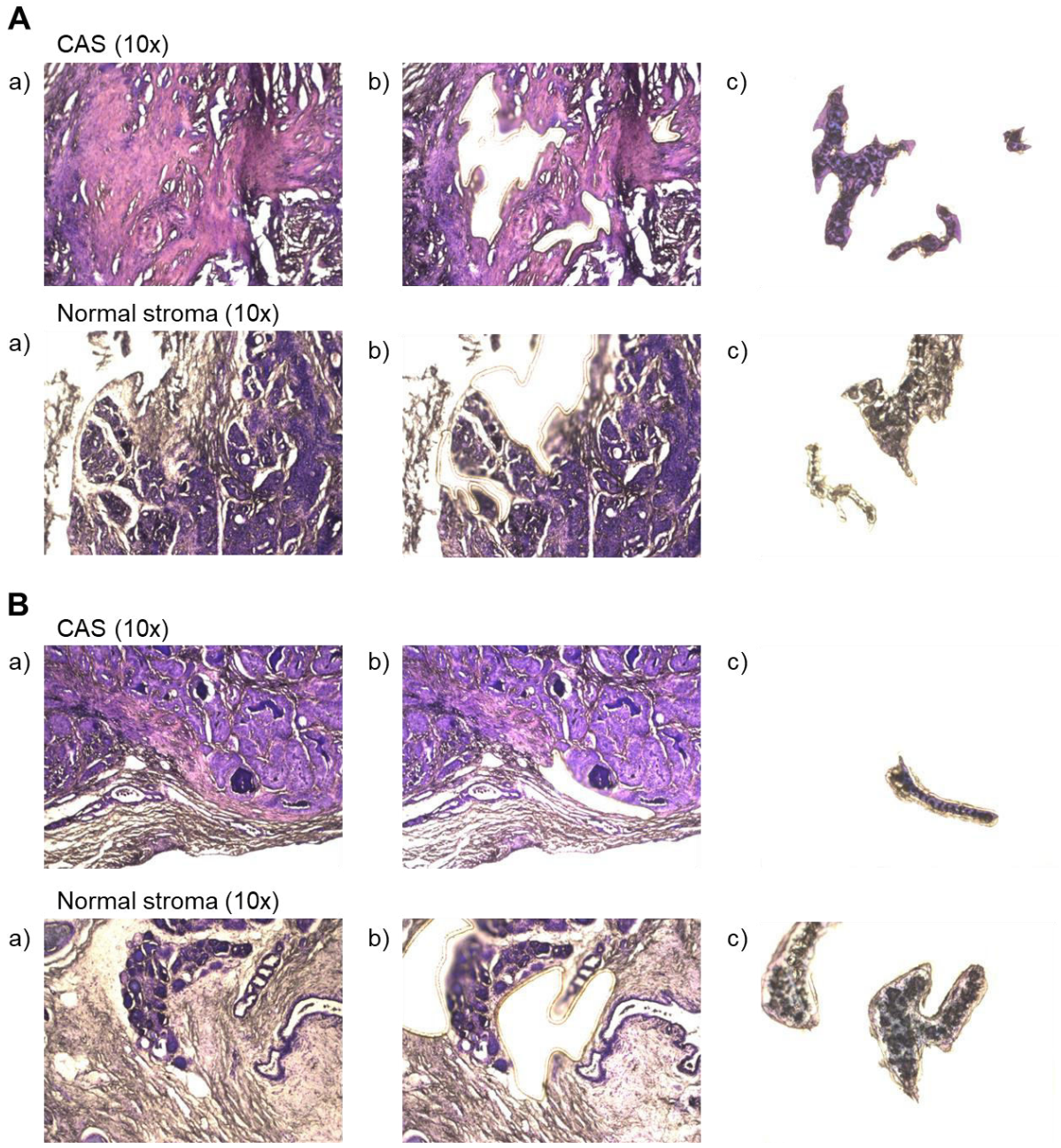

Figure 2: *Excision of CAS and normal stroma by LCM. To validate proper isolation of stromal cells, pictures of the specimen were taken at x10 magnification a) before dissection, b) after dissection, and c) of the cap. Case-IDs:* ***A:*** *H11-2840-1 (Case 13), metastatic;* ***B:*** *H11-0316-4 (Case 19), non-metastatic.*

Table 3: *Overview of RNA yields and RIN values of samples included in this study. RIN values and total yield of RNA in elution 1 (E1) are tabulated according to case# and type of tissue (normal stroma vs. CAS) in metastatic (left) versus non-metastatic (right) cases.*

metastatic cases				non-metastatic cases			
	Case #	RIN of E1	Total mRNA yield of E1 (ng)		Case #	RIN of E1	Total mRNA yield of E1 (ng)
1	Normal stroma	3.3	103.5	16	Normal stroma	2.4	198.9
	CAS	3.0	188.7		CAS	3.4	60.3
2	Normal stroma	3.3	654	17	Normal stroma	2.8	147.3
	CAS	3.1	126.3		CAS	1.1	244.8
3	Normal stroma	2.4	30.6	18	Normal stroma	2.8	52.5
	CAS	2.7	49.2		CAS	3.0	109.8
4	Normal stroma	1.0	74.1	19	Normal stroma	3.0	56.4
	CAS	3.0	82.8		CAS	3.8	103.5
5	Normal stroma	3.2	48.6	20	Normal stroma	3.3	43.5
	CAS	3.6	61.5		CAS	3.5	63.9
6	Normal stroma	2.9	183.3	21	Normal stroma	2.8	110.1
	CAS	2.8	141.6		CAS	3.1	111.9
7	Normal stroma	2.8	177	22	Normal stroma	3.3	35.4
	CAS	1.0	124.5		CAS	3.7	39.3
8	Normal stroma	1.1	120	23	Normal stroma	2.6	83.7
	CAS	2.5	118.2		CAS	3.1	62.4
9	Normal stroma	1.6	351	24	Normal stroma	2.4	135.9
	CAS	1.0	220.8		CAS	2.9	81.3
10	Normal stroma	2.3	128.7	25	Normal stroma	2.9	62.1
	CAS	3.9	67.8		CAS	3.8	48
11	Normal stroma	3.4	165	26	Normal stroma	3.4	51.6
	CAS	2.8	81.3		CAS	2.4	202.5
12	Normal stroma	3.5	71.1	27	Normal stroma	3.1	51.6
	CAS	1.0	114		CAS	2.8	59.1
13	Normal stroma	3.1	101.7	28	Normal stroma	3.3	31.5
	CAS	1.0	84.9		CAS	3.3	37.2
14	Normal stroma	3.5	23.7	29	Normal stroma	3.3	49.2
	CAS	2.9	35.7		CAS	3.7	30.6
15	Normal stroma	1.5	63	30	Normal stroma	4.0	33.3
	CAS	1.5	32.4		CAS	3.5	26.9
				31	Normal stroma	3.4	43.2
					CAS	2.8	47.4

6.3.3 Gene expression analysis of normal and tumour stroma from simple canine mammary tumours using RNAseq

To characterise differences of stromal gene expression in the different compartments of canine mammary tumour samples, an unsupervised hierarchical clustering of all samples was performed. As expected, the gene expression pattern clearly separated the normal stroma and CAS into two groups, demonstrating that CAS clearly differs from normal stroma in these canine samples and validating our isolation approach (Figure 3). Using a significance threshold of $p \leq 0.01$ and a log2 ratio threshold of 0.5 to compare CAS and normal stroma, a total of 1999 genes were identified as significantly differentially expressed. 780 genes were up-regulated in CAS compared to normal stroma, whereas 1219 genes were down-regulated. Gene ontology analysis of the deregulated genes identified six clusters (indicated by coloured blocks on the Y axis in Figure 3). To understand the biological role of genes involved in each of these clusters, gene set enrichment analysis was conducted. Analysis of biological processes in these clusters identified the following main categories: cluster 1 (blue, 559 genes) contained genes involved in cell adhesion and migration, cluster 2 (green, 174 genes) and 5 (red, 172 genes) showed genes involved in immune

response, cluster 3 (cyan, 46 genes) exhibited genes important for endodermal cell differentiation and collagen fibril organisation, cluster 4 (orange, 851 genes) showed genes related to signal transduction and angiogenesis, and cluster 6 (yellow, 197 genes) contained genes related to blood and lymph vessel development (Figure 4). Importantly, all of these categories are consistent with changes in stromal biology, thus further validating the isolation of CAS and normal stroma. To investigate whether the different histological tumour grades clustered according to gene expression, the grade of each sample was marked with a colour. However, no clear clustering of the different tumour grades could be detected (Figure 3). To get further insight into the most deregulated pathways between CAS and normal stroma, the MetaCore™ program was used. The 500 most deregulated genes were analysed with pathway maps setting a threshold of 0.5 and p-value of 0.05. For the up-regulated genes TGFβ signalling, ECM remodelling, cell adhesion and EMT were among the top 10 pathways, whereas immune response and angiogenesis were present in the top 10 pathways of the down-regulated genes (Figure 5). Taken together, these results demonstrated the validity of our approach to isolate and analyse CAS and normal stroma from FFPE subsections by RNAseq, and revealed several interesting changes between normal and tumour stroma in canine mammary carcinomas.

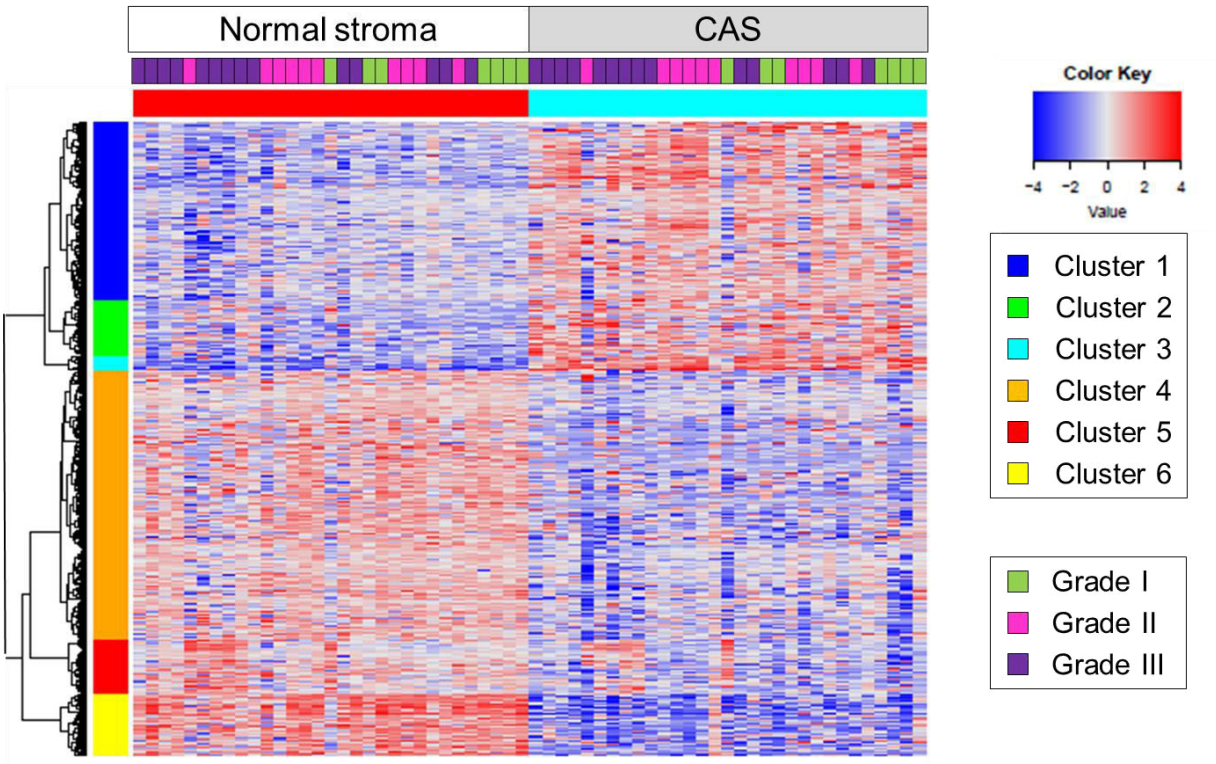

Figure 3: *Hierarchical clustering and heatmap of 31 canine mammary tumour samples analysed by RNA sequencing (p ≤ 0.01, log2 ratio threshold of 0.5). Normal stroma (left) and CAS (right) were clustered separately. Each row features one gene, and each column represents one sample. The red and blue colours represent the relative gene expression level of each gene for each sample in relation to all the other samples. Red indicates a relative up-regulation and blue indicates a relative down-regulation of the gene. The genes were clustered into six groups according to their expression pattern and marked with different colours on the Y-axis (see legend on the right). The histological tumour grade (grade I-III) is indicated for each gene on the upper X-axis (see legend on the right).*

Cluster 1 (blue)

	Term	ID	p
1	cell adhesion	GO:0007155	9.1e-9
2	cell-matrix adhesion	GO:0007160	0.0000234
3	collagen fibril organisation	GO:0030199	2.59e-8
4	positive regulation of cell migration	GO:0030335	0.00000171
5	skeletal system development	GO:0001501	0.0000234

Cluster 2 (green)

	Term	ID	p
1	immune system process	GO:0002376	1.86e-13
2	immune response	GO:0006955	2.75e-14
3	positive regulation of T-helper 1 type immune response	GO:0002827	0.0000236
4	antigen processing and presentation	GO:0019882	3.99e-9
5	antigen processing and presentation of peptide or polysaccharide antigen via MHC class II	GO:0002504	3.36e-11

Cluster 3 (cyan)

	Term	ID	P
1	endodermal cell differentiation	GO:0035987	8.48e-10
2	collagen fibril organisation	GO:0030199	1.38e-7

Cluster 4 (orange)

	Term	ID	p
1	signal transduction	GO:0007165	2.1e-7
2	lung development	GO:0030324	0.00000175
3	positive regulation of GTPase activity	GO:0043547	0.0000233
4	blood vessel morphogenesis	GO:0048514	0.0000344
5	angiogenesis	GO:0001525	0.00000104

Cluster 5 (red)

	Term	ID	p
1	immune response	GO:0006955	0.00000959
2	negative regulation of interferon-gamma production	GO:0032689	0.0000238

Cluster 6 (yellow)

	Term	ID	p
1	positive regulation of endothelial cell proliferation	GO:0001938	0.00001
2	angiogenesis	GO:0001525	0.0000149
3	lymph vessel development	GO:0001945	0.0000293
4	establishment of endothelial barrier	GO:0061028	0.0000453
5	vasculogenesis	GO:0001570	0.000094

Figure 4: *Gene ontology enrichment analysis for each cluster of deregulated stromal genes. Term = affected biological process, ID = Gene ontology accession number, p = p-value indicating the significance of overlap between biological process and the canine gene dataset.*

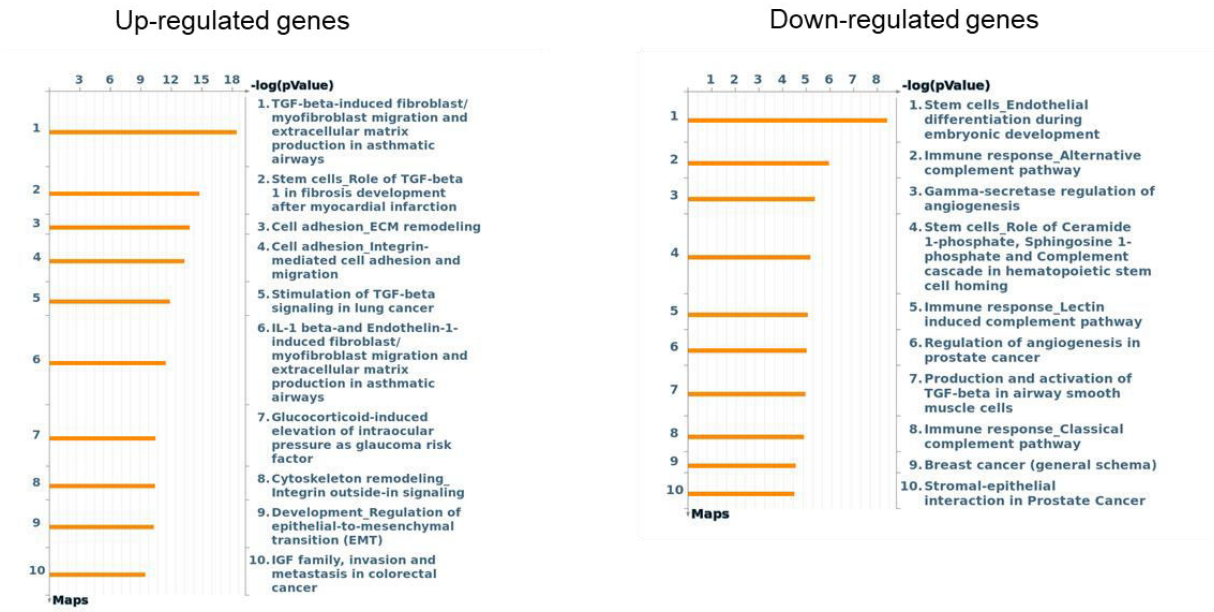

Figure 5: *Pathway analysis of up-regulated and down-regulated genes of CAS. The X-axis shows the -log(pValue) describing the extent of the intersection between the stromal genes and all the genes involved in each pathway. The 10 most significant pathways are displayed.*

6.3.3.1 Stromal gene expression of selected CAS markers in canine mammary tumours

We have previously analysed the expression of 9 known human CAS markers in stromal samples from canine simple mammary carcinomas using RT-qPCR and/or IHC [75, 76]. To see if the results from this study were comparable with the new results obtained by RNAseq with a different patient cohort, we analysed the expression patterns of the same genes in our new dataset. ACTA2 (the gene encoding αSMA), COL1A1, CXCL12, FAP, CAV1, IL6, MMP2, and PDGFRB could be identified among the significantly deregulated genes, while FGF2 was not detected in the new dataset. Similarly to our previous study, ACTA2, COL1A1 and FAP were significantly up-regulated in CAS compared to normal stroma, and CXCL12 was significantly down-regulated, thus confirming our previous results (Figure 6A, B, C and E). While our previous study did not detect significant changes in MMP2, PDGFRB and IL6 expression, mostly due to sample and analysis limitations, we now found MMP2 to be significantly up-regulated in CAS compared to normal stroma, whereas PDGFRB and IL6 were significantly down-regulated (Figure 6D, G and H). . Additionally, CAV1, expression of which had only been analysed by IHC in our previous study, showed a significant reduction in CAS compared to normal stroma in the new dataset (Figure 6F). In summary, these results validated the deregulation for ACTA2, COL1A1, FAP and CXCL12 observed in our previous study, and further underline the validity of our analytic approach. Additionally, the new dataset also revealed CAV1, MMP2, IL6 and PDGFRB to be significantly deregulated in the stroma of canine mammary tumours.

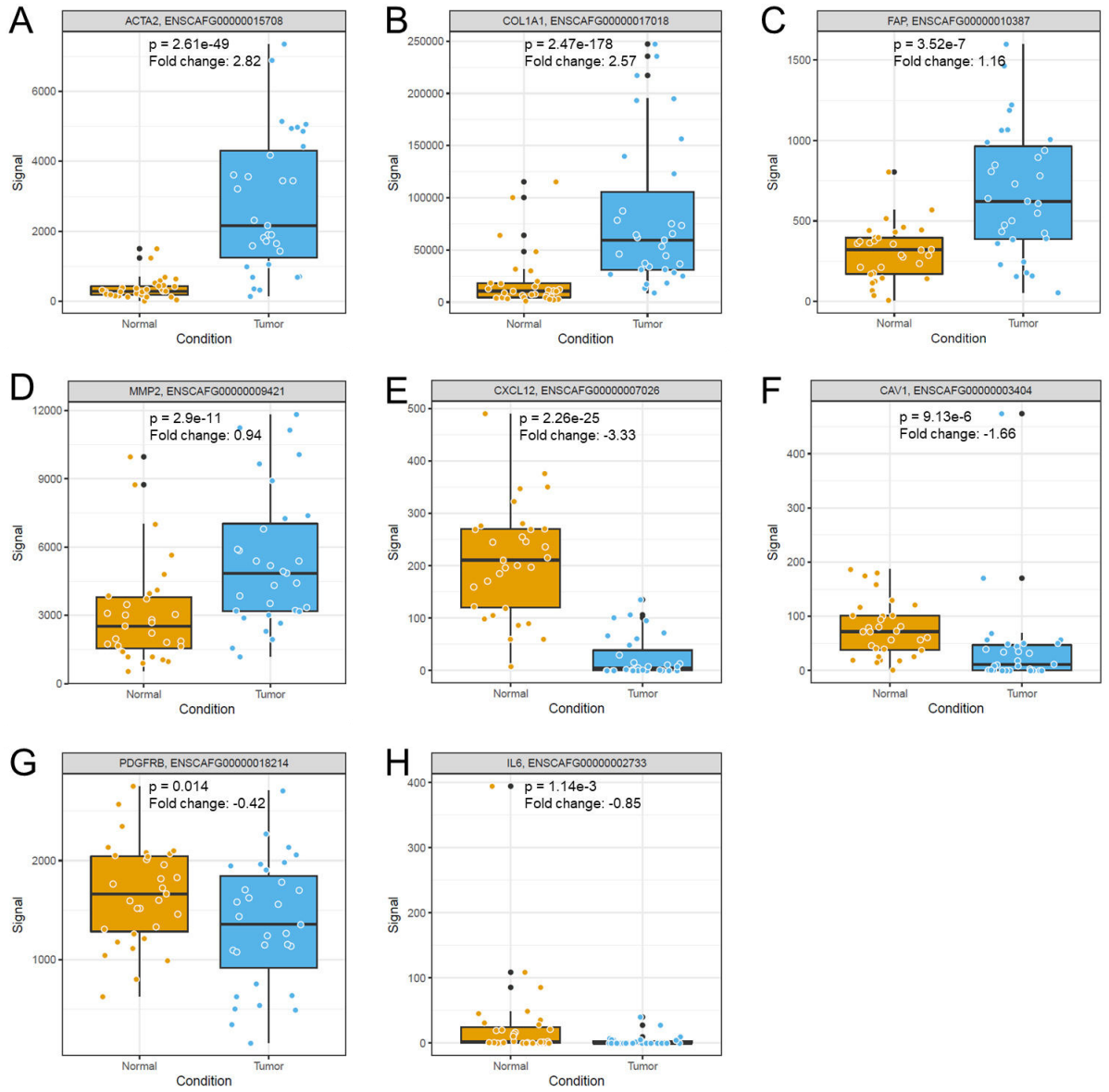

Figure 6: *Expression analysis of selected human CAS markers, in CAS from canine mammary tumours.* ***A:*** *ACTA2,* ***B:*** *COL1A1,* ***C:*** *FAP,* ***D:*** *MMP2,* ***E:*** *CXCL12,* ***F:*** *CAV1,* ***G:*** *PDGFRB, and* ***H:*** *IL6. Boxplots display the expression levels detected by RNAseq for the selected genes in normal stroma and CAS, respectively. The centre of the box indicates the median, while the top and bottom mark the 75th and 25th percentile, respectively. The whiskers indicate the 25th and 75th percentile +/- 1.5 x interquartile range. Expression levels detected in normal stroma are marked in orange, and expression levels in CAS are marked in blue. Gene expression levels (signal) indicating the amount of transcripts detected in each sample, are displayed on the Y-axis. The name of the gene and the ENSEMBL identification number are displayed in the grey box on top of each boxplot. P = p-value, fold change = the difference of the mRNA levels in CAS over to normal stroma.*

6.3.4 Identification of differentially expressed stromal genes comparing metastatic and non-metastatic canine mammary tumours

To identify changes potentially associated with tumour progression, we compared stromal gene expression of metastatic vs. non-metastatic simple canine mammary carcinomas. While the heatmap showed a similar gene expression pattern for normal stroma from the metastatic and non-metastatic samples, clear differences could be found in the CAS of metastatic versus non-metastatic cases (Figure 7). Using a significance threshold of 0.01 and log2 ratio threshold of 0.5, we identified 134 differentially expressed genes between CAS from metastatic vs. non-metastatic samples, including 68 up-regulated genes and 66 down-regulated genes in the metastatic group compared to the non-metastatic group. Six clusters were identified by gene ontology analysis and include following biological processes: cluster 1 (blue, 12 genes) showed genes involved in actin filament crosslinking, migration, cell adhesion and epithelial structure maintenance, cluster 2 (red, 23 genes) contained genes involved in ion homeostasis, regulation of cell cycle and metabolism, cluster 3 (orange, 27 genes) included genes involved in cell differentiation, osteoblast proliferation, immune response and inflammation cluster 4 (cyan, 7 genes) exhibits genes important for apoptosis, regulation of nuclear division, cell adhesion, embryonic development, and angiogenesis, cluster 5 (yellow, 51 genes) showed genes involved in hormone biosynthesis, coagulation and bone remodelling, cluster 6 (green, 14 genes) contained genes related to immune response and inflammation (Figure 8). Again, there was no clear clustering of different grades according to gene expression (Figure 7). The 500 most deregulated genes were analysed using MetaCore™ with a threshold set at 0.5 and p-value of 0.03. Pathway analysis of the up-regulated genes in the CAS of metastatic tumours showed involvement in chemotaxis, regulation of apoptosis and immune response. The down-regulated genes in the metastatic samples revealed TGFβ signalling, gonadotropin-releasing hormone (GnRH) signalling, tissue factor signalling, and genes involved in immune response and lipid metabolism among the top 10 deregulated pathways (Figure 9). Taken together, these results identify clear differences in CAS between metastatic and non-metastatic canine mammary carcinomas, suggesting that stromal changes can potentially be used as markers for tumour progression, and that some of the observed changes might present therapeutic targets to inhibit tumour metastasis.

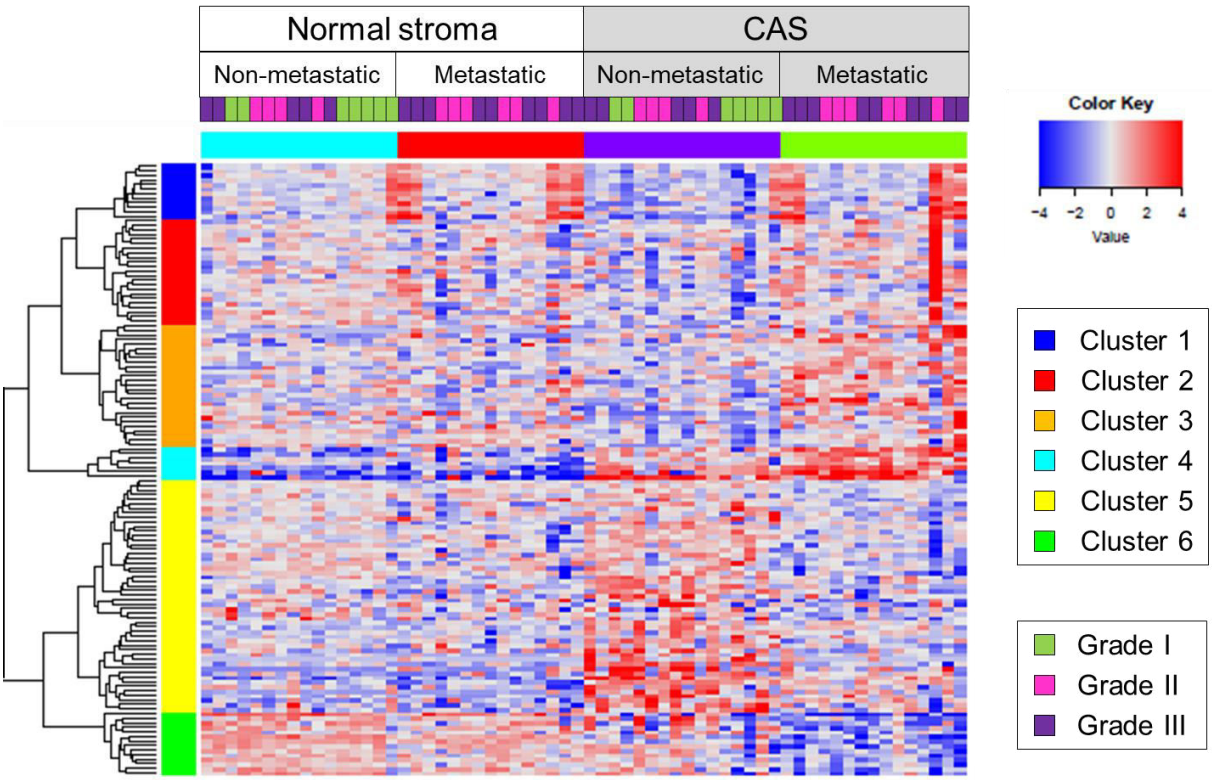

Figure 7: *Hierarchical clustering and heatmap of 31 canine mammary tumour samples analysed by RNA sequencing (p ≤ 0.01, log2 ratio threshold of 0.5). Normal stroma of non-metastatic and metastatic samples (left) and CAS of non-metastatic and metastatic samples (right) were clustered separately. Each row features one gene, and each column represents one sample. The red and blue colours represent the relative gene expression level of each gene for each sample in relation to all the other samples. Red indicates a relative up-regulation and blue indicates a relative down-regulation of the gene. The genes were clustered into six groups according to their expression pattern and marked with different colours on the Y-axis (see legend on the right). The histological tumour grade (grade I-III) is indicated for each gene on the upper X-axis (see legend on the right).*

Cluster 1 (blue)

	Term	ID	p
1	equilibrioception	GO:0050957	0.003146
2	actin filament network formation	GO:0051639	0.004044
3	regulation of cell-cell adhesion mediated by cadherin	GO:2000047	0.004492
4	actin crosslink formation	GO:0051764	0.004492
5	positive regulation of lamellipodium	GO:0010592	0.006284
6	epithelial structure maintenance	GO:0010669	0.005836

Cluster 2 (red)

	Term	ID	p
1	cellular divalent inorganic anion homeostasis	GO:0072501	0.007973
2	regulation of cell cycle checkpoint	GO:1901976	0.006980
3	cellular trivalent inorganic anion homeostasis	GO:0072502	0.007973
4	cellular phosphate ion homeostasis	GO:0030643	0.007973
5	riboflavin metabolic process	GO:0006771	0.007973
6	negative regulation of glycogen biosynthetic process	GO:0045719	0.006980

Cluster 3 (orange)

	Term	ID	P
1	regulation of transcription from RNA polymerase II promoter involved in myocardial precursor cell differentiation	GO:0003256	0.009561
2	N-terminal peptidyl-methionine acetylation	GO:0017196	0.008371
3	mRNA 5'-splice site recognition	GO:0000395	0.008371
4	auditory receptor cell differentiation	GO:0042491	0.009561
5	positive regulation of autophagy of mitochondrion	GO:1903599	0.009561
6	negative regulation of osteoblast proliferation	GO:0033689	0.009561
7	negative regulation of leukocyte chemotaxis	GO:0002689	0.01194
8	negative regulation of mononuclear cell migration	GO:0071676	0.008371

Cluster 4 (cyan)

	Term	ID	p
1	regulation of nuclear division	GO:0051783	0.00001728
2	negative regulation of embryonic development	GO:0045992	0.003296
3	somite development	GO:0061053	0.003595
4	regulation of intrinsic apoptotic signalling pathway in response to DNA damage	GO:1902229	0.005090
5	regulation of chromatin organisation	GO:1902275	0.003296
6	regulation of cell cycle process	GO:0010564	0.0003035
7	branching involved in blood vessel morphogenesis	GO:0001569	0.004492
8	positive regulation of cell adhesion mediated by integrin	GO:0033630	0.004492

Cluster 5 (yellow)

	Term	ID	p
1	regulation of hormone biosynthetic process	GO:0046885	0.0001313
2	response to heparin	GO:0071503	0.00000986
3	regulation of chemokine biosynthetic process	GO:0045073	0.0001313
4	regulation of bone remodeling	GO:0046850	0.0003633
5	negative regulation of hemostasis	GO:1900047	0.0004233
6	keratan sulfate catabolic process	GO:0042340	0.0003633
7	negative regulation of coagulation	GO:0050819	0.0005566
8	negative regulation of platelet activation	GO:0010544	0.0005566

Cluster 6 (green)

	Term	ID	p
1	regulated exocytosis	GO:0045055	0.0001097
2	regulation of glomerular filtration	GO:0003093	0.004542
3	negative regulation of interleukin-6 secretion	GO:1900165	0.004542
4	fusion of virus membrane with host plasma membrane	GO:0019064	0.005189
5	virion attachment to host cell	GO:0019062	0.006482
6	B cell chemotaxis	GO:0035754	0.004542
7	negative regulation of interleukin-1 production	GO:0032692	0.005836
8	negative regulation of dendritic cell apoptotic process	GO:2000669	0.005189
9	cellular response to interferon-alpha	GO:0035457	0.005189

Figure 8: *Gene ontology enrichment analysis for each cluster of deregulated stromal genes comparing metastatic vs. non-metastatic samples. Term = affected biological process, ID = Gene ontology accession number, p = p-value indicating the significance of overlap between biological process and the dataset.*

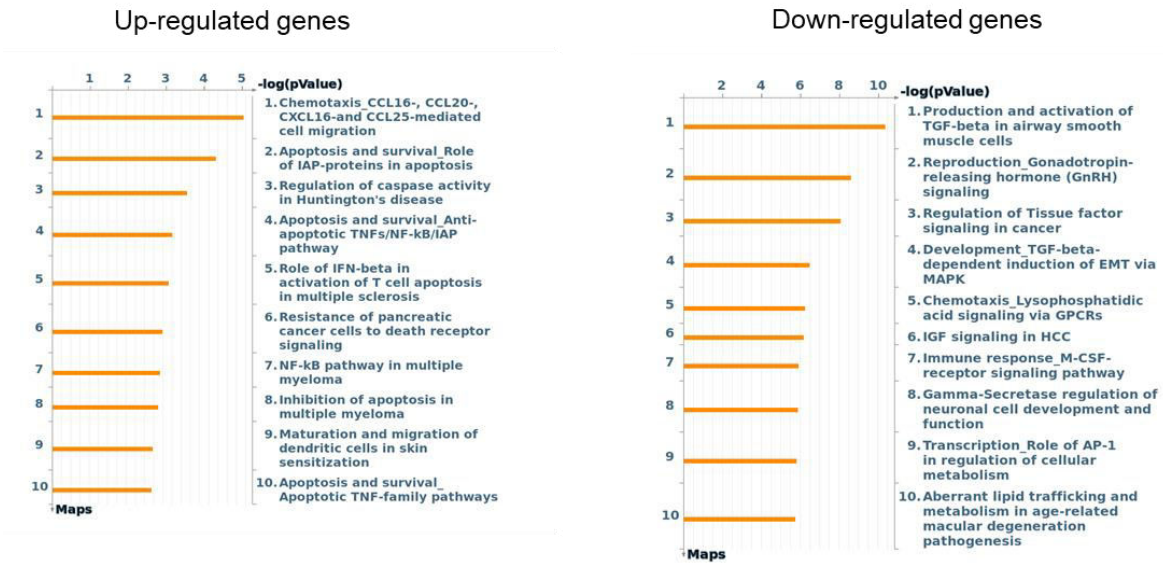

Figure 9: *Pathway analysis of genes up-regulated (left) and down-regulated (right) in CAS from metastatic compared to non-metastatic samples. The X-axis shows the -log(pValue) describing the extent of the intersection between the stromal genes from metastatic tumours and all the genes involved in each pathway. The Y-axis displays the 10 most significant pathways.*

6.3.4.1 Identification of stromal gene candidates involved in metastasis of canine mammary carcinomas

To identify genes which could potentially play an important role during tumour progression, the list with deregulated genes between non-metastatic and metastatic CAS was further analysed manually. All genes with a fold change ≥ 0.5 and p-value ≤ 0.03 were included in the analysis. First, the median level of gene expression for each gene in each condition (CAS and normal stroma from metastatic and non-metastatic samples) was analysed using “Feature view”. Interesting patterns that were identified included unchanged expression in normal and non-metastatic tumours, with a strong increase or decrease in the metastatic tumours (e.g. Figure 10A), or significant differences between non-metastatic and metastatic CAS (e.g. Figure 10B). 76 genes displayed an interesting pattern, and available literature was checked for a known involvement in cancer formation. 33 of the deregulated genes showed a known interesting association with processes involved in tumorigenesis, and could be divided into the main categories metabolism, angiogenesis and coagulation, tumour progression as well as hypoxia-inducible factor 1 (HIF-1) signalling, TGFβ signalling, immune response, and ECM remodelling (Table 4). Due to their established involvement in CAS biology in human breast cancer, several genes pertaining to the last four groups (HIF-1 signalling, TGFβ signalling, immune response, and ECM remodelling) were selected for closer analysis and validation. The deregulated genes included in these four groups can be found in Table 4.

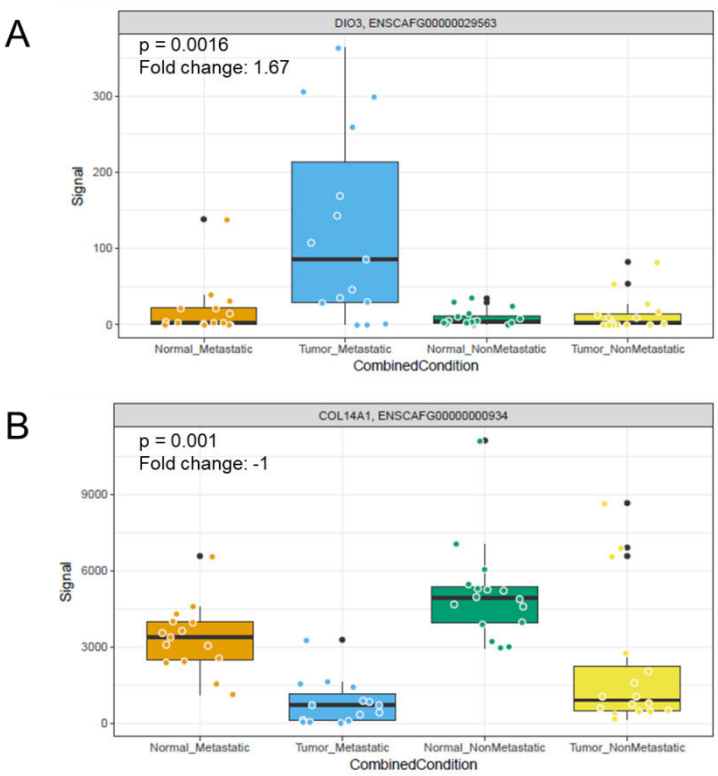

Figure 10: *Boxplots of two genes **A:** DIO3 and **B:** COL14A1 representative for genes showing an interesting pattern of median gene expression level changes. Expression levels are displayed for normal stroma of metastatic tumours (orange), CAS of metastatic tumours (blue), normal stroma of non-metastatic tumours (green), CAS of non-metastatic tumours (yellow). P = p-value, fold change = the difference of the mRNA levels in CAS of metastatic tumours over CAS of non-metastatic tumours in relation to the respective normal stroma.*

Table 4: *Overview of the 33 interesting significantly deregulated genes included in the seven groups TGFβ signalling, HIF-1 signalling, immune response, and ECM remodelling, tumour progression, angiogenesis and coagulation, and metabolism*

Up-regulated genes	Down-regulated genes
TGFβ signalling	
DIO3	TGFB2, TGFBR3, LTBP4
HIF-1 signalling	
DIO3, WT1	TGFB2, STC2, RHOBTB3
Immune response	
GIMAP8, BIN2, HLA-DRB1, FASLG	
ECM remodelling	
MMP11, OLFML2B	FN1, VIT, COL14A1
Tumour progression	
CTHRC1, MKI67, immunity-related GTPase family M protein 1 (ENSCAFG00000000497)	AKAP12, SLIT2, ABLIM1, SEMA3G, LIMCH1, SFRP1, IGFBP5
Angiogenesis and coagulation	
HHIPL1, F5	F13A1, CD36, GAS6, FBLN7
Metabolism	
	CD36, APOE

6.3.5 Validation of next-generation RNA sequencing by RT-qPCR

To validate the gene expression changes between CAS of the metastatic over non-metastatic dataset, quantitative real-time PCR (RT-qPCR) was run with 16 samples checking the expression of 7 selected genes including matrix metalloproteinase 11 (MMP11), vitrin (VIT), transforming growth factor beta 2 (TGFB2), transforming growth factor receptor 3 (TGFBR3), deiodinase 3 (DIO3), procollagen C-endopeptidase enhancer 2 (PCOLCE2), and secreted frizzled related protein 1 (SFRP1) (Figure 11 and Table 4). PCOLCE2 and SFRP1 are two interesting genes that were previously identified in CAS of canine mammary tumours in the context of a different project in our group and thus also included in the analysis. 1-way ANOVA analysis of gene expression levels in all four conditions detected significant differences for MMP11, VIT, TGFB2, TGFBR3 and PCOLCE2 (Figure 11). While the expression trends closely matched the sequencing results, the difference between CAS of the metastatic and non-metastatic samples only reached significance for MMP11 when using Bonferroni's Multiple Comparison Test to compare all conditions with each other (Figure 11A). MMP11 showed a significant up-regulation in CAS of metastatic tumours compared to all other conditions. TGFB2 displayed a significant up-regulation when comparing the normal stroma of metastatic tumours with CAS of non-metastatic tumours (Figure 11B). The trend of lower TGFB2 expression in CAS from metastatic compared to non-metastatic samples is clearly visible. VIT demonstrated a significant down-regulation between the comparison of normal stroma from non-metastatic tumours and CAS of metastatic tumours (Figure 11C). Again, the trend of lower VIT expression in CAS from metastatic compared to non-metastatic samples can be seen. TGFBR3 expression was significantly down-regulated between normal stroma and CAS (Figure 11D). Also for TGFB3, the trend of lower expression in CAS from metastatic compared to non-metastatic samples is obvious. A similar result was obtained for PCOLCE2, revealing a significant down-regulation in CAS compared to the normal stroma of non-metastatic tumours (Figure 11E). Finally, also for PCOLCE2 expression in CAS from metastatic samples is clearly lower than in non-metastatic samples. No significant deregulation between all four conditions could be found for SFRP1 (Figure 11F) and DIO3 (Figure 11G), even though the tendency of gene expression change between metastatic and non-metastatic CAS for both genes is similar to the results from RNAseq. Taken together, these results further support the findings from the sequencing analyses and identify several interesting deregulated targets in CAS between metastatic and non-metastatic canine mammary tumours.

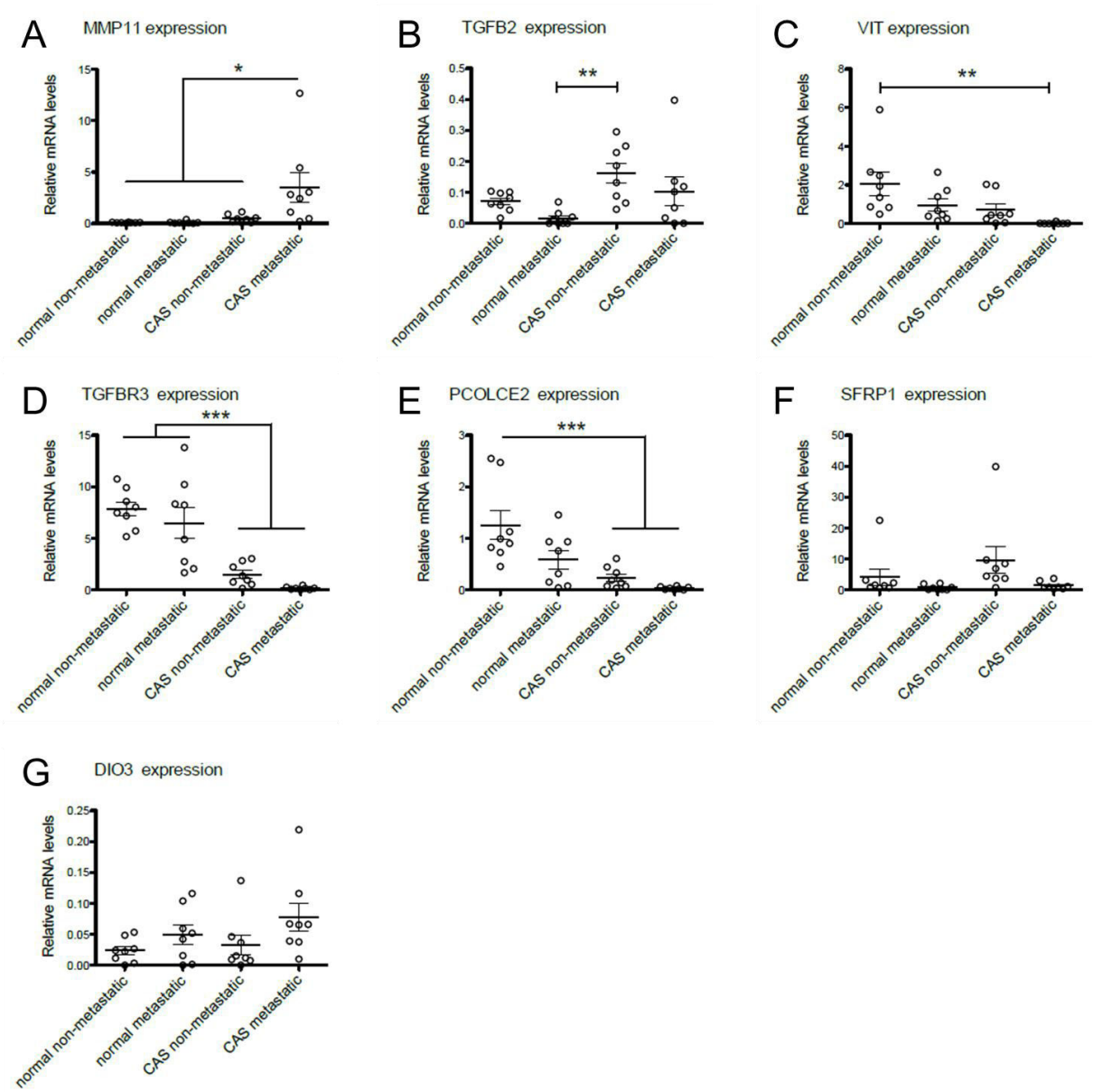

Figure 11: *Relative mRNA levels of stromal genes in CAS of metastatic tumours, CAS of non-metastatic tumours and respective normal stroma, measured by RT-qPCR. Scatter plots for* ***A:*** *MMP11,* ***B:*** *TGFB2,* ***C:*** *VIT,* ***D:*** *TGFBR3,* ***E:*** *PCOLCE2,* ***F:*** *SFRP1,* ***G:*** *DIO3. The value of each sample is displayed for each condition with a mean value ±SEM. Significance between the different conditions was calculated using ANOVA, and is indicated with (* = $p < 0.05$), (** = $p < 0.01$) and (*** = $p < 0.005$), respectively.*

6.3.6 Association of canine stromal markers of metastatic canine mammary carcinomas with survival of human breast cancer patients

Finally, we were interested to see whether some of the identified deregulated genes of the metastatic canine mammary carcinomas were associated with prognosis in human breast cancer. To assess this, we performed survival analysis of the selected 33 genes (Table 4) using the TIMER software, which allows the assessment of gene expression levels in whole tumours in correlation to survival from TCGA data. The datasets of human breast cancer patients with invasive carcinomas were checked setting a follow-up time of 100 months. A significant association with worse survival was found for down-regulation of TGFB2, VIT, collagen type XIV alpha 1 chain (COL14A1), slit guidance ligand 2 (SLIT2), and semaphorin 3G (SEMA3G) (Figure 12). Of note, TGFB2 was significantly associated with survival only when analysing data of the HER-2 subtype. These results further suggest the presence of strong similarities in expression changes in CAS between canine and human breast cancer specimen. Moreover, they identify a number of dysregulated genes that are related to tumour malignancy and survival in both species.
In conclusion, our study provides evidence that CAS in canine mammary tumours undergoes strong reprogramming mechanisms, and that a number of genes is significantly differentially expressed between CAS from metastatic and non-metastatic tumours. Finally, we demonstrate the deregulation of some of these genes in metastatic canine mammary tumours is predictive of a worse prognosis also in human breast cancers. These data support the usefulness of comparatively analysing CAS between canine mammary tumours and human breast cancer to identify potential markers of disease progression as well as novel therapeutic targets to inhibit tumour metastasis.

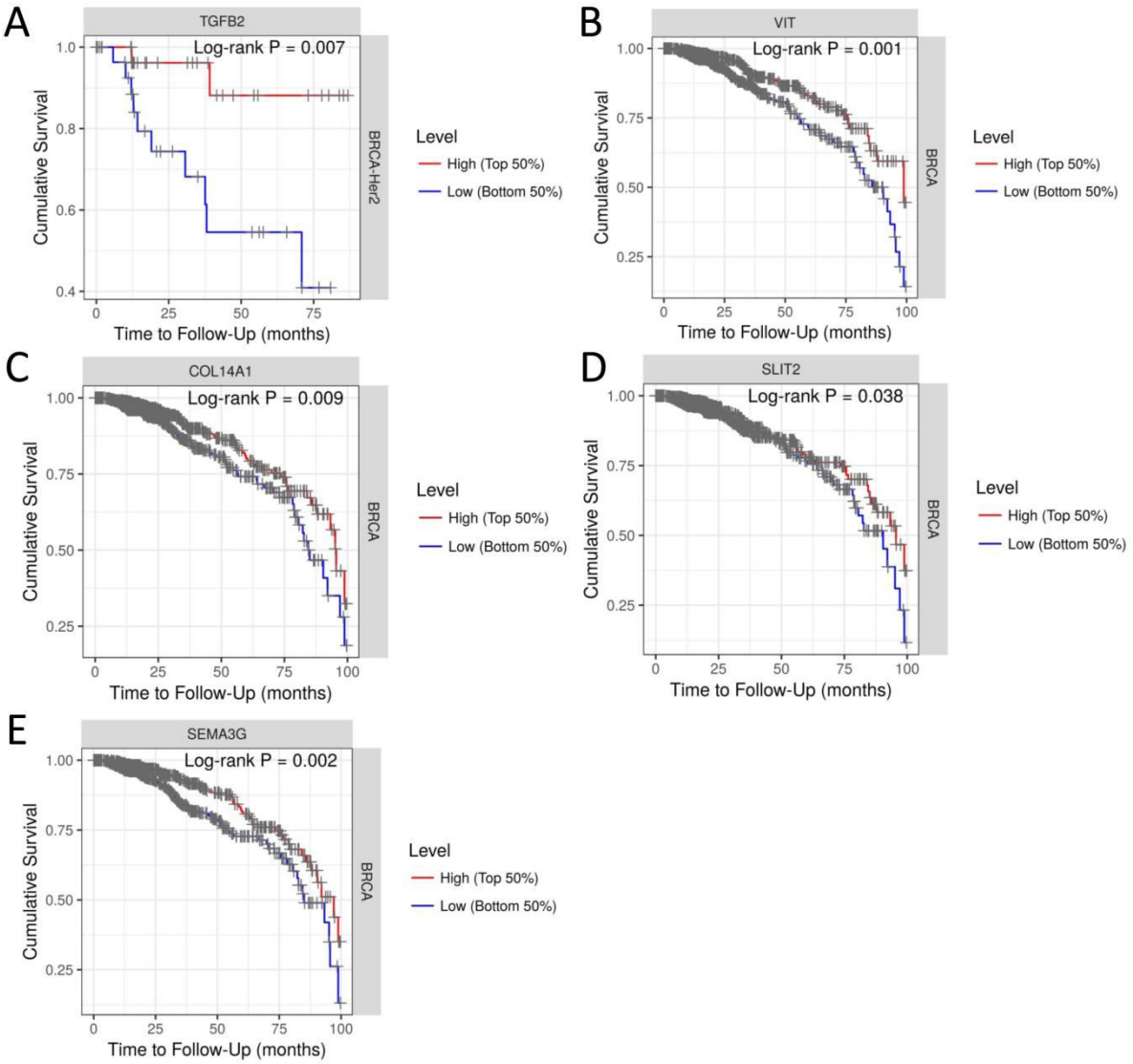

Figure 12: *Kaplan-Meier Survival Curves displaying significant association of TGFB2, VIT, COL14A1, SLIT2, SEMA3G and prognosis in human breast cancer patients. The X-axis shows the follow-up time of human patients and the Y-axis lists the percentage of patients still alive. The name of the tested gene is marked in the upper grey box, the type of human breast cancer is presented in the grey box on the right. BRCA = Breast Invasive Carcinoma, BRCA-HER2 = HER-2 subtype of Breast Invasive Carcinoma. The red line indicates patient samples with an up-regulation of the gene and blue indicates patients samples showing down-regulation of the gene with a split percentage set at 50%. Log-rank P = p-value indicating the significance of the selected gene related with survival in human breast cancer patients.*

7 Discussion

Breast cancer is the most frequent cancer both in women and female dogs. Several lines of evidence suggest spontaneously occurring mammary tumours in the dog as an interesting candidate for comparative oncology to better understand the biology of cancer and uncover novel prognostic biomarkers as well as therapeutic targets [2, 35, 48, 92]. To date, in a significant number of both humans and dogs, the clinical and histopathologic indicators that are used are not able to predict the clinical outcome. Therefore, new indicators are needed to more accurately diagnose and treat patients [48]. Especially with regards to metastasis, major efforts are being made to identify potential biomarkers and therapeutics to diagnose and treat cancer early, and to enhance survival of cancer patients, as metastases are the main factor of cancer-related deaths both in humans and dogs [1, 38, 66].
CAS is emerging as a central player in cancer biology, and it has been shown to support cancer initiation, growth, metastasis and resistance of tumour cells to cancer therapy [7, 9, 11, 12, 14]. Thus, the identification of predictive biomarkers in CAS as well as targeting of CAS components for therapeutic purposes are considered highly interesting options to advance cancer patient care [7, 8, 12, 14]. While mechanisms in CAS in human breast cancer are slowly being unveiled, CAS in canine mammary tumours remains largely uncharacterized. So far, just very few studies have investigated the involvement of stromal genes in canine mammary tumours, all of which were limited to very few markers that were analysed mostly by immunohistochemistry. To better understand the mechanisms involved in CAS formation of canine mammary tumours and be able to identify commonalities and differences between canine and human CAS, we set out to analyse the gene expression of CAS from canine simple mammary carcinomas. Specifically, the aims of my thesis were the following:

1) Establish an approach to analyse the expression of selected CAS markers for human breast cancer in CAS from canine mammary carcinomas.
2) Develop a protocol to analyse CAS and normal stroma from FFPE tissues by next-generation sequencing.
3) Analyse CAS and normal stroma from non-metastatic versus metastatic canine mammary carcinomas to investigate the changes in canine CAS and identify differentially regulated genes that could potentially be used as prognostic or therapeutic targets.

7.1 First aim: Analysis of selected CAS markers for human breast cancer in CAS from canine mammary carcinomas

In order to investigate if CAS in canine mammary carcinomas is comparable to human breast cancer, we analysed the expression of selected CAS markers for human breast cancer in canine tumour samples using laser-capture microdissection [93]. Our results suggested similarities in CAS biology between canine and human breast cancer, but also revealed some differences between the two species [75, 76]. This publication was the first report to provide an expression analysis of several of the most important human CAS markers in canine mammary carcinomas.
While yielding important results, this study was however limited, as analysis by RT-qPCR only yields results on the genes that have been chosen *a priori*. Thus, this kind of analysis is entirely relying on defined candidate genes, which precludes an unbiased view. RNAseq would allow much broader and less biased analysis of the

samples. However, as FFPE fixation is known to heavily impact on the quantity and the quality of RNA, the use of extremely small amounts of RNA recovered from laser-capture microdissected FFPE tissue was considered as incompatible with RNAseq. Nevertheless, we decided to try and improve the available RNA extraction protocols for FFPE tissue with the aim to perform RNAseq.

7.2 Second aim: Development of an optimised RNA extraction protocol from laser-capture microdissected FFPE samples amenable for RNAseq

FFPE tissues are a large and very valuable resource of patient-derived tissue samples. However, isolation and analysis of RNA from FFPE tissues has proven challenging due to chemical alteration of nucleic acids caused by formalin fixation [94-97]. In this second part of my thesis, the aim was to improve our RNA isolation technique from laser-capture microdissected samples in a manner that would allow next-generation RNA sequencing. Through optimisation of a protocol based on focused ultrasonication, we were able to develop an approach to increase the yields of RNA from laser-capture microdissected FFPE tissue samples and make them amenable to RNAseq analysis [77]. This was the first report to show that small amounts of RNA isolated from FFPE tissues can be analysed through RNAseq. One potential limitation of the approach is the low RNA quality that can be isolated from FFPE tissue [94-97]. This is the main reason that most LCM-based studies to date have been using fresh-frozen tissue rather than FFPE sections even for RT-qPCR analyses [94]. RNA degradation and crosslinking through FFPE occurs mainly at the fixation stage, and cannot be strongly influenced afterwards. Therefore, to avoid the introduction of artificial biases due to sample quality differences, it is very important for the analysis of FFPE tissues by next-generation RNAseq that RNA of similar quality is compared. Whenever possible, in our approach we strived to isolate the different areas from the same tissue section to ascertain that both samples have undergone the same treatment. If not possible, different samples from the same patient taken on the same day and fixed in the same manner were used. While these precautions certainly limit the introduction of large biases, they cannot completely be avoided. Thus, validation of results through RT-qPCR and/or immunohistochemistry should always be performed before finalising any claims. Another important aspect is that the low amount of RNA that is submitted for sequencing makes detection of very low expressed genes difficult. Therefore, results are biased towards more highly expressed genes, because these can be reliably detected and quantified. Nevertheless, as the analysis setup always compares normal stroma with CAS from the same patient, observed changes are likely to be true. A possible approach to further validate our novel protocol would be to analyse in parallel CAS and normal stroma isolated from both FFPE tissue and fresh frozen tissue from the same sample. While this would have exceeded the scope of our study, it can be considered for future projects. Concluding, this novel approach to analyse FFPE tissue subsections has the potential to become a very valuable tool for biomedical research.

7.3 Third aim: Analysis of CAS and normal stroma from non-metastatic versus metastatic canine mammary carcinomas

My third aim was to investigate the changes in CAS between metastatic and non-metastatic canine mammary carcinomas, and identify differentially regulated genes that could potentially be used as prognostic or therapeutic targets. For this, our recently developed RNAseq protocol was used to analyse CAS and matched normal stroma isolated from FFPE samples by LCM.

7.3.1 Characteristics of cases and tissue samples included in the study

31 clinical cases of canine simple mammary carcinomas were selected, including 15 metastatic and 16 non-metastatic cases (Tables 2 and 3). Among the 31 cases, no dog breed was overrepresented. The mean age of dogs included in this study was 11 years, which is in accordance with values from literature [36, 38]. Information regarding neutering was available for 21 dogs. Only 3 dogs were neutered, matching literature which shows elevated risks of mammary carcinoma development in intact bitches. Unfortunately, no information regarding the age at time of neutering was available for the 3 neutered dogs which developed mammary carcinomas. The age of FFPE tissue blocks included varied between 7 months and over 120 months. We did however not observe sample-age dependent differences in mRNA quality and quantity (Table 3), emphasising the value and usability of these patient materials for research purposes.
Among the metastatic cases the solid histological subtype was overrepresented, whereas the tubular subtype was diagnosed more frequently in the non-metastatic cases. A difference was also seen in the distribution of histological tumour grades with grade I tumours only diagnosed in non-metastatic cases. Most tubular carcinomas were classified as grade I. These results are in line with other studies that found association of histological subtypes and tumour grades in canine mammary tumours as well as association of these histological criteria with metastasis [48, 51, 52, 54]. However, a general correlation between histological criteria and prognosis was not obvious, as solid and comedocarcinomas, both of which are usually associated with worse prognosis, as well as tumours classified as grade II or grade III were also found among the non-metastatic cases (Table 2). Furthermore, several tubular and tubulopapillary carcinomas, generally associated with better prognosis, were among metastatic cases. A widely known and important point of criticism is the improper application and interpretation of histological criteria or use of different grading systems by different pathologists, leading to various diagnostic results [32, 51]. Taken together, new indicators to diagnose canine mammary carcinomas and to allow more accurate forecasting are required [48].

7.3.2 Differences in gene expression between normal stroma and CAS in canine mammary tumours

Unsupervised hierarchical clustering of samples clearly revealed significant changes in gene expression in CAS compared to matched normal stroma (Figure 3). This validated our approach to selectively isolate these tissues by laser-capture microdissection, and also demonstrated that CAS in canine mammary carcinomas undergoes strong reprogramming. A comparison of gene expression patterns

revealed no clear association with histological grades (Figure 3), matching the conclusions drawn in the previous chapter.
Gene ontology analysis of the most significantly deregulated genes revealed that genes mostly up-regulated in CAS are involved in cell-adhesion, cell migration, collagen fibril organisation, endodermal cell differentiation and immune response (Figure 4). All of these processes are consistent with changes in stromal biology. Collagen fibril organisation is often altered in tumour tissues leading to disorganisation of the ECM, thus possibly supporting the invasion of cancer cells [2, 7, 8, 11, 14]. Moreover, enhanced cell motility and migration of cancer cells is achieved through down-regulation of cell-adhesion molecules (E-cadherin) and the acquisition of a mesenchymal phenotype (EMT) induced by soluble factors like MMPs or TGFβ secreted by stromal cells [8, 9, 11, 15]. EMT and TGFβ signalling are also known to be involved in endodermal differentiation providing a possible explanation for the identification of this process [98, 99]. Altered immune response is another main category supporting tumour growth and progression [8, 9, 21]. Among the top 5 biological processes positive regulation of T-helper type 1 cells could be found suggesting a proinflammatory microenvironment, which is associated with better prognosis in cancer patients [100]. However, variable effects on patient outcome are described, due to variable effects of cytokines in the tumour microenvironment [101].
Genes mostly down-regulated in CAS were involved in signal transduction, angiogenesis and immune response (Figure 4). These processes are known to be altered in tumours and to support tumour progression [8, 9, 11]. Angiogenesis is important for the survival of tumour cells, as blood vessels provide oxygen and energy-rich metabolites [8, 11]. In our dataset genes involved in the establishment of endothelial barrier are down-regulated, which can facilitate intravasation of cancer cells, resulting in distant metastasis. Moreover, down-regulation of immune response, especially CD8+ T cells, in tumour tissue is shown to be associated with worse prognosis in cancer patients [9, 11, 14].
Detailed analysis of the pathways of the up- and down-regulated genes revealed similar categories as for the biological processes by gene ontology. For the up-regulated genes pathways involved in TGFβ signalling, ECM remodelling, EMT, cell adhesion and migration were overrepresented, and pathways involved in angiogenesis and immune response were also present (Figure 5). The main pathways affected regarding the immune system were associated with complement activation. The function of complement is still not fully understood, as a dual role has been described, where the complement either destroys cancer cells or promotes tumour growth [102]. To summarise, these results demonstrate the validity of our approach to isolate and analyse CAS and normal stroma from FFPE subsections by RNAseq, and reveal several interesting changes between normal and tumour stroma in canine mammary carcinomas.

7.3.3 Validation of selected human CAS markers in canine mammary carcinoma

The new dataset contained data for 8 of the 9 stromal markers analysed in a previous study [75, 76]. All 8 genes (ACTA2, COL1A1, FAP, MMP2, CXCL12, CAV1, PDGFRB, IL6) were significantly deregulated when comparing normal stroma and CAS (Figure 6). ACTA2, COL1A1 and FAP were up-regulated in both datasets which is consistent with findings in human studies. A detailed overview and discussion

regarding the known involvement of all these markers in tumour biology and the interpretation of their expression changes can be found in my master thesis as well as our paper [75, 76].
Differences regarding deregulation of genes detected by the RNAseq results compared to our previous study may be due to the smaller sample size in the previous study, and the different analysis method (RT-qPCR vs. RNAseq). Especially in some cases, such as for IL6, expression could only be detected in a small subset of analysed cases in the old dataset, which strongly limited the statistical power. Also, normalisation strategies differ strongly between RT-qPCR and RNAseq, which can influence detection of gene expression changes. To conclude, by comparing two independent datasets generated by two different methods, we validated deregulation of ACTA2, COL1A1, FAP and, CXCL12 in canine CAS. Furthermore, our results suggest a significant contribution of MMP2, CAV1, PDGFRB and IL6 gene expression changes in the biology of canine mammary tumours.

7.3.4 Changes in stromal gene expression during tumour progression in canine mammary carcinomas

Our results revealed significant changes in gene expression comparing CAS of metastatic and non-metastatic canine mammary tumours (Figure 7). Again, no clear difference of the gene expression pattern between the different histological grades could be seen comparing the two conditions (metastatic, non-metastatic). Therefore, these results further support the demand for more accurate prognostic indicators in cancer diagnostics besides histological and clinical criteria [48].
Hierarchical clustering of significantly deregulated genes showed a similar gene expression pattern among the normal stroma samples of metastatic and non-metastatic tumours. This demonstrates the similar behaviour of normal stroma in both tumour types and validates proper isolation of normal stroma, also because gene expression clearly differs between normal stroma and CAS (Figures 3 and 7). In contrast, clear difference could be detected comparing CAS samples of metastatic and non-metastatic tumours with greatest differences in clusters 3, 4, 5 and 6 (Figure 7). These clusters contain genes affecting cell differentiation, cell adhesion and angiogenesis, biological processes known to be altered in tumour tissues and also associated with the induction of EMT, an important mechanism needed for cancer cells to form metastasis [8, 9, 11, 15] (Figure 8). Furthermore, processes involved in bone remodelling including the negative regulation of osteoblast differentiation seem to be regulated differently in CAS of metastatic tumours. Suppression of osteoblast activity through cancer cells was associated with bone metastasis in human breast cancer [103, 104]. Another main process to be affected in the metastatic CAS is the immune response. Negative chemotaxis of leucocytes and mononuclear cells like lymphocytes leading to an immunosuppressive microenvironment is often induced by CAFs or IICs themselves and is associated with metastasis and worse prognosis [8, 9]. Pathway analysis of the up- and down-regulated genes in CAS of metastatic tumours exhibited similar categories as gene ontology analysis, and could mostly be grouped into five interesting clusters (Figure 9). The up-regulated genes were mainly involved in chemotaxis, immune response and regulation of apoptosis. Pathways overrepresented among the down-regulated genes showed involvement in immune response, GnRH signalling and TGFβ signalling. The most interesting genes were divided into seven groups of which four were further analysed in detail (Table 4).

The first group exhibited genes involved in TGFβ signalling pathway, known to play a role in cell differentiation, growth, migration and tumorigenesis including angiogenesis, EMT, and immunosuppression [8, 9, 11, 12, 14, 21, 105]. The pathway is induced by binding of TGFβ to two cell surface receptor kinases (TGFBR1, TGFBR2) and followed by phosphorylation of Smad proteins which activate specific gene transcription [105]. TGFβ is expressed by various stromal cells including CAFs, ACVs and IICs, emphasising the contribution of CAS to this pathway [7, 9, 11, 12, 14, 21]. In our dataset, genes significantly associated with TGFβ signalling include DIO3, TGFB2, TGFBR3 and LTBP4 (Table 4). DIO3, up-regulated in metastatic CAS, is a deiodinase inactivating thyroid hormones which are important for development, cell differentiation and maintenance of proper metabolism in cells. DIO3 was shown to be expressed in fibroblast under stimulation of TGFβ and activated in adults promoting growth in solid tumours. The effect may be due to local hypothyreodism induced by DIO3 which results in enhanced cell proliferation and inhibition of cell differentiation [105]. TGFB2 and TGFBR3 are directly involved in the TGFβ signalling pathway. TGFB2 encodes a protein involved in forming TGFβ, thus activating the TGFβ signalling cascade. We found TGFB2 up-regulated in CAS compared to normal stroma but down-regulated in CAS of metastatic tumours when compared to non-metastatic tumours, thus either indicating minor involvement in the formation of metastasis, or the importance of dampening TGFB2 signalling during tumour progression. TGFβ was also described to be down-regulated in stromal cells when co-cultured with metastatic tumour cells [106]. Some studies also suggest TGFβ to function as a tumour suppressor. A study in canine mammary tumours found the down-regulation of various growth factors, including their receptors like TGFBR2 or TGFBR3, in metastatic tumours when comparing with normal tissue [62]. TGFBR3 has also been shown to be down-regulated in our dataset, and decreased expression was observed in various cancers associated with poor outcome [107-109]. LTBP4, down-regulated in our dataset, is a TGFβ binding protein, and its down-regulation in canine mammary tumours was associated with malignancy [110, 152].

The second group contains genes involved in HIF-1 signalling a pathway which is activated under hypoxic condition by HIF-1 and often found in advanced solid tumours. Activation of the HIF-1 signalling pathway drives transcription of various genes and gets modulated to promote survival of hypoxic cells [105]. DIO3, TGFB2, STC2, WT1, and RHOBTB3 (Table 4) are significantly deregulated genes of our dataset associated with HIF-1 signalling [105, 111-113]. DIO3 has been shown to be induced under hypoxic conditions and to decrease the metabolic rate and oxygen consumption by inhibition of T3 (active form of thyroid hormone) [105]. RHOBTB3 is a Rho GTPase which has been shown to be involved in tumorigenesis. It suppresses the Warburg effect and deregulates the assembly of the HIFα complex, thus down-regulation as seen in our data is suggested to promote HIF-1 signalling [111, 114, 115]. WT1 encodes the transcription factor wilms tumor 1 which plays an important role in normal development. Contradicting results regarding expression of WT1 for breast cancer progression are found in literature [113, 116, 117]. Moreover, STC2 encoding a glycoprotein hormone and representing a HIF-1 target gene, has been suggested to play a role in tumour development by inhibiting tumorigenesis, metastasis and EMT of breast cancer cells. Therefore, down-regulation as seen in our dataset can promote tumour progression [112, 118].

Another main category altered in metastatic CAS was the immune response. Our data exhibits up-regulated genes like GIMAP8, BIN2, HLA-DRB1, and FASLG to be involved in this process (Table 4). GIMAP8 is a GTPase IMAP family member whose function is still not fully understood. It has been shown to be overexpressed in CAS and has been suggested to play a role in T-cell apoptosis, thus promoting an immune suppressive microenvironment [119-122]. BIN2 has been suggested to play a role in leucocyte motility and phagocytosis [123]. HLA-DRB1 belongs to the MHC II molecule complex expressed in antigen presenting cells like dendritic cells or macrophages. However, the gene has been shown to be associated with worse prognosis in human cancer patients when down-regulated or did not show significant association with prognosis [124, 125]. FASLG encodes a ligand which is a member of the TNF superfamily and induces apoptosis by binding FAS. It is known to play a role in immune system regulation including induction of T-cells apoptosis and has been suggested to be involved in tumour progression [126, 127]. Therefore, literature supports our findings of FASLG up-regulation in CAS of metastatic tumours.

The last group included genes like MMP11 and OLFML2B which were up-regulated in metastatic CAS and genes such as FN1, VIT, and COL14A1, which were down-regulated in metastatic CAS. All of these genes are involved in ECM remodelling, a process which involves genes that have been shown to be among the most deregulated genes in CAS [16]. ECM remodelling is regarded as an important step for tumour progression and metastasis [8, 14, 15]. MMP11 is a matrix metalloproteinase which, in contrast to other MMPs, has no direct influence on ECM degradation but cleaves enzymes like proteinase inhibitors [128, 129]. However, one study shows the involvement of MMP11 in collagen VI degradation, a constituent of the ECM surrounding adipocytes [130]. Expression of MMP 11 in stromal cells has been shown to be associated with higher risk of invasive tumour growth and metastasis and has been suggested as prognostic factor, as it correlates with worse clinical outcome in patients with invasive breast cancer [128, 129, 131, 132]. Up-regulation of MMP11 has also been found during progression from *in situ* to invasive breast cancer [133]. Moreover, an analysis of whole canine mammary tumours found up-regulation of MMP11 in metastatic tumours compared to non-metastatic tumours [61] . OLFML2B is a gene encoding an olfactomedin domain-containing protein, which represents a secreted glycoprotein [134]. Olfactomedins play an important role in neurogenesis, cell adhesion, cell cycle regulation, and tumorigenesis. Proteins encoded by OLFML2B have been shown to bind chondroitin sulphate-E and heparin in the ECM. Nevertheless, the function of OLFML2B is still not clear even though our dataset suggests an involvement of this gene in canine mammary tumour progression [134, 135]. FN1 encodes fibronectin, a glycoprotein and constituent of the ECM that is secreted by CAFs and involved in wound healing, fibrosis, lymphangiogenesis, proliferation and migration, and has been associated with drug resistance of cancer cells [8, 9, 12, 14, 16]. In our dataset FN1 was up-regulated comparing CAS over normal stroma, but lower in CAS of metastatic than non-metastatic tumours. This may suggest a minor role of FN1 in tumour progression of canine mammary tumours. VIT is a gene encoding vitrin, an ECM protein which may be associated with cell adhesion, matrix assembly and migration [136, 137]. In cartilage tissue vitrin has been shown to be down-regulated in the ECM surrounding hypertrophic chondrocytes, whereas high expression was detected in the ECM surrounding pre-hypertrophic chondrocytes [137]. As VIT was lower in metastatic CAS in our dataset, its downregulation may also play a role in tumour progression. COL14A1 encodes the alpha chain of type XIV collagen and is a large glycoprotein of

the ECM. It interacts with collagen fibrils, is involved in fibrillogenesis, and has been revealed to be frequently absent close to invasive tumours [138]. Moreover, COL14A1 has been shown to be mutated and down-regulated in triple-negative breast cancer patients, a molecular breast cancer subtype which exhibits the worst prognosis [139]. Therefore, similar deregulation of COL14A1 in CAS of metastatic tumours observed in our canine dataset, may suggest the same function of this gene as in human breast cancer patients.

7.3.5 Validation of RNAseq results by RT-qPCR

Validation of data obtained by RNA sequencing was performed by RT-qPCR for 7 genes (Figure 11). The expression trends of all genes analysed closely matched the sequencing results. However, comparing all conditions with each other, significant difference between CAS of the metastatic and non-metastatic samples was only detected for MMP11 (Figure 11A). It was highly up-regulated in CAS of metastatic tumours compared to all three other conditions. This is in line with literature regarding its supportive role in tumour progression in both human and canine mammary carcinoma [61, 128, 129, 131-133]. This further confirms that ECM remodelling is an important process affected during tumour progression, and MMP11 may be suggested as a biomarker for metastasis in canine mammary tumours. To further verify its contribution to tumour progression a more detailed analysis of the gene is needed.
For VIT, TGFBR3 and PCOLCE2 the gene expression declined from normal stroma of non-metastatic tumours to normal stroma of metastatic tumours followed by CAS of non-metastatic tumours and showing the lowest expression levels in CAS of metastatic tumours. Indicating that down-regulation of these genes may promote metastasis in canine mammary tumours. However, these findings have to be further validated using more samples. The same applies for SFRP1 and DIO3 (Figures 11F and G). The lack of significance for some of the genes may be due to a small sample number included in the qPCR analysis and the different normalisation strategy used, with 3 housekeeping genes that were analysed.
As expected no significant differences could be detected comparing normal stroma of metastatic and non-metastatic samples. However, a declining tendency could be observed suggesting normal stroma of metastatic tumours may already show some alterations compared to normal stroma of non-metastatic tumours. Therefore, for future studies a larger distance for isolation of normal stroma may be considered to uncover even more deregulated genes. On the other hand, hierarchical clustering of the comparison from stroma of metastatic over non-metastatic samples showed a similar expression pattern for both normal stroma of metastatic and normal stroma of no-metastatic samples, which suggests validity of the isolation approach.

7.3.6 CAS markers of metastatic canine mammary carcinomas associated with survival in human breast cancer

To see whether gene expression changes in metastatic canine CAS could also predict worse prognosis in human breast cancer, we analysed whether the expression of the identified markers for metastatic canine CAS was associated with survival in a human breast cancer dataset derived from whole tumour sequencing. Indeed, a significant association with survival was displayed for TGFB2, VIT, COL14A1, SLIT2, and SEMA3G (Figure 12). COL14A1 and TGFB2 have already

been described to be associated with prognosis in breast cancer patients, the latter showing better prognosis when up-regulated in patients without metastasis in the lymph node [139, 140]. SLIT2 encodes a glycoprotein secreted by CAFs which is involved in cell migration and which is associated with metastasis and worse prognosis when down-regulated [141-144]. SEMA3G is a gene encoding a protein involved in angiogenesis and tumour progression supporting tumour cell invasion and has been associated with longer survival when up-regulated [145-147]. More significant associations of stromal genes with survival may be found if a different dataset for comparison was used. The TCGA dataset checked by the TIMER software contains data of the whole tumour tissue, therefore presenting a mix of stromal and tumour cell gene expression signatures. As a consequence, the gene expression pattern of tumour cells could possibly overlap the gene expression signature of stromal cells. For example in case of the membrane protein CD36, worse prognosis has either been shown to be associated with CD36 down-regulation in stromal cells or has been shown to be associated with up-regulation of CD36 in cancer cells [148-151]. As MMP11 was shown to be a potential biomarker detected in CAS of metastatic mammary tumours, an association with survival would be expected. However, no significant association of MMP11 with survival was found using the TIMER software. Nevertheless, literature shows significant association of MMP11 with shorter relapse-free and overall survival in breast cancer patients [129, 132]. Taken together, these results display the usefulness of the comparison of CAS from canine and human mammary carcinomas regarding the identification of genes possibly involved in tumour progression and worse prognosis.

7.4 Conclusion/Outlook

To conclude, our findings demonstrate that CAS in canine mammary tumours undergoes strong reprogramming mechanisms, which are largely comparable with data from human breast cancer and which supports the use of the dog as a representative model for human breast cancer. More precisely, genes involved in ECM remodelling, immune response, angiogenesis, coagulation, EMT, metabolism and signalling pathways including TGFβ- or HIF-1 signalling seem to play an important role during tumour progression in both canine and human mammary carcinomas. In particular MMP11 has been shown to be significantly up-regulated in CAS of metastatic canine mammary carcinomas by RNAseq and validation with qPCR, suggesting MMP11 as a possible new biomarker in canine mammary carcinomas. To further support these results and to find even more interesting deregulated targets, a more detailed analysis of the data will be the subject of follow-up projects in the lab. These may lead to the discovery and development of new diagnostic and therapeutic targets for canine and human breast cancer.

8 References

1. World Health Organization WHO Cancer facts sheet. In: www.who.int. http://www.who.int/en/news-room/fact-sheets/detail/cancer. Accessed 5 Nov 2018

2. Zhang J, Liu J (2013) Tumor stroma as targets for cancer therapy. Pharmacol Ther 137:200–215. doi: 10.1016/j.pharmthera.2012.10.003

3. Eurostat Eurostat Statistics explained. In: ec.europa.eu. http://ec.europa.eu/eurostat/statistics-explained/index.php?title=File:Causes_of_death_%E2%80%94_standardised_death_rate,_2014_(per_100_000_inhabitants)_YB17.png. Accessed 5 Nov 2018

4. Bundesamt für Statistik B Schweizerischer Krebsbericht 2015. In: www.bfs.admin.ch. https://www.bfs.admin.ch/bfs/de/home/statistiken/kataloge-datenbanken/medienmitteilungen.assetdetail.40064.html. Accessed 8 Nov 2018

5. World Health Organization WHO breast cancer awareness. In: who.int. http://www.who.int/cancer/breast_cancer_awareness/en/. Accessed 5 Nov 2018

6. NIH National Cancer Institute Surveillance, Epidemiology, and End Results Program (SEER). https://seer.cancer.gov. Accessed 5 Nov 2018

7. Gandellini P, Andriani F, Merlino G, et al (2015) Complexity in the tumour microenvironment: Cancer associated fibroblast gene expression patterns identify both common and unique features of tumour-stroma crosstalk across cancer types. Seminars in Cancer Biology. doi: 10.1016/j.semcancer.2015.08.008

8. Luo H, Tu G, Liu Z, Liu M (2015) Cancer-associated fibroblasts: a multifaceted driver of breast cancer progression. CANCER LETTERS 361:155–163. doi: 10.1016/j.canlet.2015.02.018

9. Mao Y, Keller ET, Garfield DH, et al (2012) Stromal cells in tumor microenvironment and breast cancer. Cancer Metastasis Rev 32:303–315. doi: 10.1158/1078-0432.CCR-10-2507

10. Santos AA, Matos AJF (2015) Advances in the understanding of the clinically relevant genetic pathways and molecular aspects of canine mammary tumours. Part 2: invasion, angiogenesis, metastasis and therapy. Vet J 205:144–153. doi: 10.1016/j.tvjl.2015.03.029

11. Hanahan D, Coussens LM (2012) Accessories to the Crime: Functionsof Cells Recruited to the Tumor Microenvironment. Cancer Cell 21:309–322. doi: 10.1016/j.ccr.2012.02.022

12. Majidinia M, Yousefi B (2017) Breast tumor stroma: A driving force in the development of resistance to therapies. Chem Biol Drug Des 12:541. doi: 10.1111/cbdd.12893

13. Shan-Wei W, Kan-Lun X, Shu-Qin R, et al (2012) Overexpression of caveolin-1 in cancer-associated fibroblasts predicts good outcome in breast cancer. Breast Care (Basel) 7:477–483. doi: 10.1159/000345464

14. Soysal SD, Tzankov A, Muenst SE (2015) Role of the Tumor Microenvironment in Breast Cancer. Pathobiology 82:142–152. doi: 10.1159/000430499

15. Scully OJ, Bay B-H, Yip G, Yu Y (2012) Breast cancer metastasis. Cancer Genomics Proteomics 9:311–320.

16. Giussani M, Merlino G, Cappelletti V, et al (2015) Tumor-extracellular matrix interactions: Identification of tools associated with breast cancer progression. Seminars in Cancer Biology 35:3–10. doi: 10.1016/j.semcancer.2015.09.012

17. OBEID E, NANDA R, FU Y-X, OLOPADE OI (2013) The role of tumor-associated macrophages in breast cancer progression. Int J Oncol 43:5–12. doi: 10.3892/ijo.2013.1938

18. Duffy SW, Morrish OWE, Allgood PC, et al (2018) Mammographic density and breast cancer risk in breast screening assessment cases and women with a family history of breast cancer. Eur J Cancer 88:48–56. doi: 10.1016/j.ejca.2017.10.022

19. Shibue T, Weinberg RA (2017) EMT, CSCs, and drug resistance: the mechanistic link and clinical implications. Nat Rev Clin Oncol 14:611–629. doi: 10.1038/ncomms6241

20. Zhao X, et al (2017) Prognostic significance of tumor-associated macrophages in breast cancer : a meta-analysis of the literature. Oncotarget 8: 30576–30586. doi: 10.18632/oncotarget.15736

21. Jiang X, Shapiro DJ (2014) The immune system and inflammation in breast cancer. Mol Cell Endocrinol 382:673–682. doi: 10.1016/j.mce.2013.06.003

22. Criscitiello C, Esposito A, Curigliano G (2014) Tumor–stroma crosstalk. Current Opinion in Oncology 26:551–555. doi: 10.1097/CCO.0000000000000122

23. Schiffman JD, Breen M (2015) Comparative oncology: what dogs and other species can teach us about humans with cancer. Philos Trans R Soc Lond, B, Biol Sci. doi: 10.1098/rstb.2014.0231

24. Karlsson EK, Lindblad-Toh K (2008) Leader of the pack: gene mapping in dogs and other model organisms. Nat Rev Genet 9:713–725. doi: 10.1038/nrg2382

25. Liu D, Xiong H, Ellis AE, et al (2014) Molecular homology and difference between spontaneous canine mammary cancer and human breast cancer. Cancer Res 74:5045–5056. doi: 10.1158/0008-5472.CAN-14-0392

26. Rowell JL, McCarthy DO, Alvarez CE (2011) Dog models of naturally occurring cancer. Trends in Molecular Medicine 17:380–388. doi: 10.1016/j.molmed.2011.02.004

27. Uva P, Aurisicchio L, Watters J, et al (2009) Comparative expression pathway analysis of human and canine mammary tumors. BMC Genomics 10:135. doi: 10.1186/1471-2164-10-135

28. Rogers N (2015) Canine clues: Dog genomes explored in effort to bring human cancer to heel. Nat Med 21:1374–1375. doi: 10.1038/nm1215-1374

29. Bejerano G, Pheasant M, Makunin I, et al (2004) Ultraconserved elements in the human genome. Science 304:1321–1325. doi: 10.1126/science.1098119

30. Rivera P, Euler von H (2011) Molecular biological aspects on canine and human mammary tumors. Vet Pathol 48:132–146. doi: 10.1177/0300985810387939

31. Liu D, Xiong H, Ellis AE, et al (2015) Canine Spontaneous Head and Neck Squamous Cell Carcinomas Represent Their Human Counterparts at the Molecular Level. PLoS Genet 11:e1005277. doi: 10.1371/journal.pgen.1005277.s004

32. Lahkhani SR, Ellis IO, Schnitt SJ, et al (2012) WHO Classification of Tumours of the Breast. Fourth Edition. International Agency for Research on Cancer, Lyon

33. Rivera P, Melin M, Biagi T, et al (2009) Mammary tumor development in dogs is associated with BRCA1 and BRCA2. Cancer Res 69:8770–8774. doi: 10.1158/0008-5472.CAN-09-1725

34. Sleeckx N, de Rooster H, Veldhuis Kroeze E, et al (2011) Canine Mammary Tumours, an Overview. Reproduction in Domestic Animals 46:1112–1131. doi: 10.2460/javma.2005.226.1354

35. Sorenmo KU, Kristiansen VM, Cofone MA, et al (2009) Canine mammary gland tumours; a histological continuum from benign to malignant; clinical and histopathological evidence. Vet Comp Oncol 7:162–172. doi: 10.1111/j.1532-950X.2007.00351.x

36. Kessler M (2012) Kleintieronkologie, 3rd ed. Enke Verlag

37. Grüntzig K, Graf R, Hässig M, et al (2015) The Swiss Canine Cancer Registry: a retrospective study on the occurrence of tumours in dogs in Switzerland from 1955 to 2008. J Comp Pathol 152:161–171. doi: 10.1016/j.jcpa.2015.02.005

38. Queiroga FL, Raposo T, Carvalho MI, et al (2011) Canine mammary tumours as a model to study human breast cancer: most recent findings. In Vivo 25:455–465.

39. Pérez-Alenza MD, Peña L, del Castillo N, Nieto AI (2000) Factors influencing the incidence and prognosis of canine mammary tumours. J Small Anim Pract 41:287–291.

40. Gilbertson SR, Kurzman ID, Zachrau RE, et al (1983) Canine mammary epithelial neoplasms: biologic implications of morphologic characteristics assessed in 232 dogs. Vet Pathol 20:127–142. doi: 10.1177/030098588302000201

41. Burstein HJ, Polyak K, Wong JS, et al (2004) Ductal carcinoma in situ of the breast. N Engl J Med 350:1430–1441. doi: 10.1056/NEJMra031301

42. Simpson PT, Reis-Filho JS, Gale T, Lakhani SR (2005) Molecular evolution of breast cancer. J Pathol 205:248–254. doi: 10.1016/S0002-9440(10)64180-6

43. Makki J (2015) Diversity of Breast Carcinoma: Histological Subtypes and Clinical Relevance. Clin Med Insights Pathol 8:CPath.S31563. doi: 10.4137/CPath.S31563

44. Zardavas D, Irrthum A, Swanton C, Piccart M (2015) Clinical management of breast cancer heterogeneity. Nat Rev Clin Oncol 12:381–394. doi: 10.1038/nrclinonc.2015.73

45. Goldschmidt M, Peña L, Rasotto R, Zappulli V (2011) Classification and grading of canine mammary tumors. Vet Pathol 48:117–131. doi: 10.1177/0300985810393258

46. las Mulas de JM, Reymundo C (2000) Animal models of human breast carcinoma: canine and feline neoplasms. C Rev Oncologia 1–8. doi: 10.1007/BF02979590

47. Timmermans-Sprang EPM, Gracanin A, Mol JA (2017) Molecular Signaling of Progesterone, Growth Hormone, Wnt, and HER in Mammary Glands of Dogs, Rodents, and Humans: New Treatment Target Identification. Front Vet Sci 4:53. doi: 10.3389/fvets.2017.00053

48. Case A, Brisson BK, Durham AC, et al (2017) Identification of prognostic collagen signatures and potential therapeutic stromal targets in canine mammary gland carcinoma. PLoS ONE 12:e0180448. doi: 10.1371/journal.pone.0180448

49. Peña L, Andrés PJD, Clemente M, et al (2012) Prognostic Value of Histological Grading in Noninflammatory Canine Mammary Carcinomas in a Prospective Study With Two-Year Follow-Up. Vet Pathol 50:94–105. doi: 10.1177/0300985810377187

50. Karayannopoulou M, Kaldrymidou E, Constantinidis TC, Dessiris A (2005) Histological Grading and Prognosis in Dogs with Mammary Carcinomas: Application of a Human Grading Method. J Comp Pathol 133:246–252. doi: 10.1016/j.jcpa.2005.05.003

51. Rasotto R, Zappulli V, Castagnaro M, Goldschmidt MH (2011) A Retrospective Study of Those Histopathologic Parameters Predictive of Invasion of the Lymphatic System by Canine Mammary Carcinomas. Vet Pathol 49:330–340. doi: 10.1016/j.canlet.2006.12.036

52. Im KS, Kim NH, Lim HY, et al (2013) Analysis of a New Histological and Molecular-Based Classification of Canine Mammary Neoplasia. Vet Pathol 51:549–559. doi: 10.2754/avb200574010103

53. Nguyen F, Peña L, Ibisch C, et al (2017) Canine invasive mammary carcinomas as models of human breast cancer. Part 1: natural history and prognostic factors. Breast Cancer Res Treat 167:635–648. doi: 10.1007/s10549-017-4548-2

54. Rasotto R, Berlato D, Goldschmidt MH, Zappulli V (2017) Prognostic Significance of Canine Mammary Tumor Histologic Subtypes. Vet Pathol 300985817698208. doi: 10.1177/0300985817698208

55. Gama A, Alves A, Schmitt F (2008) Identification of molecular phenotypes in canine mammary carcinomas with clinical implications: application of the human classification. Virchows Arch 453:123–132. doi: 10.1016/S0002-9440(10)64476-8

56. Fazekas J, Fürdös I, Singer J, Jensen-Jarolim E (2016) Why man's best friend, the dog, could also benefit from an anti-HER-2 vaccine. Oncol Lett 12:2271–2276. doi: 10.3892/ol.2016.5001

57. Peña L, Gama A, Goldschmidt MH, et al (2014) Canine Mammary Tumors. Vet Pathol 51:127–145. doi: 10.1097/00125480-200007020-00005

58. Abadie J, Nguyen F, Loussouarn D, et al (2017) Canine invasive mammary carcinomas as models of human breast cancer. Part 2: immunophenotypes and prognostic significance. Breast Cancer Res Treat. doi: 10.1007/s10549-017-4542-8

59. McArthur HL, Page DB (2016) Immunotherapy for the treatment of breast cancer: checkpoint blockade, cancer vaccines, and future directions in combination immunotherapy. Clin Adv Hematol Oncol 14:922–933.

60. Nathan MR, Schmid P (2018) The emerging world of breast cancer immunotherapy. The Breast 37:200–206. doi: 10.1016/j.breast.2017.05.013

61. Klopfleisch R, Lenze D, Hummel M, Gruber AD (2010) Metastatic canine mammary carcinomas can be identified by a gene expression profile that partly overlaps with human breast cancer profiles. BMC Cancer 10:423. doi: 10.1177/0300985809353310

62. Klopfleisch R, Lenze D, Hummel M, Gruber AD (2011) The Veterinary Journal. The Veterinary Journal 190:236–243. doi: 10.1016/j.tvjl.2010.10.018

63. Yoshimura H, Michishita M, Ohkusu-Tsukada K, Takahashi K (2011) Increased presence of stromal myofibroblasts and tenascin-C with malignant progression in canine mammary tumors. Vet Pathol 48:313–321. doi: 10.1177/0300985810369901

64. Kim JH, Yu CH, Yhee JY, et al (2010) Lymphocyte Infiltration, Expression of Interleukin (IL) -1, IL-6 and Expression of Mutated Breast Cancer Susceptibility Gene-1 Correlate with Malignancy of Canine Mammary Tumours. J Comp Pathol 142:177–186. doi: 10.1016/j.jcpa.2009.10.023

65. Król M, Pawłowski KM, Majchrzak K, et al (2011) Density of tumor-associated macrophages (TAMs) and expression of their growth factor receptor MCSF-R and CD14 in canine mammary adenocarcinomas of various grade of malignancy and metastasis. Pol J Vet Sci 14:3–10.

66. Lamp O, Honscha KU, Schweizer S, et al (2011) The metastatic potential of canine mammary tumours can be assessed by mRNA expression analysis of connective tissue modulators. Vet Comp Oncol 11:70–85. doi: 10.1073/pnas.96.5.1858

67. Aresu L, Giantin M, Morello E, et al (2011) Matrix metalloproteinases and their inhibitors in canine mammary tumors. BMC Vet Res 7:33. doi: 10.1186/1746-6148-7-33

68. Santos AA, Lopes CC, Marques RM, et al (2012) Matrix metalloproteinase-9 expression in mammary gland tumors in dogs and its relationship with prognostic factors and patient outcome. Am J Vet Res 73:689–697. doi: 10.2460/ajvr.73.5.689

69. Santos A, Lopes C, Marques RM, et al (2011) The Veterinary Journal. The Veterinary Journal 189:43–48. doi: 10.1016/j.tvjl.2010.05.023

70. Santos AA, Lopes CLC, Ribeiro JR, et al (2013) Identification of prognostic factors in caninemammary malignant tumours: a multivariablesurvival study. BMC Vet Res 9:1–1. doi: 10.1186/1746-6148-9-1

71. Klopfleisch R, Euler von H, Sarli G, et al (2011) Molecular Carcinogenesis of Canine Mammary Tumors. Vet Pathol 48:98–116. doi: 10.1034/j.1600-0463.2003.t01-1-1110208.x

72. Restucci B, Papparella S, Maiolino P, De Vico G (2002) Expression of vascular endothelial growth factor in canine mammary tumors. Vet Pathol 39:488–493. doi: 10.1354/vp.39-4-488

73. Queiroga FL, Pires I, Parente M, et al (2011) The Veterinary Journal. The Veterinary Journal 189:77–82. doi: 10.1016/j.tvjl.2010.06.022

74. Santos A, Lopes C, Gärtner F, Matos AJF (2014) VEGFR-2 expression in malignant tumours of the canine mammary gland: a prospective survival study. Vet Comp Oncol 14:e83–e92. doi: 10.7314/APJCP.2012.13.9.4645

75. Ettlin J (2017) Analysis of Gene Expression Signatures in Cancer-Associated Stroma from Canine Mammary Tumours; Master thesis. Vetsuisse Faculty, University of Zurich

76. Ettlin J, Clementi E, Amini P, et al (2017) Analysis of Gene Expression Signatures in Cancer-Associated Stroma from Canine Mammary Tumours Reveals Molecular Homology to Human Breast Carcinomas. Int J Mol Sci 1–19. doi: 10.3390/ijms18051101

77. Amini P, Ettlin J, Opitz L, et al (2017) An optimised protocol for isolation of RNA from small sections of laser-capture microdissected FFPE tissue amenable for next-generation sequencing. BMC Mol Biol 18:22. doi: 10.1186/s12867-017-0099-7

78. las Mulas de JM, Millán Y, Dios R (2005) A prospective analysis of immunohistochemically determined estrogen receptor alpha and progesterone receptor expression and host and tumor factors as predictors of disease-free period in mammary tumors of the dog. Vet Pathol 42:200–212. doi: 10.1354/vp.42-2-200

79. Clemente M, Pérez-Alenza MD, Illera JC, Peña L (2010) Histological, immunohistological, and ultrastructural description of vasculogenic mimicry in canine mammary cancer. Vet Pathol 47:265–274. doi: 10.1177/0300985809353167

80. Leica (2016) SAMPLE PREPARATION FOR LEICA LASER MICRODISSECTION. 1–44.

81. Finak G, Sadekova S, Pepin F, et al (2006) Gene expression signatures of morphologically normal breast tissue identify basal-like tumors. Breast Cancer Res 8:R58. doi: 10.1186/bcr1608

82. Bolger AM, Lohse M, Usadel B (2014) Trimmomatic: a flexible trimmer for Illumina sequence data. Bioinformatics 30:2114–2120. doi: 10.1093/bioinformatics/btu170

83. Dobin A, Davis CA, Schlesinger F, et al (2013) STAR: ultrafast universal RNA-seq aligner. Bioinformatics 29:15–21. doi: 10.1093/bioinformatics/bts635

84. Bray NL, Pimentel H, Melsted P, Pachter L (2016) Near-optimal probabilistic RNA-seq quantification. Nature Biotechnology 34:525–527. doi: 10.1093/bioinformatics/bts480

85. Robinson MD, McCarthy DJ, Smyth GK (2010) edgeR: a Bioconductor package for differential expression analysis of digital gene expression data. Bioinformatics 26:139–140. doi: 10.1093/bioinformatics/btp616

86. Robinson MD, Oshlack A (2010) A scaling normalization method for differential expression analysis of RNA-seq data. Genome Biology 11:R25. doi: 10.1186/gb-2010-11-3-r25

87. Young MD, Wakefield MJ, Smyth GK, Oshlack A (2010) Gene ontology analysis for RNA-seq: accounting for selection bias. Genome Biology 11:R14. doi: 10.1186/gb-2010-11-2-r14

88. Chen EY, Tan CM, Kou Y, et al (2013) Enrichr: interactive and collaborative HTML5 gene list enrichment analysis tool. BMC Bioinformatics 14:128. doi: 10.1186/1471-2105-14-128

89. Kuleshov MV, Jones MR, Rouillard AD, et al (2016) Enrichr: a comprehensive gene set enrichment analysis web server 2016 update. Nucleic Acids Research 44:W90–W97. doi: 10.1038/srep13044

90. Kowalewski MP, Kautz E, Högger E, et al (2014) Interplacental uterine expression of genes involved in prostaglandin synthesis during canine pregnancy and at induced prepartum luteolysis/abortion. Reprod Biol Endocrinol 12:46. doi: 10.1186/1477-7827-12-46

91. Li T, Fan J, Wang B, et al (2017) TIMER: A Web Server for Comprehensive Analysis of Tumor-Infiltrating Immune Cells. Cancer Res 77:e108–e110. doi: 10.1158/0008-5472.CAN-17-0307

92. World Health Organization WHO breast cancer facts. http://www.who.int/cancer/prevention/diagnosis-screening/breast-cancer/en/. Accessed 5 Nov 2018

93. Espina V, Wulfkuhle JD, Calvert VS, et al (2006) Laser-capture microdissection. Nat Protoc 1:586–603. doi: 10.1038/nprot.2006.85

94. Liu H, McDowell TL, Hanson NE, et al (2014) Laser capture microdissection for the investigative pathologist. Vet Pathol 51:257–269. doi: 10.1177/0300985813510533

95. Ahlfen von S, Missel A, Bendrat K, Schlumpberger M (2007) Determinants of RNA quality from FFPE samples. PLoS ONE 2:e1261. doi: 10.1371/journal.pone.0001261

96. Legres LG, Janin A, Masselon C, Bertheau P (2014) Beyond laser microdissection technology: follow the yellow brick road for cancer research. Am J Cancer Res 4:1–28.

97. Erickson HS, Albert PS, Gillespie JW, et al (2009) Quantitative RT-PCR gene expression analysis of laser microdissected tissue samples. Nat Protoc 4:902–922. doi: 10.1038/nprot.2009.61

98. Kopper O, Benvenisty N (2012) Stepwise differentiation of human embryonic stem cells into early endoderm derivatives and their molecular characterization. Stem Cell Research 8:335–345. doi: 10.1016/j.scr.2011.12.006

99. VanOudenhove JJ, Medina R, Ghule PN, et al (2016) Stem Cell Reports. Stem Cell Reports 7:884–896. doi: 10.1016/j.stemcr.2016.09.006

100. Tosolini M, Kirilovsky A, Mlecnik B, et al (2011) Clinical Impact of Different Classes of Infiltrating T Cytotoxic and Helper Cells (Th1, Th2, Treg, Th17) in Patients with Colorectal Cancer. Cancer Res 71:1263–1271. doi: 10.1158/0008-5472.CAN-10-2907

101. Kaewkangsadan V, Verma C, Eremin JM, et al (2016) Clinical Study. Journal of Immunology Research 1–25. doi: 10.1155/2016/4757405

102. Afshar-Kharghan V (2017) The role of the complement system in cancer. Journal of Clinical Investigation 127:780–789. doi: 10.1373/clinchem.2004.042192

103. Du WW, Fang L, Yang W, et al (2012) The role of versican G3 domain in regulating breast cancer cell motility including effects on osteoblast cell growth and differentiation in vitro – evaluation towards understanding breast cancer cell bone metastasis. BMC Cancer 12:1–1. doi: 10.1186/1471-2407-12-341

104. YAMAGUCHI M, VIKULINA T, WEITZMANN MN (2015) Gentian violet inhibits MDA-MB-231 human breast cancer cell proliferation, and reverses the stimulation of osteoclastogenesis and suppression of osteoblast activity induced by cancer cells. Oncol Rep 34:2156–2162. doi: 10.3892/or.2015.4190

105. Vella V (2014) Type 3 deiodinase: role in cancer growth, stemness, and metabolism. 1–7. doi: 10.3389/fendo.2014.00215/abstract

106. Coulson-Thomas VJ, Gesteira TF, Coulson-Thomas YM, et al (2010) Fibroblast and prostate tumor cell cross-talk: Fibroblast differentiation, TGF. Exp Cell Res 316:3207–3226. doi: 10.1016/j.yexcr.2010.08.005

107. Jovanović B, Pickup M, Chytil A, et al (2016) TβRIII Expression in Human Breast Cancer Stroma and the Role of Soluble TβRIII in Breast Cancer Associated Fibroblasts. Cancers (Basel) 8:100. doi: 10.1167/iovs.11-7300

108. Lambert KE, Huang H, Mythreye K, Blobe GC (2011) The type III transforming growth factor-β receptor inhibits proliferation, migration, and adhesion in human myeloma cells. Mol Biol Cell 22:1463–1472. doi: 10.1182/blood-2005-11-013458

109. Meng W, Xia Q, Wu L, et al (2011) Downregulation of TGF-beta receptor types IIand III in oral squamous cell carcinoma and oralcarcinoma-associated fibroblasts. BMC Cancer 11:88. doi: 10.1186/1471-2407-11-88

110. Chandramouli A, Simundza J, Pinderhughes A, Cowin P (2011) Choreographing Metastasis to the Tune of LTBP. J Mammary Gland Biol Neoplasia 16:67–80. doi: 10.1016/0092-8674(78)90129-0

111. Zhang C-S, Liu Q, Li M, et al (2015) RHOBTB3 promotes proteasomal degradation of HIF. Cell Res 25:1025–1042. doi: 10.1038/cr.2015.90

112. Benita Y, Kikuchi H, Smith AD, et al (2009) An integrative genomics approach identifies Hypoxia Inducible Factor-1 (HIF-1)-target genes that form the core response to hypoxia. Nucleic Acids Research 37:4587–4602. doi: 10.1101/gr.3715005

113. Scholz H (2011) Oxygen-dependent gene expression in development and cancer: lessons learned from the Wilms' tumor gene, WT1. 1–11. doi: 10.3389/fnmol.2011.00004/abstract

114. Long M, Simpson JC (2017) Tissue and Cell. Tissue and Cell 49:163–169. doi: 10.1016/j.tice.2016.09.007

115. BERTHOLD J, SCHENKOVÁ K, RIVERO F (2008) Rho GTPases of the RhoBTB subfamily and tumorigenesis. Acta Pharmacologica Sinica 29:285–295. doi: 10.1007/s00018-007-7082-2

116. Wang L, Wang Z-Y (2008) The Wilms' tumor suppressor WT1 inhibits malignant progression of neoplastigenic mammary epithelial cells. Anticancer Res 28:2155–2160.

117. Wang L, Wang Z-Y (2010) The Wilms' tumor suppressor WT1 induces estrogen-independent growth and anti-estrogen insensitivity in ER-positive breast cancer MCF7 cells. Oncol Rep 23:1109–1117.

118. Hou J, Wang Z, Xu H, et al (2015) Stanniocalicin 2 Suppresses Breast Cancer Cell Migration and Invasion via the PKC/Claudin-1-Mediated Signaling. PLoS ONE 10:e0122179. doi: 10.1371/journal.pone.0122179.s001

119. Shiao Y-M, Chang Y-H, Liu Y-M, et al (2008) Dysregulation of GIMAP genes in non-small cell lung cancer. Lung Cancer 62:287–294. doi: 10.1016/j.lungcan.2008.03.021

120. Krücken J, Epe M, Benten WPM, et al (2005) Malaria-suppressible expression of the anti-apoptotic triple GTPase mGIMAP8. J Cell Biochem 96:339–348. doi: 10.1002/jcb.20552

121. Webb LMC, Pascall JC, Hepburn L, et al (2014) Generation and Characterisation of Mice Deficient in the Multi-GTPase Domain Containing Protein, GIMAP8. PLoS ONE 9:e110294. doi: 10.1371/journal.pone.0110294.s004

122. Winslow S (2015) Prognostic stromal gene signatures in breast cancer. 1–13. doi: 10.1186/s13058-015-0530-2

123. Sánchez-Barrena MJ, Vallis Y, Clatworthy MR, et al (2012) Bin2 Is a Membrane Sculpting N-BAR Protein That Influences Leucocyte Podosomes, Motility and Phagocytosis. PLoS ONE 7:e52401. doi: 10.1371/journal.pone.0052401.s011

124. Zheng T, Wang A, Hu D, Wang Y (2017) Molecular mechanisms of breast cancer metastasis by gene expression profile analysis. Molecular Medicine Reports 16:4671–4677. doi: 10.3892/mmr.2017.7157

125. Geng X-T, Hu Y-H, Dong T, Wang R-Z (2016) Associations of Human Leukocyte Antigen-DRB1 Alleles with Nasopharyngeal Carcinoma and Its Clinical Significance in Xinjiang Uyghur Autonomous Region of China. Chin Med J 129:1347. doi: 10.4103/0366-6999.182833

126. Alderson MR, Tough TW, Davis-Smith T, et al (1995) Fas ligand mediates activation-induced cell death in human T lymphocytes. J Exp Med 181:71–77.

127. Schneider P, Bodmer JL, Holler N, et al (1997) Characterization of Fas (Apo-1, CD95)-Fas ligand interaction. J Biol Chem 272:18827–18833.

128. Min K-W, Kim D-H, Do S-I, et al (2012) Diagnostic and Prognostic Relevance of MMP-11 Expression in the Stromal Fibroblast-Like Cells Adjacent to Invasive Ductal Carcinoma of the Breast. Ann Surg Oncol 20:433–442. doi: 10.1016/j.biocel.2007.06.007

129. Cid S, Eiro N, González LO, et al (2016) Expression and Clinical Signi. Clinical Breast Cancer 16:e83–e91. doi: 10.1016/j.clbc.2016.05.007

130. Motrescu ER, Blaise S, Etique N, et al (2008) Matrix metalloproteinase-11/stromelysin-3 exhibits collagenolytic function against collagen VI under normal and malignant conditions. Oncogene 27:6347–6355. doi: 10.1038/ncpendmet0456

131. González L, Eiro N, Fernandez-Garcia B, et al (2015) Gene expression profile of normal and cancer-associated fibroblasts according to intratumoral inflammatory cells phenotype from breast cancer tissue. Mol Carcinog 55:1489–1502. doi: 10.1038/nrc1926

132. Eiro N, Fernandez-Garcia B, Vazquez J, et al (2015) A phenotype from tumor stroma based on the expression of metalloproteases and their inhibitors, associated with prognosis in breast cancer. OncoImmunology 4:e992222. doi: 10.1158/1078-0432.CCR-04-0220

133. Ma X-J, Dahiya S, Richardson E, et al (2009) Gene expression profiling of the tumor microenvironment during breast cancer progression. Breast Cancer Res 11:R7. doi: 10.1186/bcr2222

134. Tomarev SI, Nakaya N (2009) Olfactomedin Domain-Containing Proteins: Possible Mechanisms of Action and Functions in Normal Development and Pathology. Mol Neurobiol 40:122–138. doi: 10.4161/cc.5.11.2804

135. Anholt RRH (2014) Olfactomedin proteins: central players in development anddisease. 1–10. doi: 10.3389/fcell.2014.00006/abstract

136. Whittaker CA, Hynes RO (2002) Distribution and evolution of von Willebrand/integrin A domains: widely dispersed domains with roles in cell adhesion and elsewhere. Mol Biol Cell 13:3369–3387. doi: 10.1091/mbc.e02-05-0259

137. Wilson R, Norris EL, Brachvogel B, et al (2012) Changes in the Chondrocyte and Extracellular Matrix Proteome during Post-natal Mouse Cartilage Development. Mol Cell Proteomics 11:M111.014159. doi: 10.1002/jor.1100070408

138. Morris MR, Ricketts C, Gentle D, et al (2010) Identification of candidate tumour suppressor genes frequently methylated in renal cell carcinoma. Oncogene 29:2104–2117. doi: 10.1016/S1535-6108(02)00215-5

139. Stirzaker C, Zotenko E, Song JZ, et al (2015) Methylome sequencing in triple-negative breast cancer reveals distinct methylation clusters with prognostic value. Nat Commun 6:1–11. doi: 10.1038/ncomms6899

140. Chen C (2015) TGFβ isoforms and receptors mRNAexpression in breast tumours: prognosticvalue and clinical implications. BMC Cancer 1–12. doi: 10.1186/s12885-015-1993-3

141. Chang PH, Hwang-Verslues WW, Chang YC, et al (2012) Activation of Robo1 Signaling of Breast Cancer Cells by Slit2 from Stromal Fibroblast Restrains Tumorigenesis via Blocking PI3K/Akt/ -Catenin Pathway. Cancer Res 72:4652–4661. doi: 10.1158/0008-5472.CAN-12-0877

142. Harburg GC, Hinck L (2011) Navigating Breast Cancer: Axon Guidance Molecules as Breast Cancer Tumor Suppressors and Oncogenes. J Mammary Gland Biol Neoplasia 16:257–270. doi: 10.1016/j.ejca.2008.10.016

143. Buchsbaum R, Oh S (2016) Breast Cancer-Associated Fibroblasts: Where We Are and Where We Need to Go. Cancers (Basel) 8:19. doi: 10.3892/ijo.2011.1073

144. Marlow R, Strickland P, Lee JS, et al (2008) SLITs Suppress Tumor Growth In vivo by Silencing Sdf1/Cxcr4 within Breast Epithelium. Cancer Res 68:7819–7827. doi: 10.1158/0008-5472.CAN-08-1357

145. Karayan-Tapon L, Wager M, Guilhot J, et al (2008) Semaphorin, neuropilin and VEGF expression in glial tumours: SEMA3G, a prognostic marker? Br J Cancer 99:1153–1160. doi: 10.1186/gb-2006-7-3-211

146. Kigel B, Varshavsky A, Kessler O, Neufeld G (2008) Successful Inhibition of Tumor Development by Specific Class-3 Semaphorins Is Associated with Expression of Appropriate Semaphorin Receptors by Tumor Cells. PLoS ONE 3:e3287. doi: 10.1371/journal.pone.0003287.s003

147. Yu R (2012) Effects of SEMA3G on migration and invasion of glioma cells. Oncol Rep. doi: 10.3892/or.2012.1796

148. Enciu A-M, Radu E, Popescu ID, et al (2018) Review Article. Biomed Res Int 1–12. doi: 10.1155/2018/7801202

149. DeClerck YA (2012) Desmoplasia: A Response or a Niche? Cancer Discov 2:772–774. doi: 10.1158/2159-8290.CD-12-0348

150. DeFilippis RA, Chang H, Dumont N, et al (2012) CD36 Repression Activates a Multicellular Stromal Program Shared by High Mammographic Density and Tumor Tissues. Cancer Discov 2:826–839. doi: 10.1158/2159-8290.CD-12-0107

151. Ren B, Best B, Ramakrishnan DP, et al (2016) LPA/PKD-1-FoxO1 Signaling Axis Mediates Endothelial Cell CD36 Transcriptional Repression and Proangiogenic and Proarteriogenic Reprogramming. Arterioscler Thromb Vasc Biol 36:1197–1208. doi: 10.1161/ATVBAHA.116.307421

152. Klopfleisch R, Klose P, Gruber AD (2010) The combined expression pattern of BMP2, LTBP4, and DERL1 discriminates malignant from benign canine mammary tumors. Vet Pathol 47: 446–454. doi: 10.1177/0300985810363904

9 Acknowledgements

At this point I would like to thank everyone who helped me during this work.
To begin with, I would like to thank my supervisor Dr. Enni Markkanen for giving me the possibility to work on this project and the great support throughout the entire time.
Next I would like to thank Prof. Dr. Hanspeter Nägeli for his support and useful inputs which helped to improve my work,
Dr. Alexandra Malbon for her expertise in case selection and characterisation as well as great support during tissue isolation,
all members of the Markkanen group including Parisa Amini, Elena Clementi, Erin Beebe, Larissa Inglin, and Zuzana Garajova for the amazing working environment which I will never forget,
all members of the Institute of Veterinary Pharmacology and Toxicology of the Vetsuisse Faculty Zurich, in particular the Nägeli group,
all members of the Institute of Veterinary Pathology of the Vetsuisse Faculty Zurich for their work and support regarding tissue processing,
the Functional Genomics Centre Zurich, in particular Lennart Opitz for the bioinformatics analysis as well as Maria Domenica Moccia for her help with RNAseq, and Prof. R. Klopfleisch for kindly providing us samples from his lab of the Freie Univeristät Berlin.
Furthermore, I want to thank the Promedica Stiftung, the A.+S. Huggenberger Stiftung, and the Heuberger Stiftung fort their financial support.

Last but not least, a big thank you to my family and friends for their unconditional support and encouraging words not only during this project but in any situation.

10 Curriculum vitae

Vorname Name	Julia Ettlin
Geburtsdatum	20.09.1992
Geburtsort	Zürich
Nationalität	Schweiz
Heimatort	Basel BS, Allschwil BL

08/1999-07/2004	Primarschule, Gesamtschule Gerlisberg, Kloten, Schweiz
08/2004-07/2007	Sekundarschule, Schulhaus Nägelimoos, Kloten, Schweiz
08/2007-09/2011	Gymnasium, Kantonsschule Zürcher Unterland, Bülach, Schweiz
08.09.2011	Matura, Gymnasium, Kantonsschule Zürich Unterland, Bülach, Schweiz
09/2012-09/2017	Studium der Veterinärmedizin, Universität Zürich, Zürich, Schweiz
29.12.2017	Abschlussprüfung vet. med., Universität Zürich, Zürich, Schweiz
02/2018-11/2018	Anfertigung der Dissertation unter Leitung von Dr. med. vet. Dr. sc. nat. Enni Markkanen am Institut für Veterinärpharmakologie und -toxikologie der Vetsuisse-Fakultät Universität Zürich Direktor: Prof. Dr. med. vet. Hanspeter Nägeli
02/2018-11/2018	Doktorandin, Institut für Veterinärpharmakologie und -toxikologie, Vetsuisse Fakultät, Universität Zürich, Zürich, Schweiz